Ankle-Foot Orthosis Stiffness: Biomechanical Effects, Measurement and Emulation

by

Deema Totah

A dissertation submitted in partial fulfillment
of the requirements for the degree of
Doctor of Philosophy
(Mechanical Engineering)
in the University of Michigan
2020

Doctoral Committee:

Associate Professor Kira L. Barton, Co-Chair
Associate Professor Deanna H. Gates, Co-Chair
Professor C. David Remy, University of Stuttgart
Professor Albert Shih

Deema Totah

deema@umich.edu

ORCID iD: 0000-0001-9258-7256

To my aunt, Suha Jubran, whose spirit lives on beyond a world with insufficient access ramps.

ACKNOWLEDGMENTS

Thank you to my advisors Kira Barton and Deanna Gates for their guidance and support. The opportunities they provided me have made me a better scholar, writer, mentor and engineer. I've been lucky to have two brilliant co-advisors with different perspectives guiding me on this journey. I am grateful for their time, patience, and flexibility as we all navigated this work. I'd also like to thank the rest of my committee, David Remy and Albert Shih, for their feedback and support to make this work possible. I'd also like to thank Alex Shorter and Noel Perkins for their support and the opportunity to become a better teacher, and Chinedum Okwudire for always having an encouraging word to say.

Most of all, thank you to my family, a constant source of support, love and encouragement at all hours of the day and night in multiple time zones. I am so grateful to my parents for giving me the freedom to choose who I want to be and the support to get there. Thank you to my father, Marwan, who taught me how to use a soldering iron and to never accept a black box solution. Thank you to my mother, Samia - no words will ever be enough. This woman does not know the phrase "it cannot be done", whether she's in a boardroom or successfully transporting Palestinian ice cream to Ann Arbor. I owe all my success to her. I've always said my mother is an enabler and I can only hope to model her leadership one day. Thank you to my sister for reminding me to enjoy life and aim high to the skies, and for understanding when no one else does.

To my true partner and best friend, Casey Harwood, thank you for everything, especially tiny champagne bottles. You've been lifting me up and making me smile since the day I met you.Thank you to Mara Harwood for being a shoulder to lean on, when I needed one, and a friend, always. Thanks to Laura and Jon Harwood for all the kindness, laughter and encouragement.Thanks to my Ann Arbor family, the Ajlouny's and their wonderful friends, for always making me feel at home.

Thank you to all the colleagues and friends - near and far, old and new - who have helped me through this process. I'd like to especially mention Rachel Vitali, Emma Treadway, Christie Rodriguez, Susannah Engdahl, Estefania Rios, Monica Oliver, Eileen Yang, Efrain Cermeno, Esteban Castro, Raya Hamoudeh, Aseel Baidoun, Samar Sakakini, Kim Ingraham, Rose Figueroa, Lianette Rivera, Leo Tse, Michael Quann, Mohammed Banani,

Luis Nolasco, Jay Kim and Michael Gonzalez (with special mention of his accountability spreadsheet for keeping me on track).

Thanks to all past and present members of the Barton Research Group, Rehabilitation Biomechanics Laboratory, Neuromechanics community, and the Biomechatronics Journal Club. I've greatly enjoyed our time together and learned so much from you. I could not have done this without your support. I'd also like to thank the undergraduate and masters students who contributed to my research whether it be included in this thesis or not, specifically I want to mention Anne Gu, Devyani Kalvit and Meghna Menon.

Thanks to Adam Mael and the Mechanical Engineering Department staff for their support and resources. Thank you to Darren Bolger, Jeff Wensman and the UM Orthotics and Prosthetics Clinic for their help with the design and fabrication of the exoskeleton in Chapter 5, providing AFOs for Chapters 3 and 4, and for helping me better understand clinician and patient perspectives. Thanks to Michael Schwartz and Andy Ries at the Gillete Gait Clinic for their help in conducting the comparative study in Chapter 3.Thanks to Qianyi (Albert) Fu, Robert Chisena and other members of the Biomedical Manufacturing and Design Lab for their collaborations. Thanks to Nikko Van Crey and Marcos Cavallin for helping with the device in Chapter 3.

The work in this thesis would not have been possible without funding from the National Science Foundation (grant number 1534003), the National Institute of Health (grant number 5 R03 HD092639-02), a Small Grant for theDevelopment of Technology to Support Health Managementand Independence from UM's Rehabilitation Engineering Research Center (supported by NIDILRR grant number H133E130014), several Rackham Research and Travel Grants, and funds from the UM Mechanical Engineering Department.

PREFACE

Chapters 2, 3 and 4 were adapted from journal manuscripts and there may be some repetition between them.

TABLE OF CONTENTS

LIST OF FIGURES

LIST OF TABLES

LIST OF APPENDICES

LIST OF ABBREVIATIONS

AFO ankle-foot orthosis

PLS posterior leaf spring (a type of AFO)

CAD computer aided design

GRF ground reaction force

IDEO Intrepid Dynamic Exoskeletal Orthosis

DF dorsiflexion

PF plantarflexion

CMT Charcot-Marie-Tooth disease

SMApp stiffness measurement apparatus

PRISMA preferred reporting items for systematic reviews and meta-analyses

SS single support

DS double support

COM center of mass

ROM range of motion

FES finite element simulation

UTM universal testing machine

BRUCE bi-articular reciprocal universal compliance estimator

MuscTM muscle training machine

DFR dorsiflexion resistance

PFR plantarflexion resistance

CoP center of pressure

EMG electromyography

MG medial gastrocnemius

MTU gastrocnemius musculotendon unit

AT achilles tendon

iEMG time-integrated electromyographic signal

SWS self-selected walking speed

ICC intraclass correlation coefficient

SEM standard error of measurement

MDD minimum detectable difference

rpm rotations per minute

PC personal computer

PEBA polyether block amide

SD standard deviation

ANOVA analysis of variance

DAQ data acquisition

ABSTRACT

Ankle-foot orthoses (AFOs) are braces worn by individuals with gait impairments to provide support about the ankle. AFOs come in a variety of designs for clinicians to choose from. However, as the effects of different design parameters on AFO properties and AFO users have not been adequately quantified, it is not clear which design choices are most likely to improve patient outcomes. Recent advances in manufacturing have further expanded the design space, adding urgency and complexity to the challenge of selecting optimal designs. A key AFO property affected by design decisions is sagittal-plane rotational stiffness. To evaluate the effectiveness of different AFO designs, we need: 1) a better understanding of the biomechanical effects of AFO stiffness and 2) more precise and repeatable stiffness measurement methods.

This dissertation addresses these needs by accomplishing four aims. First, we conducted a systematic literature review on the influence of AFO stiffness on gait biomechanics. We found that ankle and knee kinematics are affected by increasing stiffness, with minimal effects on hip kinematics and kinetics. However, the lack of effective stiffness measurement techniques made it difficult to determine which specific values or ranges of stiffness influence biomechanics. Therefore, in *Aim 2*, we developed an AFO stiffness measurement apparatus (SMApp). The SMApp is an automated device that non-destructively flexes an AFO to acquire operator- and trial-independent measurements of its torque-angle dynamics. The SMApp was designed to test a variety of AFO types and sizes across a wide range of flexion angles and speeds exceeding current alternatives.

Common models of AFO torque-angle dynamics in literature have simplified the rela-

tionship to a linear fit whose slope represents stiffness. This linear approximation ignores damping parameters. However, as previous studies were unable to precisely control AFO flexion speed, the presence of speed effects has not been adequately investigated. Thus, in *Aim 3*, we used the SMApp to test whether AFOs exhibit viscoelastic behaviors over the range of speeds typically achieved during walking. This study revealed small but statistically significant effects of flexion speed on AFO stiffness for samples of both traditional AFOs and novel 3-D printed AFOs, suggesting that more complex models that include damping parameters could be more suitable for modeling AFO dynamics.

Finally, in *Aim 4*, we investigated the use of an active exoskeleton, that can haptically-emulate different AFOs, as a potential test bed for studying the effects of AFO parameters on human movement. Prior work has used emulation for rapid prototyping of candidate assistive devices. While emulators can mimic a physical device's torque-angle profile, the physical and emulated devices may have other differences that influence user biomechanics. Current studies have not investigated these differences, which limits translation of findings from emulated to physical devices. To evaluate the efficacy of AFO emulation as a research tool, we conducted a single-subject pilot study with a custom-built AFO emulator device. We compared user kinematics while walking with a physical AFO against those with an emulated AFO and found they elicited similar ankle trajectories.

This dissertation resulted in the successful development and evaluation of a framework consisting of two test beds, one to assess AFO mechanical properties and another to assess the effects of these properties on the AFO user. These tools enable innovations in AFO design that can translate to measurable improvements in patient outcomes.

CHAPTER 1

Introduction

1.1 Research Motivation: Challenges in the AFO Fitting Process

Ankle-foot orthoses (AFOs) are assistive braces worn to provide support about the ankle joint (Figure 1.1). They have been shown to improve outcomes for a variety of patients, including those dealing with multiple sclerosis [8, 9], stroke rehabilitation [10], Charcot-Marie-Tooth syndrome [11], and cerebral palsy [12, 13]. When prescribing AFOs for such a varied patient population, clinicians have many different designs from which to choose. When considering design options, design parameters become key decision points since they can be used to alter an AFO's properties and the effective support the AFO provides to the user.

The current standard for choosing an appropriate AFO design for a specific patient largely relies on clinician experience and visual observation of the patient's gait. Once a design is chosen, the manufacturing process heavily relies upon skilled manual labor to form and cut an AFO from a thermoplastic sheet onto a plaster cast of the patient's leg [14–

Figure 1.1: A selection of posterior leaf spring ankle-foot orthoses (AFOs).

16]. This process lacks quantitative evaluation metrics in the fitting process that, together with the low manufacturing repeatability and manufacturing imperfections, results in sub-optimal AFOs and frequent repeat clinic visits to adjust AFO fit. Repeat clinical visits and AFO adjustments result in added time and cost for both the patient and the clinic. Moreover, the use of sub-optimal AFOs may lead to patient discomfort, reduce the device's biomechanical benefit, lead to patient rejection of the device, and even cause deterioration of gait and physical function in the long-term [17–20].

Recent literature has proposed additive manufacturing techniques as alternatives to traditional AFO casting and thermoforming to increase repeatability and reduce imperfections [15, 21, 22]. Additive manufacturing also increases the design space of these devices with increased customizability, making the design decision process even more complex. This places the need for more objective AFO fitting tools and standards at the forefront.

The Challenge: A key obstacle to utilizing such a broadened design space is in understanding how AFO design choices affect the mechanical properties of the AFO and, ultimately, how such choices affect appropriate quantitative patient performance metrics. It is known that changes in design parameters alter the effective ankle stiffness that an AFO provides [23, 24]. However, little is known about the effect of specific stiffness changes on patient performance metrics. This is largely due to the lack of effective AFO stiffness testing and reporting standards.

The Solution: I propose leveraging assessment tools found in gait laboratories and engineering research environments to study AFO stiffness and understand the effect of AFO design parameter changes on objective performance metrics for optimizing patient-specific AFO designs. Mechatronic actuators and sensors could be utilized to automate AFO testing and provide reliable stiffness measurements. Additionally, active exoskeleton devices could serve as test beds for studying the effects of different stiffnesses on the user. These devices, consisting of a light-weight exoskeleton tethered to an off-board motor, have been used for rapid prototyping of active device controllers and parameters (e.g. [25, 26]). The controller parameters can be tuned to emulate a specific device design. With a clear model of AFO properties, we could utilize such an emulation system to mimic a variety of AFO designs and evaluate their effects on patient performance.

By establishing methods to study AFO stiffness and understand its effects on the user, this dissertation enables the study of objective measures of patient performance as they relate to key AFO design parameters. These tools will enhance the efficacy of AFOs and ensure patients can truly benefit from properly matched AFO designs. The following section presents a summary of the state of the art in key relevant topics to reaching this goal. A summary of the dissertation aims and contributions is presented at the end of this chapter.

1.2 Background

This section contains relevant background and state of the art of select key topics. These topics and others are expanded upon further, as needed, in the other chapters of this dissertation.

AFO Design, Fitting and Manufacturing

AFO devices can be generally classified into three main types: articulating, which have a joint allowing a certain range of ankle motion; non-articulating or solid-ankle, devices that barely allow any ankle joint motion; and posterior leaf spring (PLS, Figure 1.1), which provide some energy return when flexed. AFOs may be purchased off-the-shelf or custom-manufactured. The standard method for manufacturing AFOs is the traditional plaster casting method, where a plaster cast of the patient's foot is formed and modified, then a thermoplastic sheet is formed onto the cast, cut to the appropriate trim-lines, and outfitted with accessories such as hinges, elastic bands, and straps. Recently, other manufacturing methods have emerged in research settings [27], including selective laser sintering [21] and fused deposition modeling [22]. The most common materials used in traditional AFO manufacturing are thermoplastics, e.g. polypropylene; carbon composites are sometimes used. The newer manufacturing methods also use plastics, as well as nylon and carbon composites.

Patients are typically referred to an orthotics clinic with an AFO prescription, then it is up to the orthotists at the clinic to select the appropriate AFO design. After reviewing best practice recommendations from the International Society for Prosthetics and Orthotics [28–30], guidelines from the International Committee of the Red Cross [16] and speaking to collaborators at the University of Michigan Orthotics and Prosthetics Center, we found that only general guidelines are given for AFO prescription and no specific/quantitative standards are in place. The guidelines mainly provide recommendations for choosing between the three main AFO design types (articulated, non-articulated and PLS), suggesting clinicians consider the specific pathology and type of motion needed to be supported (plantarflexion/dorsiflexion) or whether a deformity should be corrected or accommodated. In fact, insufficient descriptions of AFO devices and the pathologies of their users make it difficult to conduct conclusive literature reviews and recommendations for optimizing AFO prescription [28]. Clinicians typically use observational evaluations and their own professional experience to select the appropriate AFO design, draw trim-lines, select a material and any accessories or special features, e.g. added padding, elastic joints, or hard stops to limit range of motion. Some clinics offer more advanced gait analysis tools that go beyond

observational analysis (discussed in the next subsection). Clinicians aim to reduce patient pain and discomfort, increase gait symmetry, and decrease deviations from normative gait patterns. The personal patient-orthotist interaction and a custom-built AFO allows orthotists to make customized recommendations to alleviate pain by adding targeted cushioning for example, and to take patient weight and activity or fitness level into considerations. Typically, the more severe the deformity and more advanced the pathology, the greater the AFO rigidity needed to provide sufficient support; while patients with higher activity levels may benefit from more compliant AFOs, which offer less support but greater energy return. Considering the varying AFO types and parameters, it is concluded that all the design options can be described in terms of stiffness variation in three degrees of freedom of ankle motion (plantarflexion/dosriflexion, inversion/eversion, and suppination/pronation), with solid ankle designs and free motion hinges on opposite ends of the stiffness spectrum, exhibiting nearly infinite stiffness and nearly zero stiffness respectively.

The significance of AFO stiffness on clinical outcomes is difficult to ascertain due to differences in outcome measures, lack of consistency in patient deficits, and inability to quantify and compare stiffnesses among different studies [31]. The lack of established standards for reporting AFO design variables [32] and patient pathologies [28] makes this more challenging. Nonetheless, several studies found that AFO rotational stiffness has significant effects on movement and user performance [3, 24, 33–36]. However, one research group, while observing significant changes in ankle range of motion due to stiffness [37], concluded that overall walking performance remained unchanged [37, 38]. The group did observe changes in gait mechanics for different AFO stiffnesses during running [39]. It is likely that certain ranges of stiffness have a significant impact on gait while other ranges do not.

Discussions of AFO stiffness are not limited to clinical literature; engineering and design researchers have created computer-aided design models and finite element analyses to investigate AFO rotational stiffness [14, 27, 40, 41]. Moreover, the importance of accurately identifying AFO stiffness in simulations is highlighted in [42], where Hegarty et al. show that muscle force estimations from gait simulation models of AFO-users are very sensitive to changes in the modeled AFO stiffness, particularly dorsiflexion stiffness. In addition to computer models, researchers have attempted to quantify AFO stiffness through experimental measurements. According to a recent review article [31], the majority of publications investigating measures of stiffness, or rigidity, of an AFO used bench top testing, some with and some without a surrogate limb. A few studies collected data during functional testing from a modified or instrumented AFO during patient gait experiments. The majority of studies measured motion in the sagittal plane only (plantarflexion and dorsi-

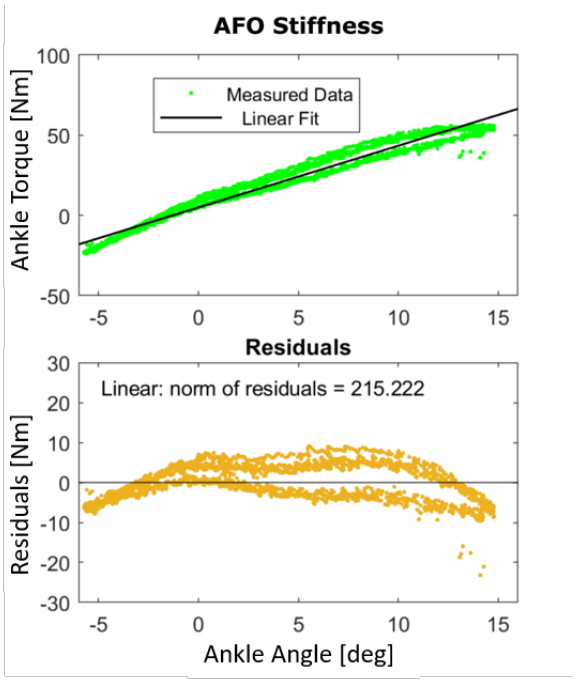

Figure 1.2: A linear fit of the stiffness data from an additively-manufactured nylon AFO shows patterned residuals, indicating that a higher-order fit is needed.

flexion) with a few additionally exploring eversion and inversion motions [43–45], and external and internal rotations [43, 44]. The AFO stiffness curve shows hysteresis effects, as is expected considering its elastic properties. However, typical representations of an AFO stiffness [46] consist of a single stiffness value, obtained by fitting a single line through an averaged hysteresis curve. These representations are therefore incomplete (Figure 1.2) and may be inadequate for emulation purposes, particularly for mimicking compliant AFO designs. Additionally, common stiffness representations ignore viscoelastic effects and do not test AFOs with different flexion speeds (with a few exceptions [47, 48]). This is may be because of anecdotal evidence that thermoplastic AFOs are not affected by flexion speed. However, this has not been adequately studied. To our knowledge, only one study systematically evaluated the effect of speed on AFO stiffness and did not find it to be statistically significant [49]. This study evaluated traditionally manufactured AFOs made from thermoplastic or carbon composites, using a manual AFO testing device to match different walking cadences. Considering the large variety of available AFO devices and the inherent elastic and hysteretic properties of the materials used to construct them, more evidence is needed before viscoelastic effects can be dismissed. This becomes increasingly important as novel materials and manufacturing methods are utilized for AFO construction.

Assessing Patient Gait Performance

Researchers and clinicians utilize various metrics to evaluate a particular assistive device and/or quantify the severity of a patient's pathological gait. The metrics utilized depend on the sensors and tools available to make these measurements. In research environments, gait analysis laboratories may be equipped with instruments such as motion capture systems, force plates, instrumented treadmills, electromyography electrodes, calorimeters, and heart rate sensors. Researchers use these tools to target reductions in metabolic cost [26, 50–53] and muscle activity to indicate better device performance [51, 54]. Joint kinematics (of the ankle, knee and hip) and segment kinetics are calculated to identify metrics of interest in joint motion and moment trajectories; many of these metrics are included in Table 1.1. In [55], Hollman et al. assessed 23 gait parameters and, using factor analsysis, identified five key domains for evaluating gait in older populations: rythm, phase, pace, base of support and variability. Each domain relates to a certain gait parameters, for example cadence, mean stance time, and single support time all fall under the rythm domain. The authors "recommend that data representing each of these domains be collected when gait analyses are conducted" [55]. Other metrics often used to asses patient gait outcomes are walking speed, with one article even dubbing it "the sixth vital sign" [56], and range of motion [57]. Additionally, symmetry between left and right gait cycle kinematics and spatio-temporal parameters is often cited as an important performance metric [58, 59]. In [60], AFO selections considered increased symmetry in muscle activity patterns. Moreover, the symmetry metric closely corresponds to visual evaluations observed by orthotists in the clinic during the AFO fitting process.

Qualitative visual observation is the most common method of assessment in clinics. While some clinics may have access to some of the tools mentioned above, they are more likely to utilize equipment like instrumented walkway mats (e.g. Strideway™ from Tekscan®) to assess kinematics measures such as stride length. Clinicians and clinical researchers also utilize gait indices or scores that quantify deviations from normative gait, such as: Normalcy Index or Gillette Gait Index [61, 62], Gait Deviation Index [63], Gait Profile Score [64], and Movement Deviation Profile [65]. These scores generally represent a cumulative deviation from normative values of several gait parameters such as angle trajectories or peak values of ankle and knee joints.

There is a gap between the metrics used in the clinic (largely visual and focusing on kinematics parameters and gait scores or indices) and those used in the lab, which tend to include kinetics, metabolic cost and muscle activity evaluations. An opportunity arises here to utilize laboratory equipment and tools to study the effects of particular design choices on clinically-relevant performance metrics. In the case of AFOs, understanding which

Table 1.1: A collection of spatiotemporal, kinematic and kinetic metrics used in pathological gait analysis studies. *GRF: ground reaction force

Spatiotemporal	**Kinematics**
Double support period [57, 66]	Peak knee extension during stance [33, 67]
Paretic single support period [57, 66]	Peak knee flexion [66]
Step width variability [68]	Knee flexion at inital contact [33, 67]
Foot placement variability [68]	Knee flexion velocity at toe-off [66]
Ankle moment zero-cross point [33]	Paretic ankle range of motion (ROM) [57]
	Peak ankle plantarflexion angle [33]
Kinetics	Peak ankle dorsiflexion angle [66]
Peak propulsion force [66]	Ankle angle at initial contact [33]
GRF* vector alignment relative to knee [67]	Ankle angle at toe-off [66]
Peak ankle plantarflexion moment [66]	Peak hip extension angle [66]
Peak ankle dorsiflexion moment [33]	Step length
Peak knee extension moment [66]	Cadence (walking speed) [68]
Peak knee flexion moment [33]	
Peak hip flexion moment [66]	

performance metrics are affected by stiffness is necessary, as those are the metrics likely to benefit from AFO design tuning.

Utilizing Robotic Devices for Prototype Emulation

While robotic assistive devices are usually required to be mobile to effectively assist the user as they navigate the world, tethered versions of these devices have their own uses inside research settings. These tethered systems consist of active exoskeleton (or prosthetic) devices controlled by off-board motors. The off-boarding of the motor systems makes for light-weight devices that can be easily controlled to facilitate the exploration of much larger parameter spaces. The separation of the actuator and controller from the device also allows researchers to vary different device parameters independently and study their effects. The presence of these emulators inside the laboratory means that a multitude of sensors and patient assessment tools could be potentially utilized that would not be otherwise available. Some research groups have utilized such systems to explore the optimality of different control parameters and schemes based on various measures, such as metabolic cost [52] or muscle activity [69]. One group used a prosthesis 'emulator' for rapid prototyping (in

an emulated-prototype sense) to evaluate candidate prosthetic devices, by measuring user performance metrics and preferences as they 'try on' the different devices [50].

These emulator systems show great potential as prototyping test beds for investigating the effect of key device design and control parameters on user performance. However, when validating these systems, prior research has focused solely on evaluating the controller's reference torque-tracking error and evaluating bandwidth. A more comprehensive validation of these systems is needed before they can be claimed as tools for candidate-device evaluation. An evaluation of the patient haptic experience with an emulated device as it compares to the actual device prototype, i.e. the physical manifestations of the candidate devices the patients take home with them, remains to be investigated. Moreover, before emulators can be deemed useful for studying the effect of a particular design parameter on the user, we need to understand which performance metrics are affected by emulation and which remain consistent between emulated and physical devices.

1.3 Key Literature Gaps

The current literature discussed in this chapter has gaps in the following areas:

(a) Effect of Stiffness on Patient Performance
The physiological measures and gait metrics affected by stiffness are not well-identified. Knowing which metrics are affected and how they are affected would greatly inform AFO device tuning.

(b) AFO Stiffness Measurement
While it is understood that rotational stiffness is an important property of AFOs, there are no standards or guidelines for AFO measurement. Current measurement methods in the literature vary in their reliability and efficacy. Additionally, the common representation of stiffness as a linear fit is not sufficient and does not capture AFO hysteretic effects.

(c) AFO Viscoelasticity
Current representations of AFO torque-angle dynamics are simplified by applying a linear fit whose slope represents the stiffness. This linear approximation ignores the likely presence of a damping parameter in a more complete model of AFO dynamics. However, the effect of angular velocity or flexion speed on AFO properties has not been adequately investigated. To study AFO behavior and its influence on the user, we need accurate models that capture all its key properties. Viscoelasticity should

not be ignored without studying the significance of its effects on key parameters of common linear representations of AFO behavior.

(d) Biomechanical Differences between Emulated and Physical Devices
While active devices used for stiffness emulation have been validated in terms of their ability to mimic reference torque-angle profiles of specific physical devices, they may differ in other ways from the physical devices (e.g. weight distribution or compliance in other degrees of freedom). Current studies have not investigated how user movement differs when walking in these tethered emulators from walking in the untethered physical devices they are emulating.

1.4 Dissertation Overview and Contributions

The objective of this work was to improve our understanding of AFO stiffness and its influence on the user. I accomplished this by addressing key gaps in the literature (Sec. 1.3) through the following specific aims, each of which are detailed in the following chapters.

Aim 1. Understand the impact of AFO stiffness on gait

This aim addresses key literature gap (a) (Sec. 1.3) through a systematic literature review on the influence of AFO stiffness on gait biomechanics, contained in Chapter 2. Accomplishing this aim shaped my AFO stiffness measurement and reporting techniques (Aims 2 and 3), and informed my focus on key kinematic lower-limb metrics affected by stiffness (for Aim 4).

Aim 2. Develop a system for reliable AFO stiffness measurement

In this aim, I designed and built an automated stiffness measurement apparatus (SMApp) to cyclically deflect AFOs non-destructively about the ankle joint, and collect reliable measurements of dynamic AFO torque (gap (b) in Sec. 1.3). Representations of stiffness, neutral angles and energy dissipation were then calculated from the experimental torque-angle data to fully characterize the non-linear, hysteretic shape of the AFO stiffness curve. A stiffness representation that balances model complexity and accuracy is necessary for comparing AFO designs and findings. The design and evaluation of the SMApp as well as calculations of the AFO properties are detailed in Chapter 3.

Aim 3. Evaluate the effect of rotational speed on AFO properties

In this aim, the SMApp built in Aim 2 was used to investigate AFO viscoelasticity (gap (c) in Sec. 1.3). A study of traditional and additively-manufactured AFOs was conducted to determine whether ankle rotational speed had an effect on the properties calculated from

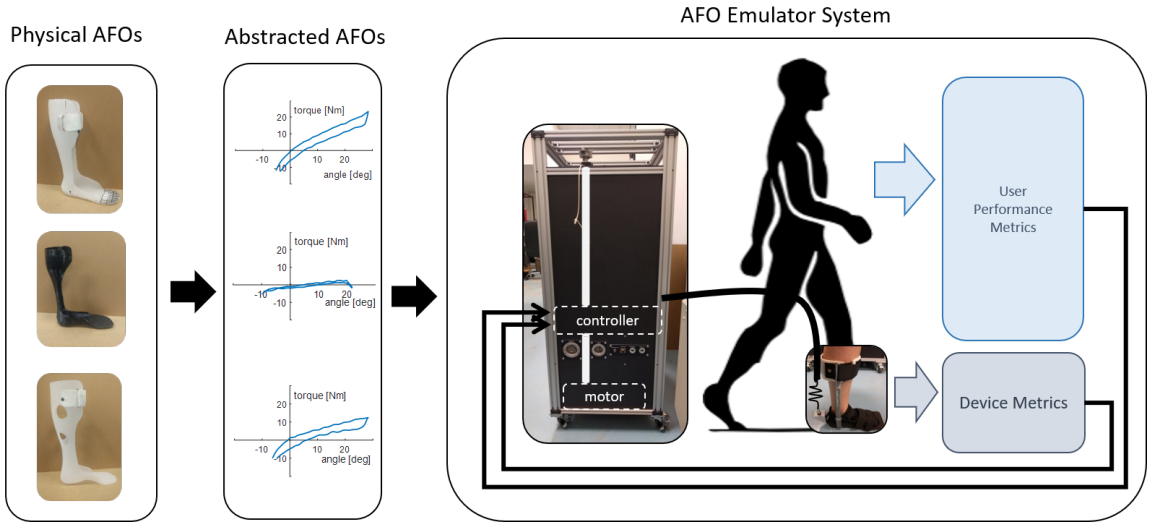

Figure 1.3: The AFO emulator system concept. A particular AFO is manually selected for emulation, then abstracted to its torque-angle representation. An instrumented exoskeleton measures device and human performance parameters, which are sent to a controller. The controller modifies the stretch of a spring on the exoskeleton to mimic the torque-angle trajectory of the AFO.

their torque-angle curves (Chapter 4). Without sufficient existing literature on speed effects, I needed to accomplish this aim to understand whether representations of the AFO torque-angle relationship (from Aim 2) needed for emulation (Aim 4) should be evaluated at specific testing velocities.

Aim 4. Quantify the kinematic differences between emulated and physical AFOs

To accomplish this aim, I built an active lower-limb exoskeleton outfitted with a sensing suite and tethered to an off-board motor and controller (Chapter 5). Using AFO torque-angle measurements (made possible by Aims 2 and 3), this 'AFO emulator' system was able to haptically emulate a physical AFO by tracking its torque-angle curve during gait (Figure 1.3). To understand the potential use of this emulator as a test bed for studying the effect of key AFO design parameters on user performance, I validated its ability to mimic passive AFO devices from a kinematics standpoint. I conducted a pilot study in which a healthy subject walked on a treadmill with physical and emulated versions of the same AFO. By comparing ankle kinematics between the two conditions, I could quantify effects arising from AFO emulation (literature gap (d) in Sec. 1.3).

Through these four aims, this work contributed to a better understanding of the influence of AFO stiffness (a key design parameter) on walking mechanics, through examining the current state of literature evidence, building a device to measure stiffness more effectively, finding the small, but significant influence of speed on torque-angle dynamics, and

exploring whether stiffness could be effectively emulated for laboratory studies of AFO design effects on user movement. These contributions form a framework for investigating AFO properties and their effects on the user. They enable future studies of user-specific assistive device design innovations and bring us closer to improving measurable patient outcomes through effective, optimized devices.

CHAPTER 2

The Impact of Ankle-Foot Orthosis Stiffness on Gait: A Systematic Literature Review[1]

Summary

Background: Ankle-foot orthoses (AFOs) are commonly prescribed to provide ankle support during walking. Current prescription standards provide general guidelines for choosing between AFO types, but are limited in terms of guiding specific design parameter choices. These design parameters affect the ankle stiffness of the AFO. **Research Question:** The aim of this review was to investigate the impact of AFO stiffness on walking mechanics. **Methods:** A literature search was conducted using three databases: Pubmed, Engineering Village, and Web of Science. **Results:** After applying the exclusion criteria, 25 of 287 potential articles were included. The included papers tested a range of stiffnesses (0.02 to 8.17 Nm/deg), a variety of populations (e.g. healthy, post-stroke, cerebral palsy) and various gait outcome measures. Ankle kinematics were the most frequently reported measures and the most consistently affected by stiffness variations. Greater stiffnesses generally resulted in reduced peak ankle plantarflexion, dorsiflexion, and total range of motion, as well as increased dorsiflexion at initial contact. At the knee, a few studies reported increased flexion at initial contact, and decreased peak extension and increased peak flexion during stance when stiffness was increased. Stiffness did not affect hip kinetics and there was low evidence for its effects on hip or pelvis kinematics, ankle and knee kinetics, muscle activity, metabolic cost, ground reaction forces and spatiotemporal parameters. There were no generalizable trends for the impact of stiffness on user preference. **Significance:** AFO stiffness is a key factor influencing ankle movement. Clear reporting standards for AFO design parameters, as well as additional high quality research is needed with larger sample

[1] A version of this chapter was published as [70]: Totah, D., Menon, M., Jones-hershinow, C., Barton, K., & Gates, D. H. (2019). The Impact of Ankle-Foot Orthosis Stiffness on Gait: A Systematic Literature Review. Gait and Posture, 69(January), 101–111. https://doi.org/S0966636218303084

sizes and different clinical populations to ascertain the true effect of stiffness on gait.

2.1 Introduction

Ankle-foot orthoses (AFOs) are braces used to provide support about the ankle joint. Gait abnormalities commonly treated with AFOs include plantarflexor [71] or dosriflexor [72] weakness, motor control deficits [73], spasticity [74], instability, and/or balance problems [75]. Three main categories of passive AFOs are available to address these deficits: non-articulated (also called solid-ankle or rigid); hinged or articulated; and posterior leaf spring (PLS) AFOs [76]. Recent guidelines for AFO prescription (e.g. [16, 28, 77]) provide recommendations for choosing between these categories. However, within each category of AFO, clinicians have to make numerous additional design decisions, e.g. drawing trimlines and material selection. These choices are likely to affect a patient's gait performance while wearing the device. Unfortunately, current clinical standards for choosing AFO design parameters are limited, likely because the impacts of design choice on patient outcomes are unclear.

One key AFO characteristic that can be affected by design decisions is the stiffness at the ankle. Here, AFO stiffness is defined as resistance to sagittal plane rotation, described by the slope of the ankle torque vs ankle angle curve of an AFO. AFO stiffness is affected by trimline location and shape, as well as material type and thickness used for fabrication [23, 24]. Clinical guidelines may suggest utilizing AFOs with higher rigidity for more severe patient deficits, for example, but do not provide specific, quantitative standards beyond this. Thus clinicians must rely on qualitative patient assessments and their own expertise to make these design choices.

An AFO's stiffness affects the level of support the AFO can provide, as well as its energy storage and return capacity, which would be expected to influence the gait performance of the user. More compliant devices may offer less support but greater energy return in comparison to their rigid counterparts. Rigid AFOs are often used to promote medial-lateral stability [78]. The increase in stability could manifest itself in increased preferred walking speeds [79] or lowered energetic cost [13]. In contrast, rigid AFOs can also help with spasticity. Muscle spasticity often results in stiff or tight muscles, which limit joint ranges of motion and cause hyper- or hypo-extension of the ankle or knee [74]. AFOs fabricated with a dorsiflexed neutral angle, for example, can prevent excessive plantarflexion of the ankle and bring its angle trajectory closer to normal gait. On the other hand, compliant PLS and hinged AFOs outfitted with spring-loaded or elastic joints can provide propulsion assistance. Depending on the location of the elastic components, energy is

stored in the AFO during dorsiflexion or plantarflexion and released to aid individuals with plantarflexor [71] or dorsiflexor [72] weakness, respectively.

Several literature reviews have found positive effects of AFO-use in general on performance in various patient populations, including individuals with cerebral palsy [80], spinal-cord injury [81], multiple sclerosis [9] and those post-stroke [28, 82]. However, none have explored the impact of AFO stiffness specifically, and many do not report it. In fact, a recent review by Eddison et al. [83] found that only 3.6% of research papers reporting AFO-use for children with cerebral palsy included AFO stiffness information. One recent review investigated the impact of a specific AFO, the Intrepid Dynamic Exoskeletal Orthosis (IDEO), on gait in individuals with lower-limb salvage [84]. The review included a brief discussion of the impact of AFO stiffness stating it significantly affected joint kinematics as a whole but had varying statistical effect sizes. The specific parameters affected were not specified. The authors also found moderate-level evidence to support the claim that “stiffness should be considered with respect to patient preference." Apart from [84], which included only one type of AFO (the IDEO) and three stiffness values (described only qualitatively as “nominal, compliant and stiff"), there are no published systematic reviews investigating the effect of AFO stiffness on gait.

The purpose of this literature review was to determine whether AFO stiffness at the ankle has a significant impact on walking mechanics. The review focused on key outcome measures related to walking performance including lower limb kinematics and kinetics, muscle activity and gait metabolic cost. Our secondary aim was to determine the specific stiffness ranges over which these parameters changed.

2.2 Methods

We used the Preferred Reporting Items for Systematic Reviews and Meta-Analyses (PRISMA) Guidelines as a methodological template for this review [1].

2.2.1 Search Strategy

We conducted database searches in February 2018 using Pubmed (1781-2018), Engineering Village (Compendex & Inspec) (1666-2018), and Web of Science (1900-2018) with the following search terms:

(ankle-foot orthosis OR AFO OR ankle foot orthosis) AND (stiffness OR resistance OR compliance OR rigidity OR flexibility OR energy storage OR energy return) AND (gait OR walking OR outcomes OR performance)

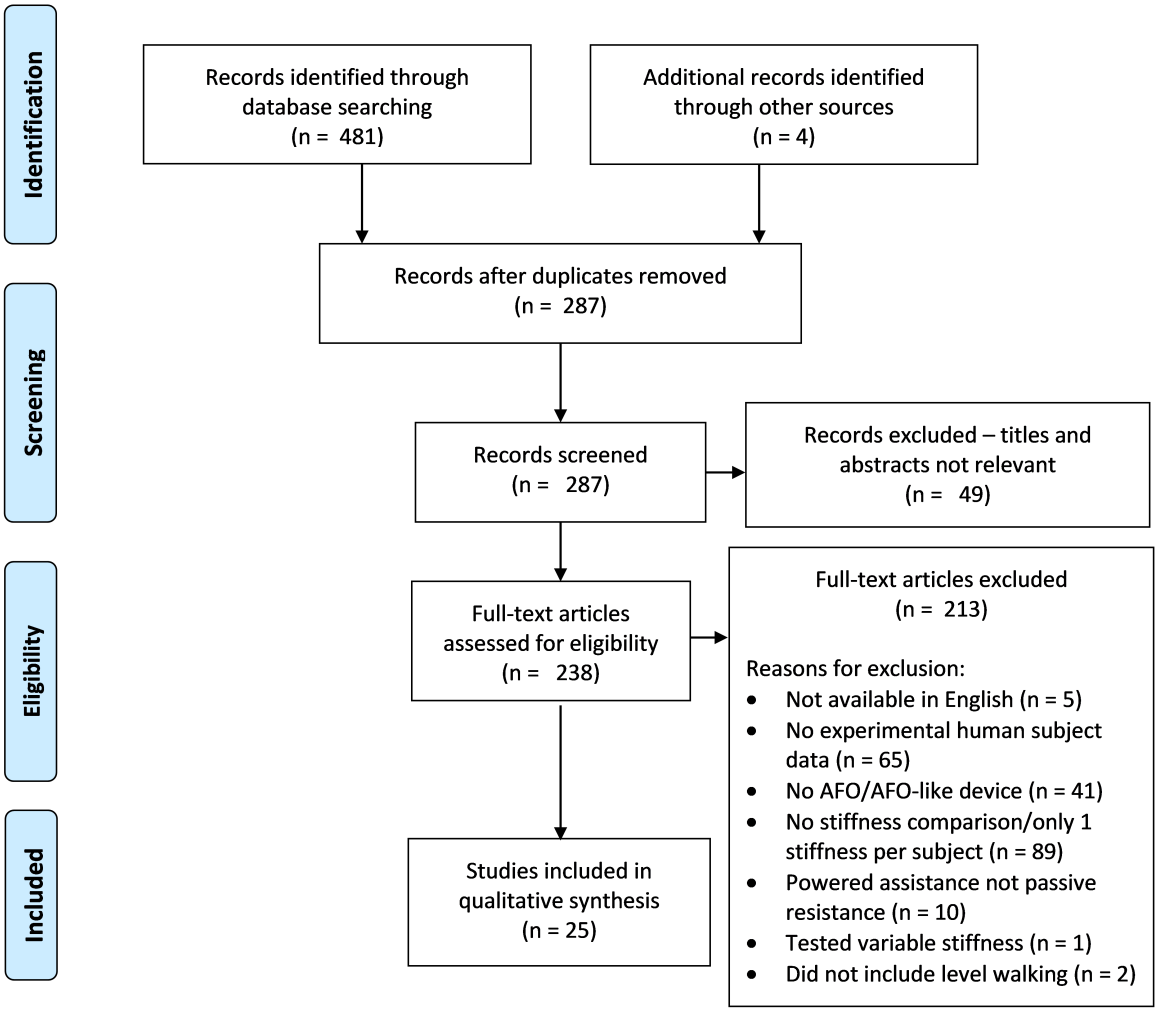

Figure 2.1: PRISMA flow diagram of article search and selection process [1].

In the Pubmed database, the species was restricted to 'human only'. Database search strategies are detailed in Appendix A.

The search process is summarized in the flow diagram in Figure 2.1. A single reviewer verified and removed duplicate works. Then, three reviewers independently selected potentially relevant articles from titles and abstracts. Finally, the full text articles were screened against the following exclusion criteria:

- No experimental subject data was presented.
- The study did not include an AFO/AFO-like device.
- No comparisons were drawn across stiffness conditions or only one stiffness was

tested for each subject.

- The intervention applied powered assistance and not passive resistance at the ankle.
- AFO stiffness varied (was not constant) within a single stiffness condition.
- The study did not test walking on level ground.

Each article was screened by two reviewers and final reasons for exclusion were agreed upon through consensus. When an article could be excluded using several criteria, a single reason for exclusion was chosen with priority given in the order listed. In addition to querying the databases, reference lists of included articles, and included and excluded review papers were reviewed for potential additional articles.

2.2.2 Assessment of Study Quality

The quality of each of the included articles was rated by three authors, using a modified PEDro scale [85] consisting of a 10-item checklist (Appendix Table B.1). Articles were given one point for each criterion met (10 possible points). The scale was adapted by excluding the therapist and assessor blinding criteria since blinding is not possible considering the nature of the AFO interventions [82]. Cross-over studies met the 'blind allocation' (3^{rd}) criterion if participants were allocated to receive all conditions since assessor bias has no influence on group allocation if all participants received all interventions [82]. Additionally, studies that tested for stiffness effects between all AFO stiffness conditions met the 'between-group statistics' (8^{th}) criterion, while papers that only compared with the baseline condition did not. The final (10^{th}) criterion, adapted from a modified STROBE scale [86], was added to evaluate whether studies reported the test-retest reliability and/or accuracy of the devices and/or analyses used to measure AFO stiffness. Studies that utilized a pre-validated measurement method such as a three point bend test also met this criterion, while articles that did not report any quantitative stiffness measurements did not. When the three raters' scores disagreed, a final score was reached by consensus.

Table 2.1: A summary of the participants and interventions included in the reviewed articles.

Paper	QS (0-10)	Participant Details	Description of AFO Stiffness Intervention
Amerinatanzi, 2016 [87]	5	1 healthy adult, age n/a	Unilateral articulated AFO that resisted ankle rotation (direction not specified) using one of two springs: a stainless steel spring and a superelastic Nickel Titanium spring
Amerinatanzi, 2017 [88]	4	2 healthy adults (all male), 30-31 yrs	Unilateral articulated AFO that resisted ankle rotation (direction not specified) using one of two springs: a stainless steel spring and a superelastic Nickel Titanium spring
Arch, 2015 [4]	7	2 healthy adults (1 female), 24-25 yrs	Unilateral passive dynamic AFO that resisted both DF and PF at three stiffnesses that spanned about 35 - 80% of each subject's natual ankle pseudo-stiffness
Arch, 2016 [89]	6	2 healthy adults (1 female), 24-25 yrs	Unilateral passive dynamic AFO that resisted both DF and PF at two stiffnesses tuned to match about 40% and 80% of each subject's natural ankle pseudo-stiffness
Bolus, 2017 [90]	7	1 healthy adult (male), 23 yrs	Unilateral articulated, instrumented AFO (iAFO) that resisted PF using four different linear springs
Brunner, 1998 [91]	5	14 children with spastic hemiplegia (8 female), 6.5-20.1 yrs	Unilateral rigid and spring-type AFOs that resisted DF and blocked any PF
Choi, 2017 [3]	8	8 healthy adults (2 female), 25.3 (4.5) yrs	Unilateral articulated AFO that resisted DF using four different elastic bands
Collins, 2015 [51]	7	9 healthy adults (2 female), 23 (3.7) yrs	Bilateral exoskeleton that resisted DF using five different linear steel springs with a clutch
Guillebastre, 2009 [92]	7	11 healthy adults (5 female), 19-37 yrs	Unilateral rigid AFO that resisted both DF and PF and a dynamic AFO with an adjustable elastic band that only resisted PF at two stiffness conditions: 30% and 70% of maximal strain
Harper, 2014 [93]	7	13 adults with unilateral lower extremity injuries (all male), 21-40 yrs	Unilateral IDEO with three interchangeable, posteriorly mounted struts that resisted both DF and PF at each patient's prescribed stiffness and $\pm$20% of prescribed
Kerkum, 2015 [94]	9	15 children with cerebral palsy (4 female), 6-14 yrs	Bilateral (n=14)/unilateral (n=1) spring-hinged ventral-shell AFO that resisted both DF and PF using different springs at three stiffness conditions (two of which had the same PF resistance but different DF resistances)
Kobayashi, 2011 [95]	6	10 adults post-stroke (all male), 46-62 yrs	Unilateral articulated AFO that resisted DF and PF independently using four oil-damper stiffness conditions[a]
Kobayashi, 2013 [2]	6	5 adults post-stroke (all male), 42-64 yrs	Unilateral articulated AFO that resisted PF using four oil-damper stiffness conditions

Kobayashi, 2015 [33]	6	10 adults post-stroke (2 female), 45-67 yrs[b]	Unilateral articulated AFO that resisted PF using three interchangeable steel springs and a baseline stiffness (close to zero) without springs
Kobayashi, 2016 [34]	6	6 adults post-stroke (all male), 38-64 yrs	Unilateral articulated AFO that resisted PF using three interchangeable steel springs and a baseline stiffness (close to zero) without springs
Kobayashi, 2017 [73]	6	10 adults post-stroke (2 female), 45-67 yrs[b]	Unilateral articulated AFO that resisted PF using three interchangeable steel springs and a baseline stiffness (close to zero) without springs
Kobayashi, 2017 [96]	5	1 adult post-stroke (female), 50 yrs	Unilateral articulated AFO that resisted DF and PF independently by adjusting the stiffness of a Becker Triple Action joint prototype to test four stiffnesses in each direction
Lehmann, 1983 [97]	5	6 adults with hemiplegia, 47-76 yrs & 4 healthy adults, 55-63 yrs	Unilateral thermoplastic AFOs (Engen and Teufel) at one trim and a unilateral polypropylene AFO (Seattle) at three trims that each resisted both DF and PF
Ramdharry, 2012 [72]	9	14 adults with CMT (5 female), 24-52 yrs	Bilateral footup splint, push brace and multifit achilles drop foot orthosis that each resisted both DF and PF at specific stiffnesses
Russell Esposito, 2014 [98]	8	13 adults with lower limb salvage (all male), 21-36 yrs	Unilateral IDEO with three interchangeable, posteriorly mounted struts that resisted both DF and PF at each patient's prescribed stiffness and $\pm$20% of prescribed
Singer, 2014 [5]	5	5 adults post-stroke (2 female), 62 (9) yrs	Unilateral articulated AFO that resisted PF using two interchangeable compression springs
Sumiya, 1996 [24]	4	1 adult with hemiplegia (male), 55 yrs	Unilateral plastic AFO that resisted both DF and PF at nine stiffness levels achieved by gradually increasing the trimline depth from 20-60% of the lateral malleolus height
Telfer, 2012 [99]	5	1 healthy adult (male), 29 yrs	Unilateral articulated AFO that resisted PF using two posteriorly-attached gas springs with adjustable pressure to test two stiffness conditions
Yamamoto, 1993 [36]	2	15 adults with hemiplegia (4 female), 38-76 yrs	Unilateral articulated AFO that resisted PF using multiple combinations of four linear springs
Yamamoto, 1997 [45]	2	33 adults with hemiplegia, age n/a	Unilateral articulated AFO that resisted PF using different linear spring combinations to test four stiffness conditions

Acronyms: quality score (QS), dorsiflexion (DF), plantarflexion (PF), Charcot-Marie-Tooth disease (CMT), Intrepid Dynamic Exoskeletal Orthosis (IDEO). [a] During the PF resistance intervention, there was no DF resistance but during the DF resistance intervention, one of the PF resistance conditions were also selected and remained constant while DF resistance varied. [b] Studies [73] and [33] had the same test subjects.

2.3 Results

The database search yielded 287 non-duplicate scholarly articles and four additional articles were identified from other sources. After applying the exclusion criteria, this number decreased to 25 papers (Figure 2.1). A majority of the studies received low to moderate methodological quality scores, below 8/10 (see Appendix Table B.2 for detailed scores). Only one study ensured subjects were blinded to the test conditions, only three specified sufficient participant eligibility criteria, 11 papers did not perform between-group statistical analyses, and 10 papers did not report the test re-test reliability of stiffness measurements. Eight of the 25 studies included only one to two participants and four studies had five to six participants.

The included papers tested a range of different populations including healthy adults (10 papers), adults with hemiplegia (11 papers), adults with severe lower limb trauma (including salvage) (2 papers), children with spastic hemiplegia (2 papers), and adults with Charcot-Marie-Tooth (CMT) disease (1 paper) (Table 2.1). They also included a variety of ankle foot orthosis designs including: passive dynamic AFOs [4, 24, 79, 89, 91, 92], the Intrepid Dynamic Exoskeletal Orthosis (IDEO) with interchangeable posterior struts [84, 93, 98], off-the-shelf commercial braces [72], articulated AFOs with elastic bands [3, 92], springs [94] or superelastic alloys [87, 88], and custom hinged, experimental AFOs or exoskeletons made from metal or carbon fiber frames with steel springs [5, 33, 34, 36, 45, 51, 73, 90], gas springs [99], oil-dampers [2, 95], or modifiable Becker joints [96]. AFO stiffness was varied to test resistance to dorsiflexion (DF) only [3, 51, 91], plantarflexion (PF) only [2, 5, 33, 34, 36, 45, 73, 90, 92, 99], DF and PF independently [95, 96], or both DF and PF concurrently [4, 24, 72, 89, 92–94, 97, 98]. Two studies did not specify the direction of resistance [87, 88]. All 25 analyzed papers used a crossover study design. In a majority, all subjects wore all AFO stiffness conditions while a variety of outcome measures were assessed (Table 2.2).

2.3.1 Quantifying AFO Stiffness

The included studies differed in how they measured and reported AFO stiffness (Table 2.3). Stiffness was reported qualitatively in four [91, 92, 97, 99] of 25 papers, estimated from finite element analyses in two papers [87, 88], and quantified experimentally in 19 papers. Of the 19 that quantified stiffness experimentally, three used functional stiffness testing methods, where measurements are taken while the subject wears the AFO [31]. Another 13 assessed stiffness on the bench top. In this method, a mechanical testing machine records the load or torque as it performs a three-point bend test on the AFO's posterior strut

[93] or flexes the AFO about the ankle in a custom fixture [73], respectively. Three studies did not specify the type of measurement method [5, 36, 45]. For each of these functional or bench top approaches, stiffness could be measured statically at one or more ankle flexion/extension positions or dynamically through the entire gait cycle or a specified range of motion.

Table 2.2: The outcome measures collected in the reviewed studies. Further details are available in the supplementary material.

Paper	Joint Kinematics			Joint Kinetics			EMG	Walking Speed	Other Metrics
	Ankle	Knee	Hip	Ankle	Knee	Hip			
Amerinatanzi, 2016 [87]	✓			✓					
Amerinatanzi, 2017 [88]	✓			✓					GRF
Arch, 2015 [4]	✓			✓					Spatiotemporal
Arch, 2016 [89]				✓			✓		
Bolus, 2017 [90]	✓			✓					Center of pressure
Brunner, 1998 [91]	✓	✓	✓					✓	Spatiotemporal, GRF, arm swing
Choi, 2017 [3]	✓	✓	✓				✓		Muscle length
Collins, 2015 [51]	✓	✓	✓	✓	✓	✓	✓		Spatiotemporal, metabolics, COM power
Guillebastre, 2009 [92]								✓	Spatiotemporal, midline length
Harper, 2014 [93]	✓	✓	✓	✓	✓	✓	✓	✓	GRF
Kerkum, 2015 [94]	✓	✓	✓	✓	✓	✓		✓	Center of pressure, metabolics
Kobayashi, 2011 [95]	✓							✓	
Kobayashi, 2013 [2]	✓	✓						✓	
Kobayashi, 2015 [33]	✓	✓		✓	✓				
Kobayashi, 2016 [34]	✓	✓		✓	✓				
Kobayashi, 2017 [73]	✓	✓		✓					
Kobayashi, 2017 [96]	✓	✓		✓	✓				
Lehmann, 1983 [97]	✓								
Ramdharry, 2012 [72]	✓	✓	✓	✓		✓			
Russell Esposito, 2014 [98]	✓	✓	✓	✓	✓	✓		✓	Spatiotemporal, GRF, preference
Singer, 2014 [5]	✓	✓		✓	✓				
Sumiya, 1996 [24]	✓†								
Telfer, 2012 [99]	✓	✓		✓	✓				
Yamamoto, 1993 [36]	✓	✓		✓					Spatiotemporal, preference
Yamamoto, 1997 [45]									Preference

Acronyms: double support (DS), single support (SS), center of mass (COM), ground reaction force (GRF). †Only qualitative descriptions of ankle kinematics during gait are reported without quantitative measures.

Table 2.3: Measurement method and value of AFO stiffnesses in the reviewed studies.

Paper	Method/Sensor	AFO Stiffnesses
Amerinatanzi, 2016 [87]	FES	Resistance to PF: 0.09, 0.24 Nm/deg/kg ([a])
Amerinatanzi, 2017 [88]	FES, Bench/weights ([b])	n/a ([c])
Arch, 2015 [4]	Functional/forceplate	Resistance to DF: 1.90, 2.94, 3.51, 3.90, 5.77, 8.17 Nm/deg
Arch, 2016 [89]	Functional/forceplate	Resistance to DF: 1.90, 3.51, 3.90, 8.17 Nm/deg
Bolus, 2017 [90]	Bench/strain gauge	Resistance to DF or PF: 0.06, 0.15, 0.30, 0.35 Nm/deg ([a,f])
Brunner, 1998 [91]	n/a	Gas spring pressure: 8-10 kPa (Spring-type), n/a (Rigid)
Choi, 2017 [3]	Bench/UTM ([g])	Resistance to DF: 0.25, 1.0, 2.0, 3.7 Nm/deg
Collins, 2015 [51]	Bench/load cell	Resistance to DF: 2.27, 3.14, 4.19, 5.41, 6.98 Nm/deg
Guillebastre, 2009 [92]	n/a	n/a
Harper, 2014 [93]	Bench/UTM	Posterior strut stiffness: 402 - 1216 N/mm
Kerkum, 2015 [94]	Bench/BRUCE	Resistance to DF: 0.7 (0.2), 1.6 (0.4), 3.8 (0.7) Nm/deg; PF: 0.11 (0.13), 0.12 (0.17), 4.6 (1.3) Nm/deg
Kobayashi, 2011 [95]	Bench/torque meter	Resistance to DF and PF: 0.32, 0.41, 0.76, 1.26 Nm/deg
Kobayashi, 2013 [2]	Bench/MuscTM	Resistance to PF: 0.5-1.4 Nm/deg ([a])
Kobayashi, 2015 [33]	Bench/torque sensor	Resistance to PF: 0.02, 0.28, 0.51, 0.58 Nm/deg ([a])
Kobayashi, 2016 [34]	Bench/torque sensor	Resistance to PF: 0.02, 0.28, 0.51, 0.58 Nm/deg ([a])
Kobayashi, 2017 [73]	Bench/torque sensor	Resistance to PF: 0.03, 0.16, 0.37, 0.48 Nm/deg ([a])
Kobayashi, 2017 [96]	Bench/torque sensor	Resistance to DF: 1.41, 2.02, 2.88, 3.99 Nm/deg; PF: 0.36, 0.46, 0.52, 0.89 Nm/deg ([a])
Lehmann, 1983 [97]	n/a	n/a
Ramdharry, 2012 [72]	Functional/isokinetic dynamometer	Resistance to DF: 0.92 (0.09), 1.11 (0.09), 1.17 (0.09) Nm/deg; PF: 0.59 (0.07), 0.87 (0.05), 0.89 (0.04) Nm/deg
Russell Esposito, 2014 [72]	Bench/UTM	Posterior strut stiffness: 392-1236 N/mm
Singer, 2014 [5]	n/a	Resistance to PF: 0.4, 1.3 Nm/deg
Sumiya, 1996 [24]	Bench/load cell	Resistance to PF: 0.40, 0.50, 0.63, 0.94, 1.13, 1.38, 1.73, 2.0, 2.25 Nm/deg; DF: 0.20, 0.23, 0.24, 0.25, 0.38, 0.48 Nm/deg ([a])
Telfer, 2012 [99]	n/a	n/a
Yamamoto, 1993 [36]	(n/a)/load cell	Resistance to PF: 0.09, 0.19, 0.50, 1.0 Nm/deg ([a,h])
Yamamoto, 1997 [45]	(n/a)/load cell	Resistance to PF: 0.5, 0.75, 1.25, 2.0 Nm/deg; DF: 0.5, 0.75, 1.5, 3.0 Nm/deg ([a,f])

Acronyms: dorsiflexion (DF), plantarflexion (PF), finite element simulation (FES), universal testing machine (UTM), Bi-articular Reciprocal Universal Compliance Estimator (BRUCE) [46], muscle training machine (MuscTM). [a]Reviewers estimated stiffness by applying linear regressions to AFO torque and angle measurements. [b]Simulations were validated with experiments by hanging known weights on the AFO. [c]Linear fits were not possible. [f]AFO could be adjusted to independently resist PF/DF, but gait trials had PF resistance only. [g]A UTM measured linear stiffness, then AFO stiffness was calculated based on geometry. [h]Unspecified combinations of two springs were also used.

Of the 21 studies that reported simulation-estimated or experimentally-measured stiffness, 19 reported AFO stiffness and two [93, 98] only reported the linear stiffness of the compliant element at the joint (a posterior strut). Comparing studies that measured stiffness linearly with those measuring rotational stiffness was not possible. Moreover, when

measuring rotational stiffness, some studies deflected the AFO towards plantarflexion or dorsiflexion only, while others tested both directions. Only eight of the 19 rotational stiffness papers directly provided quantitative stiffness values of their test conditions [3–5, 51, 72, 89, 94, 95]. We were able to estimate AFO rotational stiffness in nine additional papers by fitting a line to torque versus angle curves or measurements provided. The included studies spanned a large range of AFO stiffness from 0.02 to 8.17 Nm/deg (Figure 2.2).

Although all articles tested multiple AFO conditions, some study conditions may have had similar stiffness values [97]. This was only statistically compared in four studies. One study compared AFO stiffness measurements and found that one of three tested AFOs was not significantly different from the rest [72]. The other three studies evaluated peak AFO moment [3, 51, 73] and found significant differences across all test conditions.

2.3.2 AFO Stiffness Effects on Joint Kinematics

2.3.2.1 Ankle Kinematics

Ankle kinematics were reported in 22 papers and 11 included statistical comparisons across different stiffnesses (Appendix Table C.1). Three studies reported a significant decrease in ankle range of motion (ROM) with increasing AFO stiffness (Fig 2.3) [91, 94, 95]. Another three articles found decreased ROM but did not perform statistical analyses [87, 88, 90].

In addition to overall range of motion, several studies reported ankle angles at various points in the gait cycle. The ankle angle at initial contact was unaffected by AFO stiffness in one study in children with cerebral palsy [94], while two others found that the foot was more dorsiflexed at higher stiffnesses during initial contact in patients post-stroke [33, 73]. This difference was not significant for all tested stiffnesses. The tendency toward increased dorsiflexion with increased stiffness (Fig 2.3) was also reported as an untested observation in two additional studies of adults post-stroke [36, 96].

Peak PF angle during early stance decreased with increasing stiffness [5, 33, 34, 93, 97, 99]. This trend was significant for all stiffness conditions in one healthy-subject case study [99], and significant for a subset of stiffnesses in four papers [33, 34, 93, 97]. An additional study observed the same trend, but did not perform statistical testing [5].

While peak dorsiflexion (DF), which typically occurs in terminal stance, generally decreased with increasing AFO stiffness (Fig 2.3), the statistical findings were not consistent across studies. Changes in peak DF were significant across all stiffness conditions in three studies [3, 91, 95], significant for a subset of conditions in two studies [93, 97], and not significant in one study [98]. The trend was also observed, but not statistically tested, in three

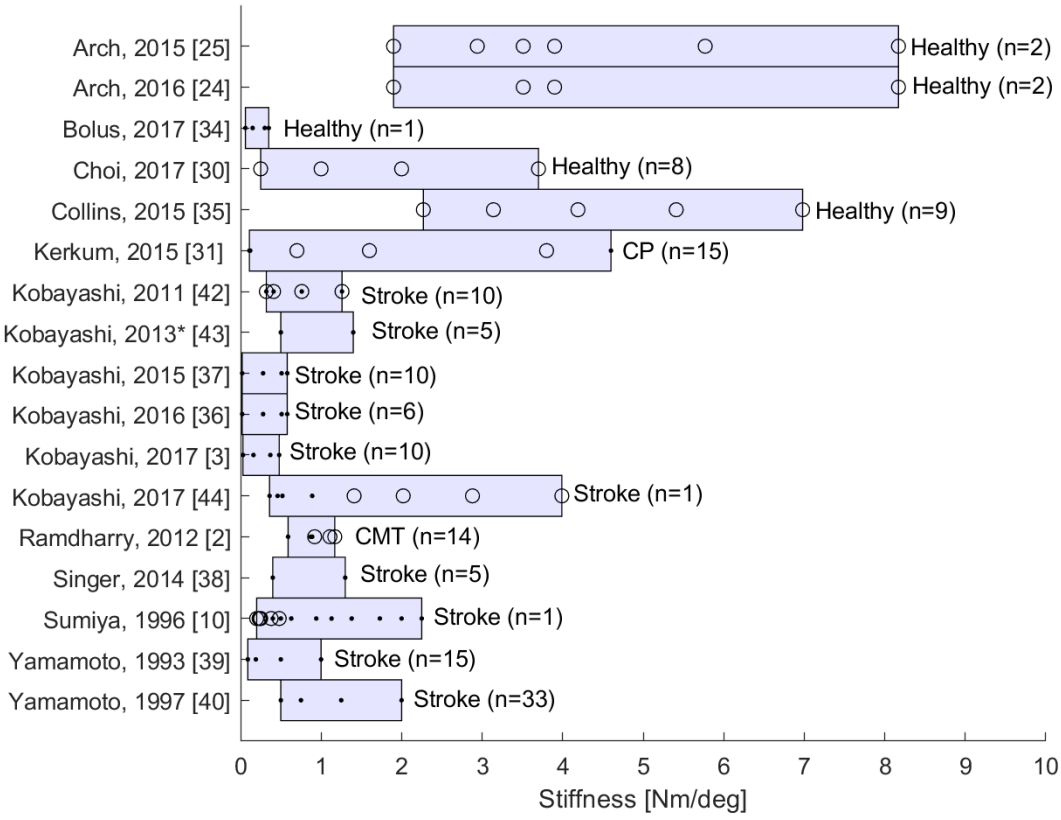

Figure 2.2: The values and ranges of tested stiffness for the studies that reported, or included sufficient information to allow estimation of, stiffness in Nm/degree. The shaded region indicates the stiffness range, the open circles (○) are stiffnesses resisting dorsiflexion, and the dots (●) are stiffness values resisting plantarflexion. The subject population and number of participants are written next to each study's stiffness range. *Study [2] only reported the range of tested stiffnesses.

case studies (n=1-2) [4, 90, 96]. Comparisons of specific stiffnesses could not be made as only four studies reported quantitative AFO stiffness values [3, 90, 95, 96]. Another case study reported a qualitative description of ankle kinematics under various stiffness conditions [24]. The subject had hemiplegia and a limited ankle DF range. As stiffness was gradually decreased, the subject's DF angle during terminal stance increased.

Four studies statistically compared peak plantarflexion (PF) angle, which typically occurs during initial swing, across stiffness conditions. Two studies found that peak PF significantly decreased with increasing stiffness for adults post-stroke [2, 95], while the two others found no effect for adults with unilateral lower limb trauma [93, 98]. An additional study with post-stroke patients also observed a decrease in PF but did not perform statistical testing [36]. A different healthy-subject case study [99] measured PF angle at toe-off and found significant differences across stiffnesses. Additionally, two studies compared ankle angle at foot clearance and found no statistically significant effects [72, 98].

2.3.2.2 Knee Kinematics

Fifteen studies reported knee kinematics and 10 included statistical comparisons between stiffness groups (Supplementary Table C2). One study measured knee range of motion and found no significant effects of stiffness [98]. Others report knee angles at various points of phases in the gait cycle. Increased stiffness resulted in a more flexed knee at initial contact [33, 73]. This effect was significant only for a subset of stiffness conditions including the least and most stiff conditions. There was a significant increase in early stance knee flexion with increasing stiffness in four studies [2, 93, 98, 99], while three others reported no change [91, 94] (Fig 2.3). This effect was significant only for a subset of stiffness comparisons (including least and most stiff) in three of the studies [2, 93, 98], and significant for all stiffnesses in the fourth study of one healthy adult [99]. Two additional studies reported peak flexion in stance without statistical testing, and neither observed notable changes [5, 96]. Peak knee extension during stance generally decreased with increased AFO stiffness (Fig 2.3). This decrease was significant across all stiffnesses [3], significant across some stiffness conditions [33, 34], and significant for only some participants [36] in different studies. Finally, there were no significant effects of stiffness on peak knee flexion during swing [2, 93].

2.3.2.3 Hip and Pelvis Kinematics

Seven studies measured hip kinematics with five including statistical comparisons (Supplementary Table C3). In general, AFO stiffness did not have an effect on sagittal plane hip

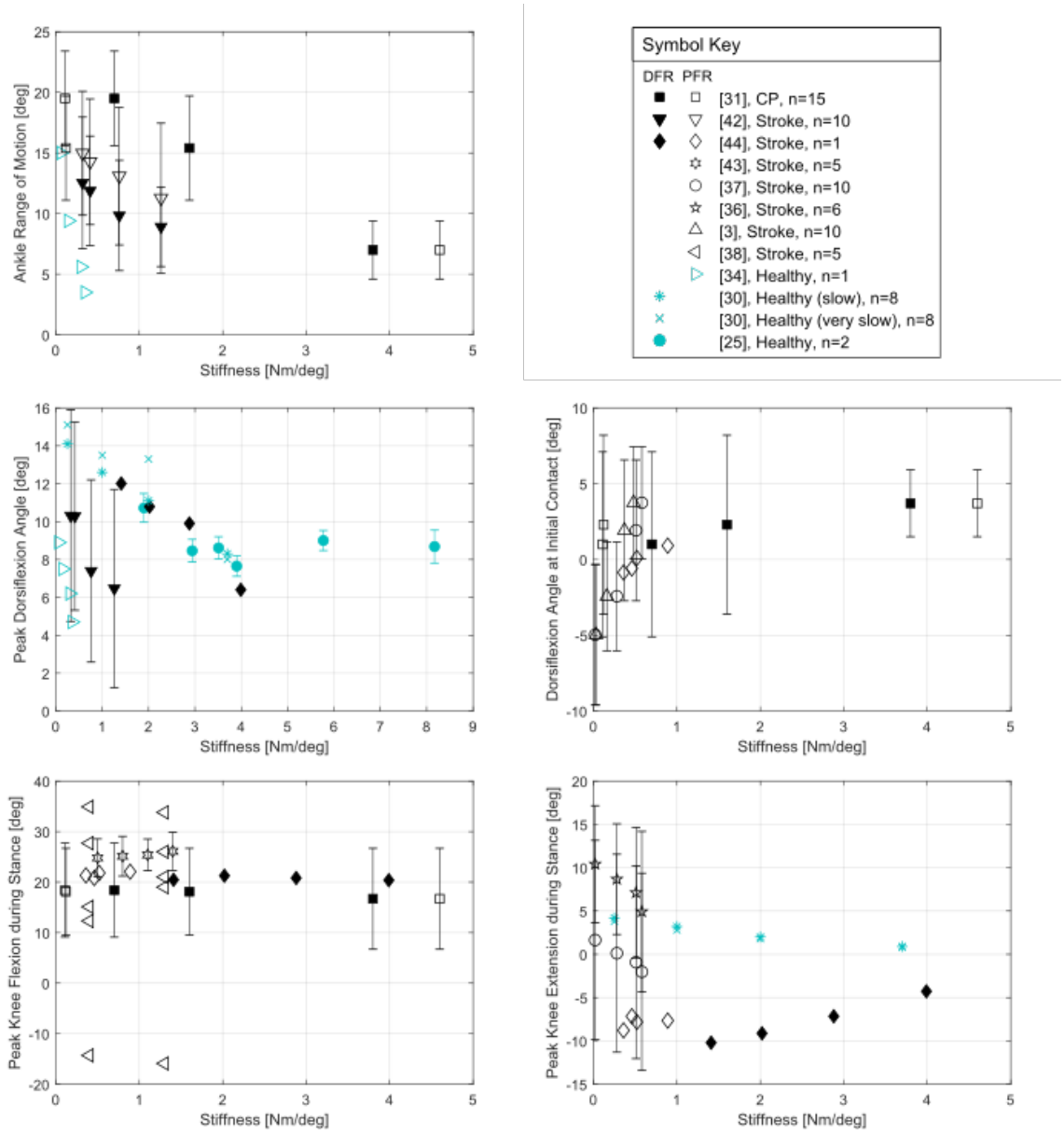

Figure 2.3: Mean values of ankle and knee kinematics measures at the tested AFO stiffness interventions, which resisted dorsiflexion (DFR), plantarflexion (PFR) or both. The error bars represent ± 1 standard deviation from the mean. Median measures are plotted instead of means for study [3] at two different walking speeds (slow and very slow). Each subject's trial-means are plotted instead of across-subject means for studies [4] and [5]. Only the papers that provided stiffness in Nm/deg and corresponding kinematics measures at each stiffness level were included in this figure. The stiffness range provided in [2] was divided into five equally spaced stiffness values for plotting purposes.

kinematics. Measures tested include hip ROM [98], peak hip flexion and extension during stance [98], peak hip flexion during swing [72, 91], and the hip angle during the second double support phase [93] and contralateral initial contact [94].

Only two studies explored transverse and coronal plane hip motion. Brunner et al. found a small ($< 1^{\circ}$), but significant decrease in minimum hip abduction, but no change in external rotation for a rigid AFO compared to a "spring-like" one [91]. Neither study found an effect of stiffness on maximum hip abduction [72, 91]. There was a significant decrease in minimum and maximum pelvic tilt [91], but no changes in pelvic rotation [91], obliquity [91], or elevation during swing [72].

2.3.3 AFO Stiffness Effects on Kinetics

2.3.3.1 Ankle Kinetics

In the 17 studies that reported ankle kinetics (Appendix Table C.4), there were few consistent significant effects of stiffness. Several studies measured peak PF and DF moments during gait. A majority found that stiffness did not affect peak PF moment [51, 93, 94, 98, 99]. However, one study found that while net moment was not affected, peak biological PF moment (without the AFO contribution) significantly decreased with greater stiffness [51]. Peak DF moment during early stance was not significantly affected by stiffness in adults with CMT [72] or those with lower limb trauma [93, 98]. In contrast, three studies [33, 34, 36] of adults post-stroke, found a significant increase in DF moment. Two [33, 34] of the three performed statistical comparisons against only the least stiff (near-zero) baseline condition. The only significant comparison was with the most stiff condition (a difference of one order of magnitude from about 0.02 Nm/deg to 0.58 Nm/deg). Singer et al. [5] also observed an increasing trend in patients post-stroke, but did not test statistical significance.

One study reported mechanical work [93] and a few others reported joint power during gait. Harper et al. [93] found that neither positive nor negative ankle work was significantly affected by stiffness. Two studies reported power absorption during stance. One found a significant decrease in average power absorption during a stride at greater stiffnesses [51], while the other found no differences in peak power absorption [98]. Peak power generation was reported in four studies, three of which performed statistical analyses with mixed results. Peak ankle power generation increased [94], decreased [72], or did not change [98] with greater AFO stiffnesses. Where there were differences, they were not seen across all tested stiffnesses. The fourth paper [96] was a case study, where increasing AFO resistance to DF resulted in reduced peak power generation, but increasing PF resistance

had no effect. Collins et al. reported average power generation, rather than peak. They found that a significant decrease in power generation with greater DF resistance [51] . Finally, one paper found no effect for the timing of peak power generation during push-off [94].

2.3.3.2 Knee Kinetics

Knee kinetics were reported in nine of the reviewed papers (Supplementary Table C5). Knee flexor moment typically has two peaks, one in early stance and another in late stance. Peak flexor moment was not affected by AFO stiffness in early stance [93], while results for terminal stance were mixed. Two studies conducted statistical comparisons across all tested stiffnesses and found no effects [93, 98]. Another two studies [33, 34] made comparisons only with the baseline (near-zero stiffness) condition and found a significant decrease in peak moment with greater stiffness for a subset of stiffnesses. An additional case study [96] found increased peak flexor moment with greater PF resistance, but no changes for increased DF resistance. A final study averaged flexor moment across late stance and found a significant increase with greater stiffness [51]. An additional paper [94] reported knee moment at midstance (33% of the gait cycle) and found no effects. However, the same study [94] also measured knee flexor moment at the timing of peak knee extension angle during single support and found it increased with greater stiffness. The increase was only significant between the least and most stiff conditions.

Five studies measured peak knee extensor moment during stance. Of these, two performed statistical testing: one study found an increase in extensor moment at greater stiffnesses [100], while the other found no difference [93]. The increase was only significant between the most and least stiff strut conditions. Three different studies [5, 96, 99] also reported an increase in peak extensor moment, without statistical testing, only when resistance to plantarflexion (not dorsiflexion) was increased [96]. Another paper [51] calculated the average extensor moment during early stance, and found a significant decrease with greater stiffness.

One study [93] measured mechanical work and two others [51, 98] reported knee power. Harper et al. [93] found that greater stiffness resulted in decreased negative work during first double support. This decrease was not significant for all stiffness conditions. Additionally, there was no effect of stiffness on knee power generation and absorption measured at various portions of the gait cycle [51, 98].

2.3.3.3 Hip Kinetics

Sagittal plane hip kinetics were measured in five studies [51, 72, 93, 94, 98]. There were no significant effects of stiffness on mean or peak hip moments, nor on peak hip power generation or absorption, during early or late stance (Appendix Table C.6).

2.3.3.4 Ground Reaction Force and Center of Pressure

Four studies measured ground reaction forces (GRFs) [88, 91, 93, 98] and all except one study [88] performed statistical analyses (Appendix Table C.7). The majority of papers reported no significant effects of stiffness on vertical GRF at initial contact [91, 93], minimum vertical GRF during stance [91], peak vertical GRF during early [91, 93, 98] and late stance [93, 98], and peak propulsive and braking GRF [91, 93, 98]. However, Brunner et al. [91] found a significant reduction only in the 2nd peak of vertical GRF with a stiffer AFO in children with spastic hemiplegia. This study had a lower quality score (5/10) than the other two studies (scoring 7/10 & 8/10) that found no significant effects in the 2nd vertical peak in adults with lower limb trauma [93, 98]. Additionally, the same two studies evaluated peak medial-lateral GRF and only one [93] found a significant increase, but only between the compliant and stiff strut conditions (40% difference). That study also observed the same trend for the sound (non-AFO) limb peak medial-lateral GRF [93].

Two studies measured the foot's center of pressure (CoP) during gait (see Supplementary Table C10 for details). Kerkum et al. [94] found that neither the excursion of CoP position during a step nor the CoP position at midstance was affected by AFO stiffness. Bolus et al. [90] noted a decrease in anterior displacement of the CoP as stiffness increased. No statistics were performed in that study.

2.3.4 AFO Stiffness Effects on Spatiotemporal Gait Parameters

Ten studies measured spatiotemporal parameters (Appendix Table C.8) and found minimal or mixed effects of AFO stiffness. Self-selected walking speed was not affected [2, 93–95, 98] or decreased [91, 92] with increased stiffness. The trend was not significant for all stiffness conditions [92]. AFO stiffness did not consistently affect step time [92] or stride time [36, 98]. A majority of studies also found no effects on step length [4, 92] or stride length [51, 98]. In contrast, [91] found step and stride length decreased when AFO stiffness increased. This effect was small (about 0.02 - 0.04 m decrease), however. There was no effect of AFO stiffness on stride width [98] or step width [51].

A few studies measured the time spent in various phases of the gait cycle. Two studies measured double support time: one found no changes [91], and the other performed

within-subject comparisons and had mixed results [36]. Two studies reported single support time: one found a significant increase with greater stiffness [91] and the other had mixed results [36]. Another study found no significant effects for the percentage of gait spent in stance phase [92]. A healthy-subject case study (n=2) also found that stance time remained generally consistent across stiffness conditions [4].

2.3.5 AFO Stiffness Effects on Muscle Activity and Length

Muscle activity was only measured in four of the reviewed studies, one of which [89] did not perform statistical testing (Supplementary Table C9). The mostly commonly measured muscles were the gastrocnemius, soleus and tibialis anterior.

There is low evidence that ankle plantarflexor electromyography (EMG) is affected by AFO stiffness. One study found no effects for peak medial gastrocnemius (MG) activity during stance [3]. Another study found that the average integrated MG signal during late single-leg support decreased with increased stiffness [93]. The decrease was not significant for all stiffnesses. A third study found a significant increase for the combined medial and lateral gastrocnemius activity integrated over the whole stride [51]. The increase was not significant when the signal was integrated over the early stance to midstance region only. In addition to gastrocnemius muscle activity, one study reported muscle and tendon length and length velocity (Supplementary Table C10). Choi et al. [3] measured normalized lengths of the gastrocnemius musculotendon unit (MTU), achilles tendon (AT) and MG muscle, as well as muscle velocity (change in length per second) of the MG during the gait cycle in healthy adults. Increasing AFO stiffness caused statistically significant decreases in peak MTU and AT length during mid- to terminal-stance, and increases in AT length at heel contact and in peak MG length. However, the effect was small (0.4% - 2.9% change). Normalized peak MG eccentric velocity was not affected. The time-integrated electromyographic signal (iEMG) of the soleus was not affected by stiffness in one study [93] and significantly decreased with stiffness in another [51].

Two studies compared ankle dorsiflexor activity. Collins et al. [51] found that tibialis anterior iEMG increased with increased AFO stiffness while Harper et al. [93] found no changes. Additionally, Harper et al. [93] found no significant stiffness effects on the gluteus medius, rectus femoris, biceps femoris long head, and vastus medialis iEMG signals during various regions of the gait cycle.

2.3.6 AFO Stiffness Effects on Metabolic Cost

Only two papers measured the effects of stiffness on metabolic cost [51, 94]. Collins et al. [51] found a significant decrease and then increase in net metabolic cost as stiffness increased in healthy adults, with a minimum cost for moderate stiffness (3.14 Nm/deg). In contrast, Kerkum et al. [94] found no significant effects of AFO stiffness on metabolic cost in children with cerebral palsy. Collins et al. [51] increase dorsiflexion resistance from 2.27 to 6.98 Nm/deg, while Kerkum et al. varied resistance in both directions from 0.7 to 4.6 Nm/deg.

2.3.7 User Preference

Three studies surveyed subject preference for particular stiffness conditions [36, 45, 98]. Results varied and there were no generalizable preferences among the different stiffness values tested (Appendix Table C.11). Moreover, one study [36], evaluating adults with hemiplegia, found no consistent correlations between a subject's preferred stiffness and the stiffness at which they had optimal gait performance measures, including peak knee extenion/flexion, peak dorsiflexion/plantarflexion moments, single support phase and second double support phase length.

2.3.8 Other Collected Metrics

Several studies reported outcomes we did not specifically include in our aims. These included: foot midline length [92], functional ankle joint stiffness [88], and arm swinging motion quality [91]. There were no significant effects for any of these measures. More details can be found in Appendix Tables C.10 and C.11.

2.4 Discussion

We investigated the impact of the stiffness of ankle-foot orthoses (AFOs) on gait outcomes. The literature suggests that altering AFO stiffness mainly impacted kinematics directly at the ankle and, more proximally, at the knee. As the stiffness of the AFO increases, the user must generate a larger torque to deflect the AFO at the ankle. Thus, increased stiffness led to lower peak dorsiflexion and plantarflexion and consequently, decreased ankle range of motion. Stiff AFOs with increased plantarflexion resistance kept the foot in a more dorsiflexed position throughout gait, with some higher stiffnesses preventing *any* plantarflexion. Reduced plantarflexion counters the effects of functional drop foot, commonly found in

people recovering from stroke [2, 95] or those with spastic cerebral palsy [91]. It also promotes an initial contact with the heel rather than forefoot. Altered ankle mechanics resulted in compensations at the knee. There is moderate evidence that greater AFO stiffness results in increased in knee flexion during stance. This effect was seen in both healthy unimpaired populations [3, 99] and people with lower limb injuries [93, 98] or those recovering from stroke [2]. As described in [2], an AFO that is too stiff can cause abrupt forward rotation of the tibia at initial contact causing the knee to be pushed forward, thereby increasing knee flexion at early stance and inducing gait instability. The addition of dorsiflexion resistance in conjunction with the plantarflexion stiffness, like in [94], prevents the tibia from collapsing over the foot and reduces the knee flexion effect.

AFO stiffness did not affect hip kinetics and there was low evidence for its effects on hip or pelvis kinematics, ankle or knee kinetics, muscle activity, metabolic cost, ground reaction forces or spatiotemporal parameters. Given the small number of available studies, we could not find sufficiently high evidence to support either the lack or presence of stiffness effects on these secondary outcome measures. It should be noted that the level and type of impairment may influence these findings. In particular, proximal muscle contractures may affect the extent to which proximal biomechanics can be normalized. As many of these studies included only healthy participants, these findings may not be applicable to individuals with impairments.

Self-selected walking speed (SWS) is a common clinical measure and is often used to gauge gait performance during patient evaluation and AFO fitting. There is low evidence that AFO stiffness affects walking speed. Walking speed was only significantly affected by stiffness in two of seven studies that measured it [91, 92]. These studies found that people with cerebral palsy [91] and healthy adults [92] walked slower as AFO stiffness increased. Comparison of these two studies with the others is difficult as neither measured the actual stiffness of the AFOs they tested. However, SWS did improve (increase) with an AFO compared to barefoot walking [91].

In a recent review, Highsmith et al. suggested that stiffness should be considered with regard to user preference [84] as stiffness affected user preference more than it affected gait parameters. Only four of the reviewed articles evaluated patient preference. The results were varied with no generalizable patterns. Only one study investigated outcomes at the preferred stiffness compared to the other stiffness conditions [36]. Yamamoto et al. found that the stiffness selected by each subject did not necessarily coincide with the stiffness at which maximum dorsiflexion corrective moment was generated [36]. Therefore, there is insufficient evidence to establish a relationship between patient preference and quantitative measures of gait performance. Future work should focus on understanding what factors

drive user preferences and whether preferred stiffnesses result in improved gait mechanics.

In general, it was difficult to draw comparisons between studies when trends differed due to differences in how stiffness was measured or reported. Because of this, we were unable to achieve our secondary aim of determining the stiffness ranges that impact walking mechanics. Other reviews exploring AFO design parameters also note both the lack of sufficient detail in AFO design descriptions [32] and inconsistency of measurement techniques [31]. AFO ankle stiffness, in particular, may be less frequently reported since there are no commercially available tools or standardized procedures to measure it. As such, research groups must create and validate their own testing devices. Accordingly, many did not test AFO stiffness, with some measuring only linear stiffness of the posterior strut [93, 98] and others reporting nothing at all [92, 97, 99]. A few studies utilized *functional* measurement methods, where it was unclear whether the reported stiffness was that of the AFO alone or the AFO with the biologic ankle. Only about half of the reviewed studies reported both AFO stiffness and the test re-test reliability of their measurement method (Appendix Table B.2). Additionally, the direction and speed at which the AFO was deflected during stiffness testing was inconsistent across studies. While velocity effects are not significant for thermoplastic AFOs [47, 49], the effect on other materials such as printed composites remains unknown. Finally, in some cases, AFOs were chosen by type, with the assumption that one would be stiffer than another. However, one study that statistically compared the stiffnesses of the various devices it tested, found that the actual stiffness did not differ between some of the AFOs [72]. Thus, it is possible that not all conditions included here had uniquely different stiffnesses.

In this review, we utilized the standard approximation of stiffness as the slope of a linear regression through the AFO's torque-angle curve. However, many AFOs have a hysteretic torque-angle curve due to their viscoelastic properties; the torque required to flex the AFO to a specific angle is not equal to the torque generated when it is released. Thus, a description that also includes the regression intercept, width of the curve, and/or area inside the hysterisis loop [49] may be a better representation of the AFO's energy storage and dissipation properties.

It is likely that stiffness effects would differ depending on the deficits of a particular population. The current literature has an insufficient number of high quality articles that evaluated the same clinical population under similar stiffness interventions and using the same outcome measures for us to make meaningful conclusions. Most of the articles had low to moderate quality rating scores (below 7/10); many did not provide sufficient participant eligibility details or perform between-group statistical analyses across stiffness conditions. A third of the articles were case studies of one to two individuals. About

half of the reviewed studies tested individuals recovering from stroke but had inconsistent stiffness ranges resisting plantarflexion, dorsiflexion or both (Fig 2.2). Differences in reported outcome measures between the studies also made comparisons challenging. Similar challenges were noted in a review by Chisholm [28].

There were several possible confounding factors in the reviewed studies. First, we only considered AFO stiffness at the ankle joint in the sagittal plane. It is possible that other factors such as lateral or torsional stiffness of the AFO or compliance of the footplate impacted the findings across different studies. The profile and shape of the sole as well as the pitch, i.e. the height of the sole at the heel relative to at the toe, of the AFO or AFO-footwear combination may also impact user comfort and outcomes. Sole profile plays a key role in the timing of knee flexion during pre-swing. A higher pitch AFO-footwear combination would increase plantarflexion during midstance. For individuals with gastrocnemius contractures, if the increased plantarflexion is insufficient, the contracture might limit the user's ability to extend the knee. Second, we did not consider the shank to vertical angle of the studied AFOs as it was often not provided. This angle affects where the AFO stiffness (torque versus angle) curve intersects the horizontal axis. The shank to vertical angle likely affects the timing of AFO PF or DF resistance during the gait cycle, thus affecting several parameters including where the ground reaction force vector passes through the knee during midstance. Third, the acclimation period for different conditions differed between studies, with a majority testing all conditions in a single session. Longer accommodation periods may affect outcomes differently. Fourth, the user's walking speed may have affected stiffness comparisons. The included articles required participants to walk either at a self-selected or predetermined walking speed. Joint kinematics and kinetics are impacted by walking speed and thus any changes might be the result of speed rather than stiffness. However, self-selected speed was only affected in two studies [91, 92]. In addition, the impact of stiffness may be different at different speeds. One study [3] evaluated the impact of stiffness separately at slow and very slow walking speeds and did not find differences. The study included only healthy adults who would choose to walk much faster. The impact may be different for clinical populations or at faster walking speeds. Finally, the available literature is not sufficient to determine whether other activities, such as running [100] or walking on an incline [101], are impacted differently than level-walking by AFO stiffness.

2.5 Conclusion

This review found sufficient evidence to indicate that increasing AFO stiffness decreases ankle range of motion and increases stance knee flexion during gait. There was low evi-

dence for the effect of stiffness on other outcome measures including hip mechanics, muscle activity and metabolics. However, differences in measured outcomes, subject populations and stiffness reporting made determining the influence of AFO stiffness on walking performance difficult. Standardized stiffness testing and reporting guidelines should be established to ensure AFO device characteristics are sufficiently communicated and allow comparison across studies. Based on this review, we suggest the following guidelines for future studies: 1) Researchers should provide the type, material, pitch, manufacturing method and torque-angle curve for each AFO used. They should also cite the measurement instrument and technique used to obtain those curves. 2) AFO stiffness should be measured in both plantarflexion and dorsiflexion directions and the speed of flexion testing should be reported. 3) Participants should be tested at both a prescribed walking speed and preferred speed to facilitate inter-subject comparisons. 4) Detailed descriptions of subject characteristics should be provided, including noting any contractures. 5) Each subject's raw data, including preferred walking speed, rather than across-subject averages should be provided to allow deeper analyses for individual stiffness effects. 6) Considering AFO-footwear interaction effects, authors should note the type, make and model of the footwear used with the AFO. When possible, we recommend standardizing footwear across participants. With future studies providing this level of detail we can better understand the effects of a wide range of stiffnesses on specific populations, and thus improve patient outcomes.

CHAPTER 3

Design and Evaluation of the SMApp: a Stiffness Measurement Apparatus for Ankle-Foot Orthoses[1,2]

Summary

Background: Ankle-foot orthoses (AFOs) are braces worn by individuals with gait impairments to support ankle motion. AFO rotational stiffness is a key mechanical property that affects gait biomechanics. However, it is unclear how design choices affect AFO stiffness and what specific stiffness ranges impact gait. This stems largely from the absence of commercial devices or established guidelines for measuring AFO stiffness. **Aim:** This chapter details the design and evaluation of the AFO Stiffness Measurement Apparatus (SMApp). **Methods:** The SMApp is a non-destructive, automated system that measures torque and angle as an AFO is moved through a range of motion at a set speed. Using the derived torque-angle curve, we can calculate rotational stiffness, neutral angle and hysteresis of any AFO for speeds up to 74 deg/s. The repeatability of the SMApp was evaluated between and within two operators and three testing sessions using three AFOs cycled 10 times through flexion and extension. We also measured the stiffness of three different AFOs with the SMApp and another published system in a comparative case study. **Results:** The SMApp had excellent reliability (ICC ≥ 0.97) for all measured AFO properties. The standard error of measurement and minimum detectable difference were comparable to published parameters from other devices for stiffness (SEM < 0.32 Nm/°, MDD < 0.88 Nm/°)

[1] A version of this chapter was submitted for publication to the Journal of Mechatronics: D. Totah, M. Menon, D. Gates, and K. Barton. Design and Evaluation of the SMApp: a Stiffness Measurement Apparatus for Ankle-Foot Orthoses. Mechatronics. (submitted May, 2020)

[2] Supplementary files for this chapter, including an operation manual for the SMApp and code files, can be found at this link: https://drive.google.com/drive/folders/11203bS2ZBxkzoXIUXlWmh7sLdPkfaDYD?usp=sharing

and neutral angle (SEM < 0.30 °, MDD < 0.84 °). In comparison to a previously described, reliable manual stiffness measurement device, the SMApp measurements had similar stiffness, but different neutral angle values for one of three AFOs. **Significance:** We built a device that can test a large variety of AFO types and sizes non-destructively across a wide range of flexion angles and at speeds exceeding current alternatives. The SMApp can be utilized in future studies for AFO material fatigue testing, to validate finite element models, and to evaluate speed effects on AFO properties.

3.1 Introduction

Ankle-foot orthoses (AFOs) are braces worn around the lower leg and foot, inside a shoe, to support ankle motion. These devices are often prescribed to individuals with neurological impairments to compensate for muscle weakness or contracture. Clinicians have a variety of AFO designs to choose from, including rigid or articulated AFOs and off-the-shelf or custom-manufactured, all with varying mechanical properties. An important mechanical property of an AFO is its rotational stiffness, or the resistance of an AFO when it is displaced about the ankle joint into plantarflexion and dorsiflexion. This is often determined from the AFO's ankle torque-angle curve (Figure 3.1). AFO rotational stiffness has important functional consequences for the user, as a device that is very stiff will prevent ankle motion, and may require compensations at the knee [70]. In contrast, AFOs that are too compliant may not provide sufficient support to lift the toes and clear the ground during swing. Determining the range of acceptable stiffnesses has proven difficult as stiffness is infrequently measured or reported in clinical research [70].

Currently, there are no commercially available devices or established guidelines for measuring rotational stiffness. Several research groups have developed custom devices to measure stiffness using a variety of approaches, each with their own advantages and disadvantages. Some stiffness measurement techniques use custom surrogate limbs to load a particular AFO [102], while others compromise accurate ankle location matching for a more modular loading mechanism that accommodates multiple AFO sizes [46, 49]. Other approaches prioritize ensuring the AFO is securely fastened into the measurement device, potentially damaging the AFO in the process [103, 104]. Moreover, many of the approaches have not been evaluated for reliability or validity. A representative selection of the relevant literature is shown in Table 3.1 and discussed in Section 3.2. From these, we have identified three main criteria for the accurate measurement of AFO stiffness. First, testing should mimic functional AFO use. The device should test the full range, direction, and speed of ankle flexion during gait. The device should be able to do this for several AFO sizes and

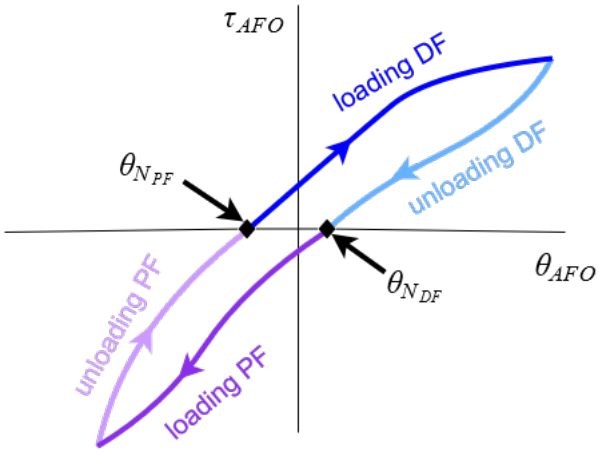

Figure 3.1: Schematic of an AFO's ankle torque versus angle curve showing plantarflexion (PF) and dorsiflexion (DF) loading and unloading regions and neutral angles (θ_N).

types as well as be non-destructive to the AFO. Second, gravitational and device dynamics effects should be isolated and removed from the AFO measurements. Finally, the reliability of the measurements should be assessed.

Therefore, drawing from the strengths of existing designs and addressing each criterion noted, we have designed a bench top device termed the Stiffness Measurement Apparatus (SMApp, /'es.mæp/). To our knowledge, this is the first device to address the three criteria identified above. The SMApp measures torque and angle as an AFO is moved through a range of motion at a set speed. Using the derived torque-angle curve, we can then calculate rotational stiffness, neutral angle and hysteresis area.

This chapter details the design of the SMApp and evaluation of the reliability of stiffness measurements obtained with the device. The chapter is organized as follows. Section 3.2 discusses key features of current measurement methods of AFO rotational stiffness in the literature. The SMApp design and operation details are presented in section 3.3. Section 3.4 details the data processing methods, dynamics equations used to isolate device dynamics and gravitational components, and calculation of AFO properties including stiffness, neutral angle, and hysteresis area. Section 3.5 details an evaluation of the SMApp reliability within and between sessions and operators. Section 3.6 describes a comparison of SMApp measurements with those made with an alternative, highly reliable, manual measurement device, termed the BRUCE [46]. A discussion of the results and a summary with conclusions are provided in sections 3.7 and 3.8, respectively.

Table 3.1: A representative selection of existing bench top stiffness measurement techniques in the literature and their key features. A dash (-) means that this feature or criterion was not addressed in the corresponding publication. Abbreviations: Automatic, automatic continuous device operation; Manual, manually-operated continuous flexion; Discrete, manually-operated discrete flexion (static measurements); s, between-session reliability; o, between-operator reliability; c, between-cycle reliability; v, velocity effect testing; n/a, insufficient information available.

	Mimic Functional AFO Use							Account for Device Effects	Assess Device
Author, Year	Operation	Flexion Speed	Flexion Range	Flexion Direction	*Not Destructive*	*Multi-size/ type Accommodation*	*Matched Flexion Axis to Ankle Location*	*Gravitational Components/ Friction*	*Tested Reliability/ Validity*
Bedard, 2016	Auto.	5 deg/s	-11 to 17	Both	✓	-	✓	✓	-
Bregman, 2009	Man.	-	-10 to 20	Both	✓	✓	-	✓	✓ (s,o,c)
Cappa, 2005	Auto.	-	-7 to 15	Both	✓	-	✓	✓	-
DeToro, 2001	Discrete	-	-10 to 10	PF	-	-	✓	-	-
Faustini, 2008	Discrete	-	n/a	PF	✓	✓	-	-	-
Golay, 1989	Discrete	-	0 to 16	DF	✓	-	✓	-	-
Ielapi, 2018	Auto.	1 deg/s	-25 to 25	Both	✓	-	✓	✓	✓ (s,o,c)
Kasahara, 1996	Discrete	2 deg/s	n/a	Both	-	-	✓	✓	✓ (s)
Klasson, 1998	Discrete	-	-2 to 3	Both	-	-	✓	-	-
Kobayashi, 2010	Auto.	10 deg/s	-15 to 15	Both	✓	-	-	-	-
Lee, 2006	Discrete	-	2 to 16	DF	✓	✓	-	-	-
Lunsford, 1994	Discrete	-	0 to 10	DF	✓	-	✓	-	-
Major, 2004	Auto.	2.3 deg/s	0 to 14	DF	✓	✓	-	-	-
Nagaya, 1997	Discrete	-	-12.2 to -1.2; 2 to 14.8	Both	✓	✓	-	-	-
Novacheck, 2007	Man.	-	-20 to 20	Both	✓	✓	-	-	✓ (s,v)
Polliack, 2001	Discrete	-	n/a	DF	✓	-	✓	-	-
Singerman, 1999	Man.	-	-14 to 13	Both	-	-	✓	✓	-
Takahashi, 2010	Man.	-	0 to 10	DF	✓	✓	-	✓	-
Walbran, 2016	Disc.	-	0 to 20	DF	✓	✓	n/a	n/a	-
SMApp	Auto.	up to 74 deg/s*	-20 to 17, -17 to 20	Both	✓	✓	✓	✓	✓

* The SMApp servomotor can operate at much higher speeds, but it has been tested up to 74 deg/s

3.2 Current Methods to Measure Stiffness

There are generally two approaches to measuring AFO stiffness [31]: functional and bench top. In functional methods [95, 105] an AFO is worn by a human user while the stiffness is measured. As it is difficult to isolate the AFO's stiffness from the user's ankle stiffness, we instead focus on bench top measurement techniques, which do not include a user (Table 3.1). Key attributes of bench top measurement techniques are discussed in the following subsections.

3.2.1 Mimicking Functional AFO Use

3.2.1.1 Device Operation

The majority of AFO flexion testing devices are operated manually and deflect the AFO to static angle positions [21, 44, 103, 104, 106–111] or continuously between two angles [46, 49, 112, 113]. Manual devices deflect AFOs using hanging weights [21, 44, 109], lead screw mechanisms [111], or lever arms [46, 49, 104, 112, 113]. However, thermoplastics, carbon fiber and other materials used to manufacture AFOs can exhibit hysteretic and sometimes viscoelastic properties [107]. This means that the velocity of flexion testing could affect the measured stiffness properties. Thus, automatic operation [23, 43, 102, 114, 115] is necessary for continuous flexion at a controlled speed. Since different AFO-users have varying mobility levels, AFO properties should be characterized at the walking speeds they are expected to be used.

3.2.1.2 Range and Direction of Flexion Testing

AFOs exhibit hysteretic and nonlinear torque-angle relationships. Accordingly, the direction and range of deflection during stiffness testing should be carefully designed. To capture the unloading and loading portions of the hysteresis loop, AFOs should be flexed in both plantarflexion (PF) and dorsiflexion (DF) directions. Bregman et al. [46] asserted the importance of testing AFOs from 10° in PF to 20° DF and back to 10° PF to assess functional gait ranges. However, some AFOs are designed to restrict the range of motion to satisfy a functional need.

One solution is to determine the range to deflect each AFO from the range of ankle movement during user gait trials with the AFO [115]. Another approach that does not require clinical gait assessment is testing the AFO at the full range of motion during typical gait of healthy individuals or until a maximum torque threshold is reached [21].

3.2.1.3 Ankle Location Matching

Measuring stiffness by deflecting the AFO about an axis that does not match the ankle's axis of sagittal-plane rotation results in a shifted torque-angle curve. In some studies, forces were applied directly at the shank and/or footplate without using a joint, forgoing a fixed rotation axis altogether [23, 110].

For measurement devices that use a joint, the device's deflection axis can be made to match the location of the ankle, marked by the lateral malleolus protrusion, by using a custom surrogate lower-limb model for each AFO-user [103, 104, 106, 107, 113]. Making custom surrogates can be laborious. Bregman et al. [46] proposed a compromise by manufacturing a selection of surrogate feet in several sizes to choose from. While the different sizes may not perfectly match the ankle axis, they can get close without the need to manufacture custom surrogates. Alternatively, a more modular approach is to make the device's surrogate ankle axis translatable so it can be shifted to match the biological location for each tested AFO [115]. Another approach, which we employ in this chapter, does not require any additional hardware and simply shifts the collected data in post-processing by applying a coordinate transformation using geometric parameters of the device and AFO [44].

3.2.2 Device Dynamics and Gravitational Effects

The devices used to deflect the AFO are assembled from multiple components. The inertia of these components, their weight due to gravity and any resulting friction from their motion will cause disturbances and increase measured torques. These extraneous torques should be minimized and/or subtracted from sensor data to ensure that the resulting torque-angle curves represent the AFO properties alone.

Design choices can also help reduce extraneous torques. Gravitational effects can be reduced by mounting the AFO horizontally such that gravity acts in the transverse rather than sagittal plane [104]. Torques due to the surrogate limb weight can be countered by pre-loading the device with a spring [46]. Alternatively, initial gravitational effects can be accounted for by zeroing the torque sensors prior to mounting the AFO [23, 113], or estimated through torque calculations and subtracted from the original signal [43, 102]. Finally, spurious hysteresis, resulting from slip between the AFO and the surrogate limb during testing, can be mitigated by adding lubrication [104] or a linear bearing [46] between the surrogate calf the AFO is mounted on and the surrogate shank it slides along during deflection (Figure 3.2).

While these approaches successfully minimize extraneous torques, they do not account

for all device inertial and damping effects during the entire range of flexion testing. Utilizing redundant sensors (3-axis load cell for single-axis motion), Cappa et al. [43] was able to account for mechanism friction effects in off-axis planes of motion. To account for the remaining inertial and damping effects along the plane of interest (sagittal plane), torques resulting from device dynamics can be measured by operating the device, without an AFO, through its full range of flexion at the same speed an AFO will be tested, then subtracting these torques from the torque measurements obtained with the AFO. Ielapi et al. [115] employed a similar approach, but did not specify the speed at which these calibration curves were acquired.

3.2.3 Device Assessment and Evaluation

When a new measurement device is designed, it is important to evaluate the precision (i.e. reliability) and accuracy (i.e. validity) of the measurements it produces. However, only a few studies included a formal analysis of the stiffness measurement systems. A reliability analysis provides insight into the robustness or repeatability of measurements of the same AFO under different experimental conditions. A few devices were found to be reliable for torque or stiffness measures across different operators [46, 115], sessions [46, 49, 104, 115], and cycles [46, 115]. Cycling an AFO refers to flexing it through a specified range without removing it from the testing apparatus. One testing session may consist of multiple cycles. Between-cycle (within-session) reliability, also called test-retest reliability, captures inconsistencies in the device's operation. The AFO is removed from the device fixture between each session. This way the between-session reliability testing captures errors due to differences in AFO placement in the measurement apparatus for a single-operator.

Validity refers to measurement accuracy as compared to a true known stiffness. Making a reference specimen is difficult, which is why most studies forego experimental validation altogether. While validity assessment is not common in AFO testing, some methods used in literature include estimating measurement accuracy through a theoretical uncertainty analysis [43], or using a steel sheet reference specimen whose 'true' stiffness was measured with a commercial, universal mechanical testing machine [115]. Given the limitations of these approaches, we instead chose to compare measurements of a sample set of AFOs from the SMApp with another reliable, manual measurement device [46].

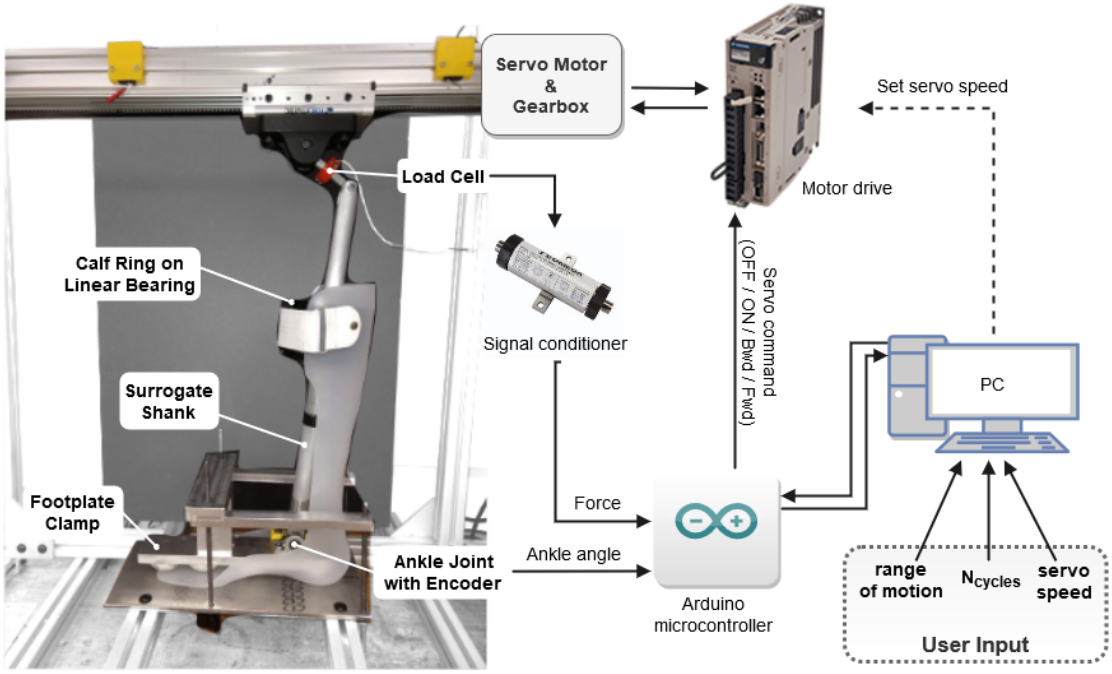

Figure 3.2: The stiffness measurement apparatus (SMApp) components.

3.3 SMApp System Design and Operation

3.3.1 Hardware

The stiffness measurement apparatus (SMApp) is comprised of a surrogate leg driven by a linear actuator to rotate about a surrogate ankle joint (Figure 3.2). The surrogate leg consists of a metal foot, shank and calf ring. The AFO is clamped to the base of the testing device by tightening four lead screws. The clamp is made of an aluminum surrogate foot and a steel bottom plate. Rubber half-spheres, lining the clamp, mold to the shape of the AFO insole and hold it in place during testing. The surrogate ankle joint was custom-machined from a steel bar and is connected to the foot with a shoulder screw through two bearing mounts, which allow it to rotate freely. The steel ankle joint is also fixed to an aluminum rod or "surrogate shank". The AFO cuff is mounted on a 3-D printed PLA ring and held in place with a hook and loop strap. The PLA ring is attached to the aluminum rod with a linear bearing to minimize slip. Several sizes of calf rings are available, and custom geometries can be produced, to accommodate different AFO sizes. The proximal end of the surrogate shank is attached to a linear belt drive actuator (MXB32S, Tolomatic, Hamel, MN) through an in-line tension/compression load cell (LC201, Omega, Norwalk, CT). The

load cell attachments on both ends consist of eye-bolts with bearings allowing free rotation in the sagittal plane and some minimal movement in the frontal plane (to accommodate any misalignment). The linear actuator is driven by a servo motor (SGM7J-06A7D6C, Yaskawa, Waukegan, IL) to allow continuous and autonomous operation. The servomotor is rated for 3000 rpm but was tested in the SMApp to up to 1200 rpm which corresponded to a 74°/s ankle angular speed. Additionally, the SMApp has a maximum flexion range of 37° starting from either -17° or -20°, which meets functional gait assessment needs (Section 3.2.1.2). The surrogate leg assembly is rotated about its' vertical axis by 180° to switch between the two range of motion options.

3.3.2 Device Control and Software Interface

The user specifies the range of motion, rotational speed, and number of cycles. The SMApp flexes an AFO according to these specifications and outputs a time series of the surrogate ankle angle and force applied to the shank through the load cell connection. The SMApp control architecture involves an outer control loop employing ankle position feedback and an inner loop for servo speed control. An Arduino Mega 2560 microcontroller board manages the outer control loop and communicates with a motor drive (Servopack SGD7S, Yaskawa, Waukegan, IL) that executes the inner loop. The motor drive modulates the SMApp's servo speed through closed-loop feedback control using the servo's built-in encoder. The desired rotation speed is inputted through the motor drive's proprietary software (SigmaWin+ v7, Yaskawa, Waukegan, IL). For the outer control loop, a user specifies the desired flexion range and number of cycles for AFO testing through a PC interface that communicates with the Arduino controller through a serial connection. The Arduino reads the current ankle angle from a magnetic rotary encoder (AS5048B, ams, Unterpremstätten, Styria, Austria) mounted to the surrogate ankle joint. A bang-bang position-feedback control loop on the Arduino sends a command of forward or backward rotation to the motor drive (through a serial connection) until the desired maximum or minimum flexion angle is reached. This is repeated until the desired number of cycles is reached. The Arduino controller also collects sensor data from the ankle encoder and load cell through I^2C protocol. The load cell force, outputted as a voltage differential signal, is first amplified and filtered through an in-line signal conditioner (IN-UVI, Omega, Norwalk, CT) before it is sent to an analog-to-digital converter chip (ADS115, Texas Instruments, Dallas, TX), which transfers it to the Arduino via an I^2C communication protocol. The Arduino then converts the voltage to a force reading using a calibration curve. Both the magnetic encoder and load cell readings were calibrated experimentally using a goniometer and calibration weights

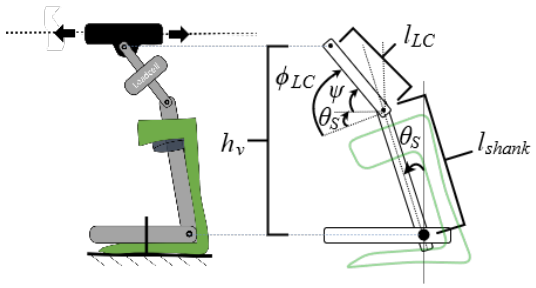

Figure 3.3: Illustration showing parameters used to calculate torque applied to the shaft from the load cell force measurements.

to validate angle and force readings, respectively. The Arduino outputs the collected data including timestamps, ankle angle, current cycle and load cell force values to a PC through a serial port at a sampling rate of about 35 Hz. The data is saved into a text file on the PC for post-processing in Matlab® (The MathWorks Inc., Natick, MA).

3.3.3 Safety Considerations

Several features were added to ensure safety during device operation:

- **Hardware-activated Soft Limits** - a limit switch was placed at each end of the linear actuator. If triggered, these switches stop motor rotation using dynamic braking to ensure the actuator does not move beyond a specified range.
- **Manually-activated Stop Button** - an emergency stop button can be manually activated to trigger the motor limit switches and stop the motor through its driver software.
- **Emergency Power Shut-off** - a power shut-off switch can be manually activated in case of an emergency to cut power to the motor.
- **Hard Stops** - long metal screws attached to the bearing mount on the surrogate foot prevent the surrogate ankle joint from rotating beyond a specified maximum range from $-30°$to $32°$.

3.4 Calculating AFO Properties

3.4.1 Data Processing

The surrogate limb ankle angle (θ_S) and the force from the SMApp's load cell (F_{LC}) were input into a custom code to identify and remove artifacts. Artifacts were identified as points

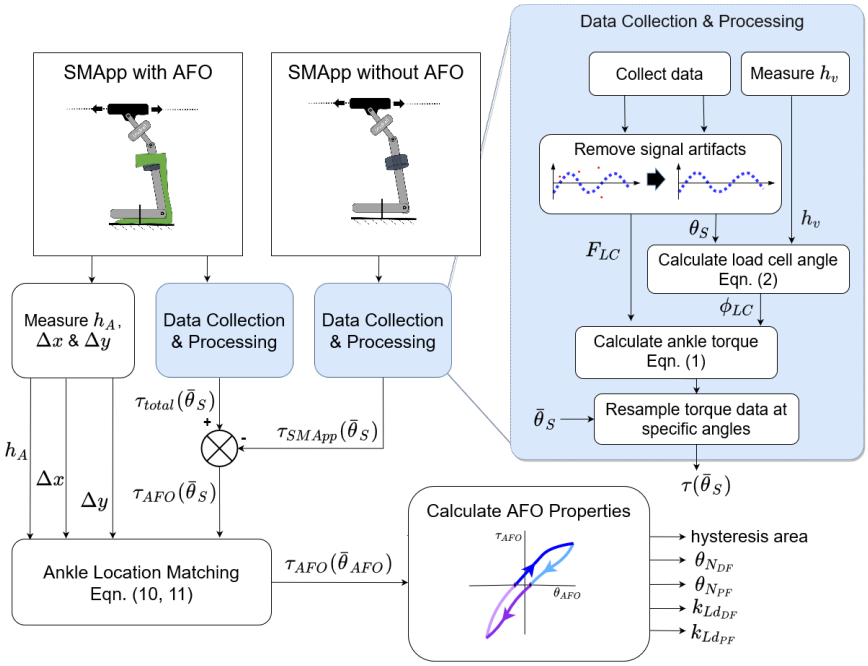

Figure 3.4: Flowchart of the data processing steps for isolating AFO torque to produce a torque versus angle stiffness curve to calculate AFO properties.

with sample-to-sample variations of greater than 10 degrees or 10 N, which corresponded to approximately a 350 °/s or N/s slope. This threshold was determined empirically through visual inspection. The signals were then interpolated such that they retained the same number of data points. Ankle torque was then calculated using:

$$\tau = l_{shank} F_{LC} \cos(\phi_{LC}) \tag{3.1}$$

where l_{shank} is the length of the SMApp's surrogate shank (0.4817 m) and ϕ_{LC} is the angle of the load cell joint (Figure 3.3). The angle ϕ_{LC} was calculated from θ_S as:

$$\phi_{LC} = \theta_S + \psi, \tag{3.2}$$

$$\text{where } \psi = \sin^{-1}\left(\frac{h_v - l_{shank}\cos(\theta_S)}{l_{LC}}\right) \tag{3.3}$$

Parameter l_{LC} is the length of the load cell segment (0.0770 m) and h_v is the vertical height from the surrogate ankle joint to the joint connecting the actuator to the load cell segment. Height h_v is measured when the AFO is clamped in the SMApp as it is affected by the thickness and shape of the AFO footplate.

The total torque when the AFO is in the SMApp can be represented as a linear combi-

nation of the torque resulting from the AFO dynamics and the torque contribution from the SMApp device dynamics (equation 3.4).

$$\tau_{total} = \underbrace{[k_{AFO}\theta_S + B_{AFO}\dot{\theta}_S + I_{AFO}\ddot{\theta}_S]}_{\tau_{AFO}} + \underbrace{[k_{SMApp}\theta_S + B_{SMApp}\dot{\theta}_S + I_{SMApp}\ddot{\theta}_S + G_{SMApp}]}_{\tau_{SMApp}} \quad (3.4)$$

The stiffness (k) and damping (B) terms come from the compliance and hysteretic properties of the AFO materials and from the compliance and friction in the SMApp joints and bearings. The mass of the SMApp components contributes to the inertia (I) and gravitational (G) terms. The following assumptions were made when formulating this torque equation:

A1. The gravitational contribution to AFO torque (G_{AFO}) is negligible,

A2. The SMApp's surrogate shank is modeled as a rigid body with infinite stiffness.

The first assumption holds since $G_{AFO} =$ (moment arm) $\times\ mg\ \sin(\theta_S)$ and the only portion of the AFO that moves is the upright section, whose mass (m) is small. The range of motion is also small enough that the $\sin(\theta_S)$ term lowers the gravitational contribution even further. The second assumption (A2) allows the stiffnesses of the SMApp and AFO to be modeled as two in-parallel springs and ignores any in-series stiffness components. The in-series stiffness comes from the compliance of the surrogate shank on which the AFO is mounted. The shank's compliance can be neglected because its' stiffness is far greater than the AFO's. We verified this with a beam equation calculation. A maximum applied moment of 150 Nm would deflect this aluminum beam by a negligible angle of less than 2×10^{-10} degrees.

This representation (equation 3.4) allowed us to treat the system dynamics (stiffness, damping, inertia and gravity) of both the SMApp and the AFO as independently measurable. We measured these by first collecting data with the AFO in the SMApp and then repeating the test without the AFO. We then subtracted the SMApp dynamics from the total dynamics in order to isolate the AFO's torque. In a pilot study of the device, we found a negligible effect of speed on SMApp torque, with a 6 °/s speed increase resulting in a < 0.02 Nm change in torque. Therefore, the values for τ_{SMApp} can be subtracted from τ_{total} at each θ_S value to isolate the τ_{AFO} values even if they were collected at different speeds,

$$\tau_{AFO}(\theta_S) = \tau_{total}(\theta_S) - \tau_{SMApp}(\theta_S). \tag{3.5}$$

Importantly, to collect τ_{SMApp}, the AFO is removed but the surrogate calf ring used to fit the AFO onto the SMApp must stay in place. A piece of electrical tape placed on the surrogate leg rod directly below the ring's linear bearing kept the ring at the same height as when the AFO was placed in the SMApp in the upright position (zero degrees). This insured the inertia of the system remained consistent between the with AFO and without AFO data collections. The motion of the linear bearing along the surrogate leg during testing is assumed sufficiently small that its effects on the system's inertia can be neglected.

Before equation 3.5 could be practically applied, two data processing steps were needed. First, the torque and angle signal pairs for each test (with and without the AFO) were separated according to the rising and then falling portions of the torque versus angle curve (Figure 3.1). Next, these monotonic rising and falling sections of each of the τ_{total} and τ_{AFO} signals were resampled to find their values at a set of angles $\bar{\theta}_S$ that lie within the range of the measured θ_S, i.e. $\bar{\theta}_S \in [\theta_{S_{min}}, \theta_{S_{max}}]$. Then, the AFO torque corresponding to each angle in $\bar{\theta}_S$ was found by applying equation 3.5 to each of the falling and rising segments when $\dot{\bar{\theta}}_S < 0$ and $\dot{\bar{\theta}}_S > 0$, respectively.

Recall from equation 3.4, the AFO's dynamics were modeled as: $\tau_{AFO} = K\theta_S + B\dot{\theta}_S + I\ddot{\theta}_S$. Flexion speed is constant during each of the rise and fall portions of the torque-angle curve, meaning $\ddot{\theta}_S = 0$ and AFO torque becomes a function of θ_S and a constant $\dot{\theta}_S$:

$$\tau_{AFO} = f(\theta_S, \dot{\theta}_S) \tag{3.6}$$

3.4.2 Ankle Location Matching

Custom AFOs are made to match a user's anthropometry. An AFO's ankle location may not match the SMApp's surrogate limb ankle location. This results in a mismatch in the center of rotation and, therefore, the AFO's ankle angle (θ_{AFO}) will not match the measured surrogate ankle angle (θ_S). We utilized geometric relationships when an AFO is mounted in the SMApp to find an expression relating θ_S to θ_{AFO}. First, consider the AFO in the SMApp at a particular instant in time during a testing cycle (Figure 3.5), where the instantaneous point P is located on the surrogate calf ring. Two origins were defined in this system, one at the AFO's ankle location (O_A) and one at the SMApp's surrogate ankle (O_S). The location of P was described relative to the AFO's ankle ($\vec{r}_{P/O_A}$) and to the surrogate ankle location ($\vec{r}_{P/O_S}$). The two position vectors were related by equation 3.7 (unknown variables are in bold, all others are measured):

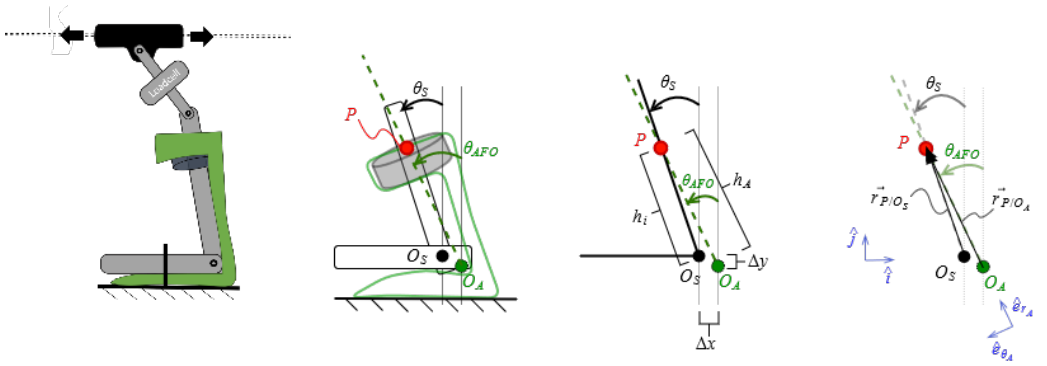

Figure 3.5: Schematic for ankle location matching between the surrogate limb ankle (origin O_S) and the AFO's ankle (origin O_A). The schematic is drawn for an instantaneous point P located at the top of the surrogate calf ring and the middle of the surrogate shank.

$$\vec{r}_{P/O_A} = \vec{r}_{O_S/O_A} + \vec{r}_{P/O_S} \tag{3.7}$$

$$\vec{r}_{P/O_S} = \boldsymbol{h_i}[-\sin(\theta_S)\,\hat{i} + \cos(\theta_S)\,\hat{j}] \tag{3.7a}$$

$$\vec{r}_{P/O_A} = h_A[-\sin(\boldsymbol{\theta_{AFO}})\,\hat{i} + \cos(\boldsymbol{\theta_{AFO}})\,\hat{j}] \tag{3.7b}$$

$$\vec{r}_{O_S/O_A} = -\Delta x\,\hat{i} + \Delta y\,\hat{j} \tag{3.7c}$$

The variables θ_S, $\boldsymbol{\theta_{AFO}}$ and $\boldsymbol{h_i}$ are time-varying, where $\boldsymbol{h_i}$ is the instantaneous distance of point P from the surrogate ankle (Figure 3.5). The parameters h_A, Δx and Δy are constants measured for each tested AFO.

Substituting equations 3.7a-c into 3.7 yielded:

$$h_A[-\sin(\boldsymbol{\theta_{AFO}})\,\hat{i} + \cos(\boldsymbol{\theta_{AFO}})\,\hat{j}] = -\Delta x\,\hat{i} + \Delta y\,\hat{j} + \boldsymbol{h_i}[-\sin(\theta_S)\,\hat{i} + \cos(\theta_S)\,\hat{j}] \tag{3.8}$$

and applying small angle approximations linearized equation 3.8 to:

$$h_A[-\sin(\boldsymbol{\theta_{AFO}})\,\hat{i} + \cos(\boldsymbol{\theta_{AFO}})\,\hat{j}] = -\Delta x\,\hat{i} + \Delta y\,\hat{j} + \boldsymbol{h_i}[-\sin(\theta_S)\,\hat{i} + \cos(\theta_S)\,\hat{j}]$$

$$-h_A\,\boldsymbol{\theta_{AFO}}\,\hat{i} + h_A\,\hat{j} = -\Delta x\,\hat{i} + \Delta y\,\hat{j} - \boldsymbol{h_i}\theta_S\,\hat{i} + \boldsymbol{h_i}\,\hat{j} \tag{3.9}$$

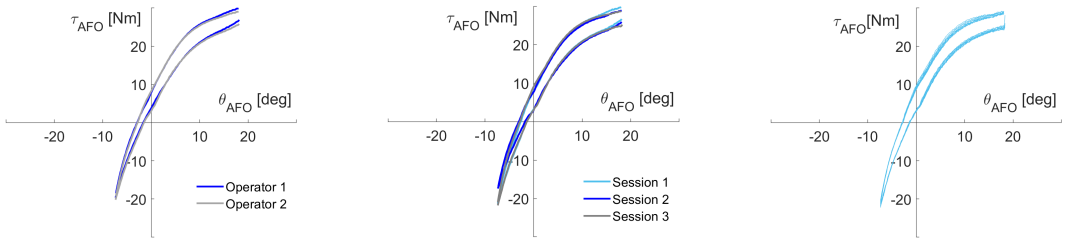

(a) Inter-operator Reliability (b) Inter-session Reliability (c) Inter-cycle Reliability

Figure 3.6: Example torque-angle curves from the SMApp reliability analysis of one AFO. a) The average of all sessions for each operator. b) The average of all cycles in each session for one operator. c) 10 cycles from a single session.

Grouping the $\hat{i}$- and $\hat{j}$-component directions resulted in the following two equations with:

$$\hat{i}: \; -h_A \, \boldsymbol{\theta_{AFO}} = -\Delta x - \boldsymbol{h_i}\theta_S \tag{3.9a}$$

$$\hat{j}: \; h_A = \Delta y + \boldsymbol{h_i} \tag{3.9b}$$

We solved for $\boldsymbol{h_i}$ from equation 3.9b and substituted it into equation 3.9a to derive an expression for $\boldsymbol{\theta_{AFO}}$ that depends only on the collected signal θ_S and other measured geometric parameters:

$$\boldsymbol{\theta_{AFO}} = \frac{\Delta x}{h_A} + \left[1 - \frac{\Delta y}{h_A}\right] \theta_S \tag{3.10}$$

Let $g(\theta_S)$ represent the function in equation 3.10. Then, taking the inverse of $g(\theta_S)$ allowed us to transform the torque equation from a function of θ_S to a function of $\boldsymbol{\theta_{AFO}}$:

$$\boldsymbol{\tau_{AFO}} = f(\theta_S) = f(g^{-1}(\boldsymbol{\theta_{AFO}})) \tag{3.11}$$

3.4.3 AFO Neutral Angle

The neutral angle of an AFO is the angle (measured from vertical) at which the torque is equal to zero. A neutral angle for each of plantarflexion and dorsiflexion was found from the x-intercepts of the rising and falling sections of the torque versus angle curve, respectively.

$$\theta_N := \begin{cases} \theta_{N_{PF}} = \{\theta_{AFO} \mid \tau_{AFO_{rise}}(\theta_{AFO}) = 0\} \\ \theta_{N_{DF}} = \{\theta_{AFO} \mid \tau_{AFO_{fall}}(\theta_{AFO}) = 0\} \end{cases} \tag{3.12}$$

3.4.4 AFO Stiffness

Stiffness can be calculated as the slope of a linear torque versus angle curve. This linear model assumes the damping term is negligible. A piece-wise linear regression of four segments was applied to the AFO ankle torque versus angle curve to yield four stiffness values (Fig. 3.1). The four segments were found by splitting the rising and falling portions of the curve at the neutral angle, where angles larger than the neutral angle were considered dorsiflexion angles and those smaller as plantarflexion. A linear regression was fitted to each combination of plantarflexion or dorsiflexion during loading or unloading portions of the torque-angle curve. Loading and unloading states were determined from the flexion direction. For example, plantarflexion loading is when the AFO ankle angle is negative (plantarflexed) relative to neutral and the AFO is flexed in the direction of increasing plantarflexion (making the ankle angle more negative).

Only the loading portions of the curve were used to acquire a linear fit slope representing loading plantarflexion and loading dorsiflexion AFO stiffness ($k_{LD_{PF}}$ and $k_{LD_{DF}}$, respectively). The unloading portions were not considered good estimates of the AFO stiffness. This is because during unloading the AFO springs back and exerts a torque in the same direction as the actuator torque. The load cell measures both these torques and we cannot separate them.

3.4.5 Hysteresis Area

The area inside the hysteresis loop represents the energy dissipation of an AFO. The integral of the rising curve was subtracted from the integral of the falling portion to find the loop's inner area. Numerical integrals were calculated in Matlab (Mathworks, Natick, MA, USA) from the collected torque versus angle data. The result was then multiplied by $\pi/180$ to convert the angle units from degrees to radians such that the energy value had units of Joules.

3.5 Evaluation of SMApp Reliability

We evaluated the reliability of SMApp stiffness measurements across different operators, testing sessions, and flexion cycles with three custom made AFOs (Figure 3.7): a tradi-

(a) PEBA AFO

(b) Nylon AFO

(c) Thermoplastic AFO I

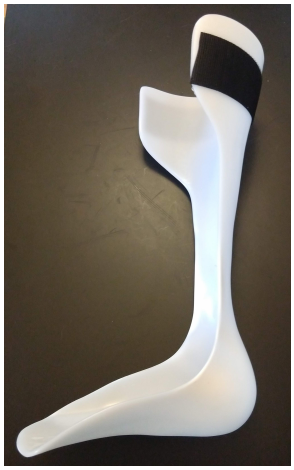

(d) Thermoplastic AFO II

Figure 3.7: The four AFOs tested in this chapter. AFOs (a), (b), and (c) were used in the SMApp reliability study. AFOs (b), (c), and (d) were used in the cross comparison with an alternative device. The AFOs had wall thicknesses of 7.5, 3.6, 3.5, and 4.0 mm, foot lengths of 27.0, 28.0, 27.0, and 20.0 cm, and heights of 39.0, 36.0, 41.5, and 36.5 cm, respectively.

tional polypropylene and polyethylene composite AFO thermoformed under vacuum over a plaster cast, a 3-D printed nylon, and 3-D printed polyether block amide (PEBA) AFO. The latter two were printed using fused deposition modeling. Two operators tested each AFO during three different sessions on a single day. At the start of a session, the operator tightly clamped the AFO's footplate into the SMApp, using a level to ensure the footplate clamp fasteners were tightened equally. Next, a custom-sized surrogate calf was fixed to the linear bearing on the shank and the AFO upright portion was secured tightly around the surrogate calf with a hook and loop strap. The SMApp then flexed the AFO through its full range of motion 10 times. The AFOs were removed from the SMApp after each testing session. Both operators followed the same randomized testing order and ran the SMApp at the same actuator speed (78 rpm). The geometric measurements needed to calculate torque and angle using the equations in Section 3.4 were collected by one operator (Operator 2) and used for all data analyses.

3.5.1 Statistical Analysis

We assessed the reliability of five parameters measured by the SMApp: the stiffness of plantarflexion loading and dorsiflexion loading, the neutral angle in plantarflexion and dorsiflexion, and the hysteresis area. Reliability of each parameter was measured using intraclass correlation coefficients (ICCs) using SPSS v 22 (IBM, Armonk, NY, USA). ICCs were calculated as a measure of relative within- and between-operator or session reliability for each AFO parameter using a two-way mixed model for absolute agreement. A valid ICC ranges between 0 and 1, with a value of 0.95, for example, meaning that 95% of the total error of a measurement comes from the true error and conversely only 5% of the total error is due to measurement error [116]. A high ICC indicates low *relative* measurement error between the different cycles, operators, or sessions. Between-operator reliability calculations used averaged parameters across sessions and cycles for each operator. Between-session (within-operator) reliability calculations used the average of 10 cycles for each session for one of the operators (Operator 2). Finally, Between-cycle (within-session) reliability calculations used the data collected by operator 2 during their first testing session. As suggested in [117], an $ICC > 0.75$ indicated good reliability and an $ICC > 0.90$ was considered good for clinical measures.

The standard error of measurement (SEM) and the minimum detectable difference (MDD) were calculated as measures of *absolute* error. The SEM was estimated as the root mean square average of the within-AFO standard deviations for each measurement

Table 3.2: The intraclass correlation coefficients (ICCs) for between-cycle (within-session), between-operator, and between-session (within-operator) reliability for five key AFO properties.

		ICC Values [95% confidence intervals]				
		Ankle Stiffness		Neutral Angle		Hysteresis
		$k_{Ld_{DF}}$	$k_{Ld_{PF}}$	$\theta_{N_{DF}}$	$\theta_{N_{PF}}$	$Area$
Between-cycle (within-sess.)	Single Score	1.00 [1.00-1.00]	1.00 [1.00-1.00]	1.00 [1.00-1.00]	1.00 [1.00-1.00]	0.99 [0.97-1.00]
	Mean Score	1.00 [1.00-1.00]	1.00 [1.00-1.00]	1.00 [1.00-1.00]	1.00 [1.00-1.00]	1.00 [1.00-1.00]
Between-operator	Single Score	1.00 [0.95-1.00]	1.00 [0.91-1.00]	1.00 [0.94-1.00]	1.00 [0.92-1.00]	0.97 [0.61-1.00]
	Mean Score	1.00 [0.96-1.00]	1.00 [0.95-1.00]	1.00 [0.97-1.00]	1.00 [0.96-1.00]	0.99 [0.76-1.00]
Between-session (within-oper.)	Single Score	0.99 [0.95-1.00]	1.00 [0.97-1.00]	1.00 [0.98-1.00]	1.00 [0.98-1.00]	0.98 [0.85-1.00]
	Mean Score	1.00 [0.98-1.00]	1.00 [0.99-1.00]	1.00 [0.99-1.00]	1.00 [0.99-1.00]	0.99 [0.94-1.00]

Table 3.3: The standard error of measurement (SEM), minimum detectable difference (MDD) and average measured values for five key AFO properties.

	Ankle Stiffness [$Nm/°$]				Neutral Angle [°]				Hysteresis [J]	
	$k_{Ld_{DF}}$		$k_{Ld_{PF}}$		$\theta_{N_{DF}}$		$\theta_{N_{PF}}$		$Area$	
	SEM	MDD	SEM	MDD	SEM	MDD	SEM	MDD	SEM	MDD
Between-cycle	0.01	0.03	0.05	0.13	0.07	0.20	0.06	0.16	0.07	0.20
Between-operator	0.20	0.55	0.28	0.78	0.27	0.75	0.30	0.84	0.15	0.41
Between-session	0.32	0.88	0.24	0.68	0.25	0.70	0.21	0.59	0.14	0.40
AFO	$k_{Ld_{DF}}$		$k_{Ld_{PF}}$		$\theta_{N_{DF}}$		$\theta_{N_{PF}}$		$Area$	
PEBA	0.85		1.15		2.15		0.79		0.29	
Nylon	7.30		8.26		-9.45		-10.05		1.83	
Thermoplastic	1.33		3.38		-1.60		-2.87		1.87	

parameter:

$$\text{SEM} = \sqrt{({SD_{AFO1}}^2 + {SD_{AFO2}}^2 + {SD_{AFO3}}^2)/N} \tag{3.13}$$

where N equaled 2 (operators), 3 (sessions), and 10 (cycles) for between-operator, between-session, and within-session reliability, respectively. The MDD was derived from the SEM as follows [116]:

$$\text{MDD} = \text{SEM} \times 1.96 \times \sqrt{2} \tag{3.14}$$

where 1.96 is the z score for a 95% confidence interval.

3.5.2 Reliability Results

All measured AFO parameters had high reliability within-session, between-sessions, and between-operators (ICC ≥ 0.97; Table 3.2) for both single and mean scores. Single scores show the reliability of a typical cycle, operator, or session; while mean scores show the reliability of average measurements from multiple cycles, operators or sessions. The SEM

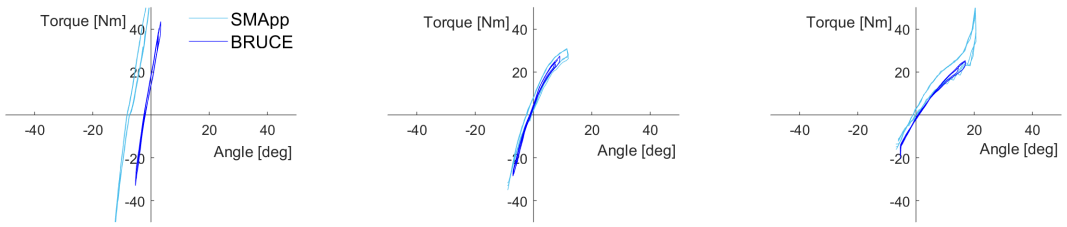

(a) Printed Nylon AFO (b) Thermoplastic AFO I (c) Thermoplastic AFO II

Figure 3.8: Torque and angle curves for three AFOs measured with the SMApp (light blue) and the BRUCE (dark blue). Data are shown for three full test cycles.

for stiffness, neutral angle, and hysteresis area parameters ranged between $0.01 - 0.32$ Nm/°, $0.06 - 0.30$ °, and $0.07 - 0.15$ J, respectively (Table 3.3). The within-session SEM ranges were < 1.2 % of AFO measurements for stiffness and < 8 % of the neutral angle values, while between-session and between-operator reliability SEM's were 3-38 % of stiffness and angle measurements. The hysteresis area had the lowest absolute reliability of 4-24 % of the tested AFOs' values for within-session, and 8-52 % for between-session and between-operator reliability.

3.6 Cross Comparison with an Alternative Device

We compared the SMApp measurements of three AFOs (a printed nylon and two thermoformed plastic composite AFOs; Figure 3.7) to those taken with another, reliable (ICC > 0.90) testing device, the BRUCE [46]. The BRUCE is a manually operated bench-top device that measures the torque versus angle curve of an AFO at an operator chosen speed. Each AFO was tested for at least three flexion cycles using the BRUCE and 10 cycles in the SMApp. The first three full cycles from each device were used. We compared the measures of dorsiflexion and plantarflexion loading stiffness, dorsiflexion and plantarflexion neutral angles, and area inside the hysteresis loop between the measurement devices for each AFO.

For this cross-comparison study, the operator attempted to set the SMApp test speeds to match each AFO's tested speed in the BRUCE. However, the BRUCE speeds varied both within and across cycles since it is a manually-operated device. Therefore, the SMApp speed was set to within 2 °/s of the median speed for each AFO with the BRUCE. The median speeds for the nylon and two thermoplastic AFOs were 10 °/s, 18 °/s, and 31 °/s in the BRUCE and 8 °/s, 20 °/s, and 33 °/s in the SMApp, respectively.

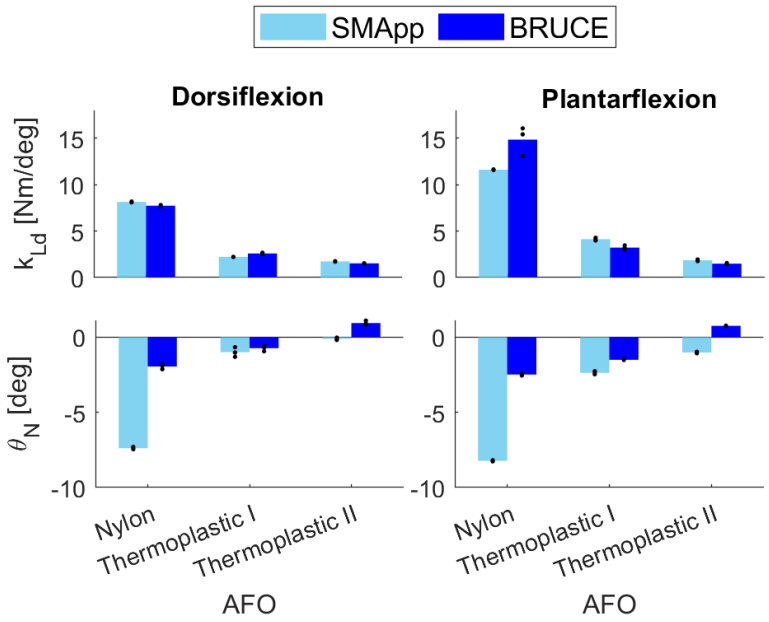

Figure 3.9: The average stiffness in loading (k_{Ld}) and neutral angles (θ_N) for three AFOs measured with the SMApp and the BRUCE devices. Each (•) represents data from an individual cycle.

3.6.1 Comparison Results

For all three AFOs, loading stiffness values were similar between the SMApp and Bruce. The torque-angle curves were more similar between the SMApp and BRUCE for the two thermoplastic AFOs compared to the 3-D printed nylon AFO (Figure 3.8). The curves for the SMapp and BRUCE were similarly sloped, but offset. This is also seen in the large difference in neutral ankle for this AFO (Figure 3.9). Neutral angles were more plantarflexed with the SMApp compared to the BRUCE for all AFOs. The torque-angle curves with the SMApp demonstrate a hysteretic effect at the end range, not seen with the BRUCE.

3.7 Discussion

In this study, we designed a non-destructive, automated AFO testing device that could accommodate a variety of AFO sizes and types, flexion speeds and ranges of motion. The SMApp had excellent reliability between operators, sessions and cycles when measuring AFO loading stiffness, neutral angle, and hysteresis area. The main function of the SMApp is to measure AFO stiffness. The loading stiffness had excellent relative and absolute reliability. Stiffness ICC, SEM, and MDD values obtained were similar to or better than

other devices [46, 115]. Stiffness also matched closely between the SMApp and BRUCE devices (Figure 3.9).

The neutral angle measures had high reliability, and SEM and MDD values, comparable to those found in a published reliability study of the BRUCE [46]. In our comparison study, the BRUCE measures had a shifted neutral angle for the Nylon AFO, but similar values for the two thermoplastic AFOs tested. The shift could be due to the placement of the AFO in the BRUCE. The nylon AFO's ankle location may not have matched the surrogate ankle of the dummy leg used. The BRUCE has a number of finite surrogate limbs of different sizes, which makes it more modular while the SMApp uses a custom fitted calf and shifts the ankle location in post-processing, which may improve the accuracy. Because of the difference in locating the ankle between the two devices, the BRUCE's angle data (Figure 3.8) corresponds to the device's surrogate ankle angle, while the SMApp's data include the true AFO angle θ_{AFO} shifted from the surrogate angle θ_S (Equation 3.10, Section 3.4.2).

The area inside the hysteresis loop of the stiffness curve is a measure of energy dissipation. Few studies have calculated this measure. The area values measured in the SMApp had very good relative reliability and an SEM < 0.2 J, which represented an error of 4-8% of the mean for the Nylon and Thermoplastic AFOs (Table 3.3). This is compared with another published device that had differences up to 40% of the mean area of tested AFOs [49]. For AFOs with a small hysteresis area, such as the PEBA AFO we tested, this small SEM accounts for a larger percent error, up to 52% of the PEBA's mean area. Such low-hysteresis curves are described as highly linear, elastic curves with low energy dissipation. It follows that the area measure is only relevant for AFOs with sizable hysteresis areas > 1 J, where the SEM is <10% of the measured area.

The SMApp design has several advantages not explored in this study. First, the automated speed control can be used to study the viscoelastic properties of AFOs. While a few others have implemented automatic speed control, the SMApp's range of speed and range of motion exceed current alternatives (Table 3.1). The automatic operation allows the SMApp to be used to cyclic test the AFO for analysis of material fatigue. Fatigue testing is especially important for ensuring AFOs manufactured from new materials and methods such as 3-D printing are suitable for long-term use. Finally, while only posterior leaf spring AFOs were tested in this study, the SMApp can test both the plantarflexion and dorsiflexion dynamic stiffness of a multitude of AFO types including anterior leaf spring designs.

Backlash is often an issue in mechanical devices such as the SMApp. While there is some play in the joints, backlash does not affect the control of nor the data collected with the SMApp. This is because the speed control is handled through the servo drive with feedback from the servo encoder which is placed *before* the gear box and any joints that

would be affected by backlash. Conversely, the AFO torque and angle data is collected from sensors placed *after* the gearbox and hinge joints. Additionally, The SMApp pre-loads the AFO to the maximum dorsiflexion angle before beginning the cyclic testing. This keeps any initialization effects confined to the start of the rise and fall segments of the torque-angle curve. Since the stiffness and neutral angle properties are calculated from the loading portions of the rise and fall segments, the initialization dynamics, which occur during unloading, do not affect the calculated properties.

The design of the SMApp is not without its limitations. First, the SMApp does not test AFO footplate stiffness about the MTP joint [46, 109], inversion/eversion nor internal/external rotation [43, 44]. The SMApp only tests sagittal plane loading about the ankle, which is the dominant plane of ankle motion during walking. Second, the AFO sometimes twisted during testing. This occurred due to the geometry of some AFOs, where the AFO's vertical axis through the shank was not always centered about its ankle width. This torsional motion contradicts modeling the AFO as a single-degree-of-freedom rotational spring acting on a hinge joint. It may be accommodated in future work by fitting custom-footplate clamps and allowing rotation of the clamp fixture and/or adjustment of the surrogate leg to better align the SMApp's loading action with the AFO's primary plane of motion. Third, during the unloading portions of the curves, the actuator torque and AFO's torsional spring torque are both contributing to the AFO's return to its neutral angle and cannot be decoupled in the SMApp's load cell readings. This could potentially be resolved by compromising on speed control and releasing the AFO from the actuator during unloading. Finally, while the SMApp can accommodate a variety of AFO sizes, it is restricted to AFOs with a minimum ankle width of about 2 inch (5 cm) due to the footplate clamp geometry.

The SMApp's speed is set as a rotational speed of its motor that can correspond to different ankle flexion speeds for different AFOs. This occurs because the thickness of the AFO changes the height of the SMApp's footclamp. This change in geometry alters the gear ratio between the linear actuator speed, dictated by the motor's rotational speed, and the angular speed at the surrogate ankle. Therefore, while we performed the reliability study at the same motor speed for all AFOs, each AFO had a different angular speed at the ankle. In this study, all comparisons were made within an AFO rather than between them, so this difference did not affect the comparisons. Future studies comparing AFOs directly should adjust the motor speed for each AFO to match the same angular speed at the surrogate ankle. Speed transitions in the SMApp were handled by the internal set speed control of the servo drive. We selected a square velocity profile, with zero acceleration/deceleration times and a constant speed, however, a square profile is not physically

possible and transition times are limited by the motor capabilities. While the transitions had minimal effects on our AFO properties, which are calculated from steady-state segments of the torque-angle curve, future work should consider a trapezoidal velocity profile and explore different acceleration/deceleration rates to soften speed transitions. Additionally, utilizing a reference generator to perform speed control would allow tracking of velocity profiles, to match profiles during gait, rather than a set constant speed currently utilized through the servo's internal set speed control method.

3.8 Conclusion

The stiffness measurement apparatus (SMApp) is a non-destructive, automated device that can test a large array of AFO sizes and types across ranges of motion and flexion speeds that exceed current alternatives. The SMApp measurements were shown to be highly repeatable and the stiffness properties were comparable to an alternative manual measurement device. Future work will include using the SMApp for material fatigue testing to ensure longevity of new and existing AFOs, to validate finite element models, and to evaluate speed effects on AFO properties.

CHAPTER 4

The Effect of Rotational Speed on Ankle-Foot Orthosis Properties[1]

Summary

Background: Ankle-foot orthoses (AFOs) are devices that support ankle motion. The rotational stiffness of the AFO in the sagittal plane, can affect gait kinematics. Stiffness is calculated from linear regressions of an AFO's torque-angle curve. These regressions do not include damping and viscoelastic parameters. Because AFOs are often made from viscoelastic materials, their torque-angle dynamics may vary at different walking speeds and these models may not capture true AFO properties. The influence of rotational speed on AFO dynamics has not been thoroughly investigated. **Research Question:** What is the impact of ankle rotational speed on AFO properties? **Methods:** We tested a sample of three AFOs: one thermoplastic, one 3-D printed nylon and one 3-D printed polyether block amide (PEBA). Each AFO's dynamic ankle torque was measured as it was flexed at four speeds ($5 - 20$ °/s) using a custom-built stiffness measurement apparatus (SMApp). We compared linear approximations of loading stiffness, neutral angle, and energy dissipation parameters for each AFO across speeds. **Results:** There was a statistically significant effect of speed on stiffness for all AFOs tested ($p < 0.05$). The neutral angle of the thermoplastic AFO was affected by flexion speed ($p < 0.001$), while there was no effect on the two printed AFOs. Energy dissipation, as indicated by hysteresis area, was significantly affected by speed for all AFOs ($p < 0.001$). **Significance:** Flexion speed can influence the properties of a variety of different AFOs. The differences in AFO stiffness, neutral angle, and energy dissipation were quite small (< 0.5 Nm/°, < 0.6 °, and < 0.6 J), however. Future work should assess whether these small variations of stiffness and neutral angle have a

[1] A version of this chapter was submitted for publication to the Journal of Biomechanics: D. Totah, K. Barton, and D. Gates. The Effect of Rotational Speed on Ankle-Foot Orthosis Stiffness. Journal of Biomechanics. (submitted July, 2020)

clinically meaningful impact on user performance, explore effects of higher speeds on a variety of AFO materials and designs, and investigate more complex models for representing AFO dynamics that include damping and viscoelastic parameters.

4.1 Introduction

Ankle-foot orthoses (AFOs) are used to support the ankle during walking. The benefit of an AFO may depend on its design. In particular, AFO rotational stiffness affects ankle and knee kinematics during gait [70]. Many of the thermoplastics used to make AFOs are viscoelastic, meaning their properties are speed-dependent. The AFO's effectiveness may therefore vary at different walking speeds.

AFO behavior is often represented and discussed by its stiffness parameter, which is typically the slope of a linear regression applied to either a segment of or the entire torque-angle curve for that AFO. This representation follows a model without damping parameters. If an AFO's dynamics are not affected by speed, then this model should hold regardless of speed, and stiffness can easily be calculated from this linear model. However, if viscoelastic effects are present, then the linear model no longer applies and the stiffness it approximates will be muddied by torque components from a missing damping term. In this chapter refer, 'stiffness' refers to the slope of this linear model that ignores damping.

Only a few studies have investigated the effect of speed on AFO properties [31]. Two studies visually observed the stiffness curve when AFOs were tested at different speeds. One noted that thermoplastic AFOs were not affected by speed [47], while the other had mixed results across speeds for an AFO with oil-damper joint [48]. A third study statistically compared stiffness of thermoplastic AFOs across speeds and found no effect [49]. This study used a manual testing device, where speed cannot be controlled precisely. Thus, there is limited evidence of the true effect of speed variations on AFO stiffness.

Given the limited prior evidence and increased prevalence of new materials and orthosis manufacturing methods, such as 3-D printing [14, 15, 118], the purpose of this study was to determine if ankle rotational speed affects the stiffness of traditional and printed AFOs. We used a custom-designed mechatronic testing apparatus to control speed consistently within a cycle and from trial to trial. We also measured effects on AFO neutral angle and energy dissipation, since much of an AFO's supportive function comes from its energy storage and return capabilities due to material elasticity.

(a) Nylon AFO

(b) PEBA AFO

(c) Thermoplastic AFO

Figure 4.1: The three AFOs used in this study. The nylon, PEBA, and thermoplastic AFOs had wall thicknesses of 7.5, 3.6, and 3.5 mm, foot lengths of 27.0, 28.0 and 27.0 cm, and heights of 39.0, 36.0, and 41.5 cm, respectively.

4.2 Methods

We tested a sample of three solid-ankle, i.e. non-articulated, AFOs (Figure 4.1): one traditionally-manufactured thermoplastic AFO made from a polyethylene and polypropylene composite, and two 3D-printed AFOs made using fused deposition modeling, one with carbon fiber enforced nylon and one with polyether block amide (PEBA). Each AFO was clamped, by the same operator, to a custom Stiffness Measurement Apparatus (SMApp, Figure 4.2a) [119]. The SMApp cycled the AFO through its range of motion in dorsiflexion and plantarflexion, 10 times, at each of four speed conditions in ascending and then descending order. Forty cycles were collected for each of the three AFOs, for a total of 240 cycles. Eight cycles were excluded because a sensor error caused them to terminate before completion.

The four commanded motor speed conditions (78, 156, 234 and 313 rotations per minute) corresponded to sagittal plane ankle speeds of 5, 10, 15 and 20 °/s, calculated without an AFO in the device. The rotational speeds varied slightly when the AFOs were mounted in the SMApp due to differences in AFO geometries, specifically in footplate thickness and ankle location. The differences in speed conditions between the AFOs has no effect on the results since all comparisons were made within each AFO group.

Measurements from the SMApp were used to create a torque-angle curve for each AFO. Several AFO properties were calculated from these curves (Figure 4.2b). First, AFO stiffnesses in plantarflexion and dorsiflexion were calculated as the slope of a linear regression of the loading portions of the rising and falling curve segments, respectively. AFO dorsiflexion and plantarflexion neutral angles were the x-intercepts of the falling and rising curves, respectively. Due to material hysteresis, the resistive torque during unloading is

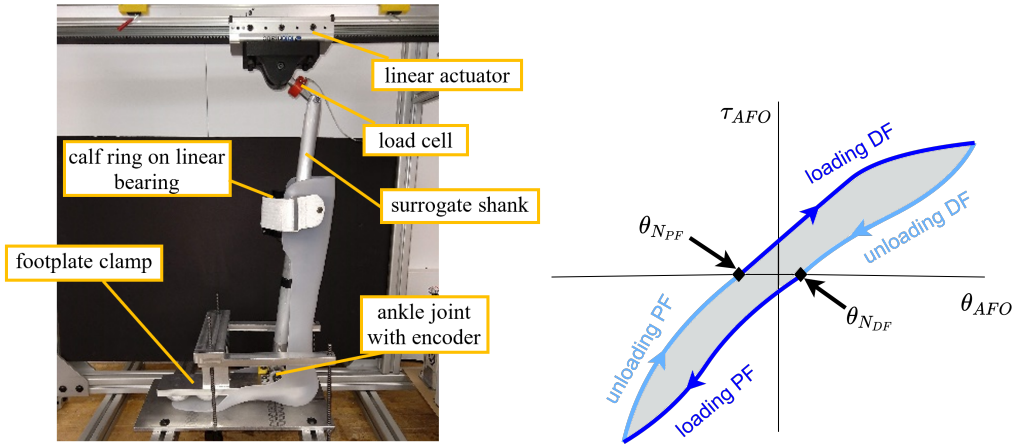

(a) (b)

Figure 4.2: (a) An AFO mounted in the Stiffness Measurement Apparatus (SMApp). (b) Schematic of an AFO's ankle torque versus angle curve showing plantarflexion (PF) and dorsiflexion (DF) loading and unloading regions and neutral angles (θ_N). The shaded area inside the hysteresis loop represents the AFO's energy dissipation.

different than that during loading, resulting in a torque angle curve with a loop shape. The area in this hysteresis loop represented the AFO's energy dissipation.

We tested for differences in each of these AFO properties across speed conditions using a series of one-way ANOVAs ($\alpha = 0.05$), separately for each AFO, using SPSS v26 (IBM, Armonk, NY, USA). To aid in interpretation, we then compared the measured differences to their minimum detectable difference values [119].

4.3 Results

While the torque-angle curves may appear similar at different speeds (Figure 4.3), statistical analyses of the AFOs' properties reveal significant effects. Differences in dorsiflexion loading stiffness were significant across speeds for all three AFOs ($p \leq 0.010$; Figure 4.4). There were also significant speed effects for plantarflexion loading stiffness for the printed AFOs ($p \leq 0.002$), but not for the thermoplastic AFO ($p = 0.612$). Of these effects, only differences in the nylon AFO's plantarflexion stiffness ($0.43 - 0.50$ Nm/°) were greater than the minimum detectable difference (MDD) of 0.13 Nm/° [119] (Table 4.1).

The neutral angles in dorsiflexion and plantarflexion were affected by speed. These effects were significant for the nylon ($p \leq 0.015$) and thermoplastic ($p < 0.001$) AFOs, but not the PEBA ($p = 0.241$ and $p = 0.519$). While the differences in neutral angle were quite small ($< 0.6°$), those for the thermoplastic AFO were greater than the MDD of $0.2°$.

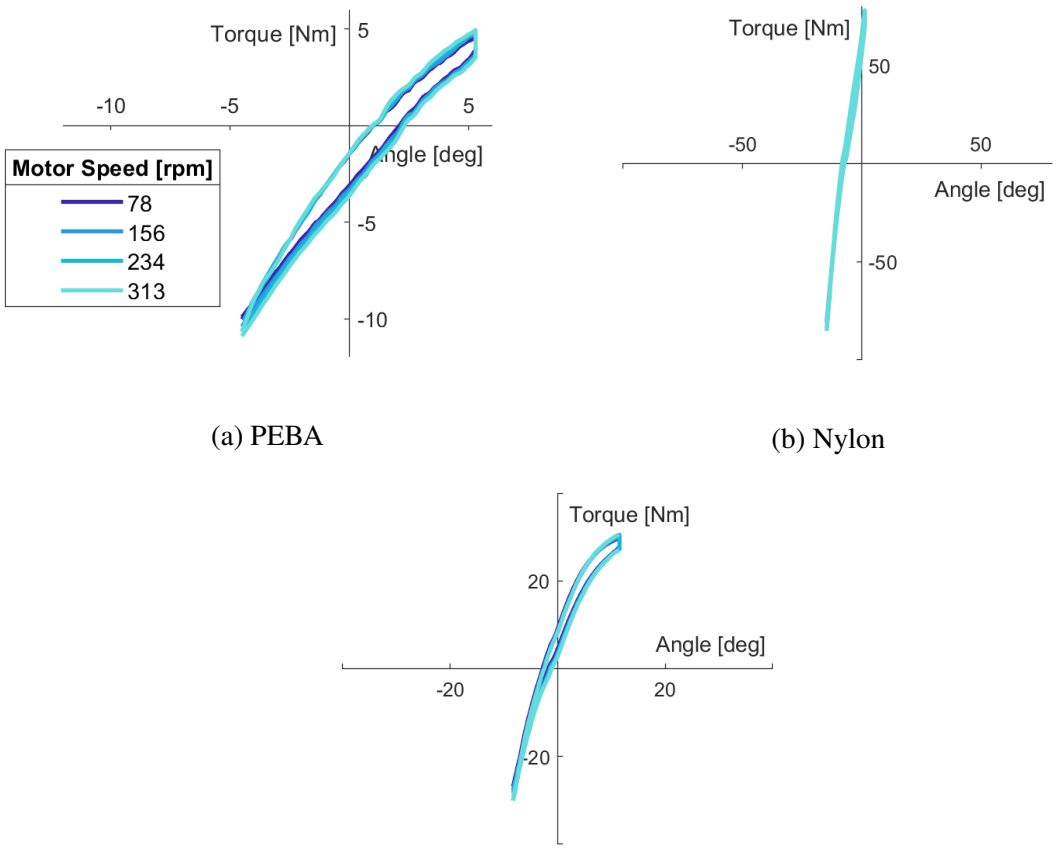

(a) PEBA

(b) Nylon

(c) Thermoplastic

Figure 4.3: The torque-angle curves of three AFOs at four different flexion speeds.

Following the same trend as dorsiflexion stiffness, differences in hysteresis area across speeds were significant for all three AFOs ($0.03 - 0.57$ J; $p < 0.001$). However, differences in the PEBA AFO's area were lower than the MDD of 0.20 J.

4.4 Discussion

This study demonstrated that traditional and 3-D printed AFOs exhibit viscoelastic effects. Changes in ankle rotational speed caused small but statistically significant differences in approximations of AFO stiffness, neutral angle and hysteresis area. Changes in stiffness or energy dissipation patterns could alter the orthosis's resistance torques and degree of support it provides. For example, for patients using AFOs to assist with drop-foot, alterations to stiffness and neutral angle may mean changes to plantarflexion resistance affecting the ability to achieve ground clearance during swing [120].

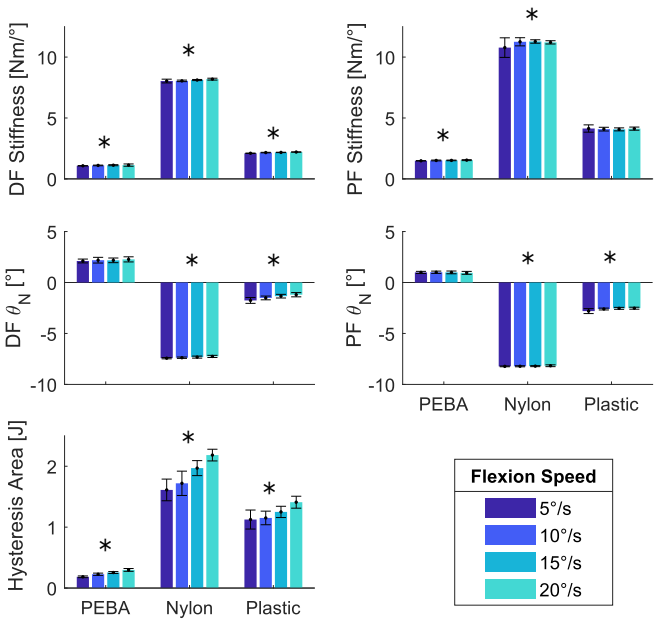

Figure 4.4: AFO properties of dorsiflexion (DF) and plantarflexion (PF) loading stiffness and neutral angle (θ_N), and hysteresis area at the four tested flexion speeds for the three AFOs (PEBA, nylon, and thermoplastic). * Significant main effect of speed ($p < 0.05$).

Our results differ from those of another study, where there were no speed effects on the stiffness of 18 traditionally-manufactured, thermoplastic AFOs [49]. There are several differences between these studies that may explain the contrasting findings. First, the measurement devices differed in their approaches to controlling speed. While we used a mechanical device to automate angular speed, the study in [49] used a manually-operated measurement device, where the operator targeted specific walking cadences ($30-60$ steps/min.) by following a metronome. Second, there are differences in how stiffness was quantified between the two studies. Novachek et al. measured stiffness by fitting a linear regression to the entire torque-angle hysteresis loop, rather than separately to the loading and unloading phases [115, 119]. The slope of the overall curve may mask the effects on hysteresis. Finally, the AFOs tested in this study had larger stiffness ranges ($1 - 13$ Nm/°) than those tested in [49] (≤ 1.3 Nm/°).

While the SMApp followed a constant speed in each flexion direction (PF and DF), the velocity profile at the transition between the two directions is not known. The profile was dictated by the servo motor's capabilities and controlled through an internal speed control loop within the servo drive. Nonetheless, the transition profile has a minimal effect on the calculated AFO properties in this chapter. This is because the speed transitions occur at the

edges of the flexion testing range of motion and the dynamics described by the stiffness, neutral angle and hysteresis mainly occur during the steady-state portions.

In conclusion, this study provided preliminary evidence that both printed and traditional AFOs have viscoelastic properties. Current representations of AFO stiffness as a linear fit ignore these viscoelastic effects and so a more complex model that includes damping and viscoelasticity parameters may be more appropriate. Future work should investigate the development of such a model. Future work should also assess whether the small variations of AFO stiffness, neutral angle, and energy dissipation found in this study have a clinically meaningful impact on user performance, as well as explore effects of higher speeds and different velocity profiles on a variety of AFO materials and designs, including different printing techniques and orientations.

Table 4.1: The measured properties of each AFO at four speed conditions (S1, S2, S3, and S4) and the results of statistical testing for speed effects.

(a) PEBA AFO

		Speed Condition						
		S1	**S2**	**S3**	**S4**			
Motor Speed [rpm]		78	156	234	313		**Speed Effects p-value**	**Significant Pairwise Comparisons[1] (absolute mean difference)**
Ankle Speed [$°/s$]		5	10	15	20	**Total**		
AFO Property								
DF k [$Nm/°$]	Mean	1.0754	1.1049	1.1238	1.1321	1.1094	0.010*	S1-S4 (**0.06**), S3-S4 (**0.05**)
	N	19	16	20	19	74		
	SD	0.01151	0.02748	0.0437	0.0933	0.0577		
PF k [$Nm/°$]	Mean	1.4847	1.5122	1.5169	1.5394	1.5134	<0.001*	S1-S2 (0.03), S1-S3 (0.03), S1-S4 (0.05), S2-S4 (0.03)
	N	19	16	20	19	74		
	SD	0.01390	0.03363	0.0263	0.0393	0.0351		
DF θ_N [°]	Mean	2.1106	2.1886	2.1743	2.2691	2.1854	0.241	
	N	19	16	20	19	74		
	SD	0.18798	0.2804	0.2288	0.2512	0.2395		
PF θ_N [°]	Mean	0.9905	1.0060	0.9910	0.9468	0.9828	0.519	
	N	19	16	20	19	74		
	SD	0.10274	0.11172	0.1345	0.1434	0.1242		
Hysteresis Area [J]	Mean	0.1846	0.2266	0.2548	0.2977	0.2417	<0.001*	S1-S2 (0.04), S1-S3 (0.07), S1-S4 (0.11), S2-S3 (0.03), S2-S4 (0.07), S3-S4 (0.04)
	N	19	16	20	19	74		
	SD	0.01422	0.01850	0.0157	0.0231	0.0456		

Continued on next page

(b) Nylon AFO

		Speed Condition						
		S1	**S2**	**S3**	**S4**		**Speed Effects p-value**	**Significant Pairwise Comparisons[1] (absolute mean difference)**
Motor Speed [rpm]		78	156	234	313			
Ankle Speed [°/s]		5	8	13	17	**Total**		
AFO Property								
DF k [$Nm/°$]	Mean	8.0336	8.0478	8.1164	8.1893	8.0973	<0.001*	S1-S3 (**0.08**), S1-S4 (**0.16**), S2-S4 (**0.14**)
	N	19	20	19	20	78		
	SD	0.15370	0.06329	0.0455	0.0767	0.1112		
PF k [$Nm/°$]	Mean	10.7783	11.2562	11.2804	11.2097	11.1338	0.002*	S1-S2 (**0.48**), S1-S3 (**0.50**), S1-S4 (**0.43**)
	N	19	20	19	20	78		
	SD	0.80416	0.33510	0.1415	0.1341	0.4795		
DF θ_N [°]	Mean	-7.4286	-7.3801	-7.3200	-7.2531	-7.3447	<0.001*	S1-S3 (0.11), S1-S4 (0.18), S2-S4 (0.13)
	N	19	20	19	20	78		
	SD	0.06261	0.0670	0.0999	0.1055	0.1072		
PF θ_N [°]	Mean	-8.2294	-8.2183	-8.2070	-8.1688	-8.2056	0.015*	S1-S4 (0.06)
	N	19	20	19	20	78		
	SD	0.03972	0.05266	0.0498	0.0875	0.0637		
Hysteresis Area [J]	Mean	1.6112	1.7198	1.9693	2.1833	1.8730	<0.001*	S1-S3 (**0.36**), S1-S4 (**0.57**), S2-S3 (**0.25**), S2-S4 (**0.46**), S3-S4 (**0.21**)
	N	19	20	19	20	78		
	SD	0.17795	0.19968	0.1231	0.0961	0.2709		

(c) Thermoplastic AFO

		Speed Condition						
		S1	**S2**	**S3**	**S4**		**Speed Effects p-value**	**Significant Pairwise Comparisons[1] (absolute mean difference)**
Motor Speed [rpm]		78	156	234	313			
Ankle Speed [°/s]		5	11	16	21	**Total**		
AFO Property								
DF k [$Nm/°$]	Mean	2.1029	2.1607	2.1730	2.2045	2.1603	<0.001*	S1-S2 (**0.06**), S1-S3 (**0.07**), S1-S4 (**0.10**), S2-S4 (**0.04**), S3-S4 (**0.03**)
	N	20	20	20	20	80		
	SD	0.01646	0.02141	0.0150	0.0154	0.0407		
PF k [$Nm/°$]	Mean	4.1351	4.0845	4.0654	4.1257	4.1027	0.612	
	N	20	20	20	20	80		
	SD	0.29976	0.15298	0.1231	0.1287	0.1890		
DF θ_N [°]	Mean	-1.7606	-1.5144	-1.3420	-1.1986	-1.4539	<0.001*	S1-S2 (**0.25**), S1-S3 (**0.42**), S1-S4 (**0.56**), S2-S4 (**0.32**)
	N	20	20	20	20	80		
	SD	0.28589	0.1846	0.1796	0.2078	0.3007		
PF θ_N [°]	Mean	-2.8057	-2.6025	-2.5369	-2.5226	-2.6169	<0.001*	S1-S2 (**0.20**), S1-S3 (**0.27**), S1-S4 (**0.28**)
	N	20	20	20	20	80		
	SD	0.24327	0.09076	0.0961	0.0978	0.1835		
Hysteresis Area [J]	Mean	1.1249	1.1512	1.2503	1.4096	1.2340	<0.001*	S1-S3 (0.13), S1-S4 (**0.28**), S2-S4 (**0.26**), S3-S4 (0.16)
	N	20	20	20	20	80		
	SD	0.15611	0.11169	0.0925	0.0982	0.1608		

*Indicates a significant p-value with $\alpha = 0.05$.

[1] Post-hoc pairwise comparisons between speed conditions were performed, with Sidak corrections, for AFO properties with significant speed effects, using SPSS v26 (IBM, Armonk, NY, USA). Only pairs with significant effects are shown. Mean differences greater than the measurement's minimum detectable difference are bolded.

CHAPTER 5

Quantifying the Kinematic Effects of AFO Emulation

5.1 Introduction

Actuated exoskeleton devices with tethered off-board motors (i.e. not mounted to the exoskeleton body) have been proposed for rehabilitation robotics [121]. Recently, their use as emulation test beds for prototyping and device parameter tuning has emerged [25, 50, 52, 69]. The off-boarding of the motor systems makes for light-weight devices that can be easily controlled to facilitate the exploration of much larger parameter spaces. The separation of the actuator and controller from the device also allows researchers to vary different device parameters independently and study their effects.

These emulator systems show great potential as prototyping test beds for investigating the effect of key device design and control parameters on subject performance and patient benefit. Some research groups have utilized such emulator systems to explore the optimality of different control parameters and schemes based on various measures, such as metabolic cost [52] or muscle activity [69] for unimpaired individuals. One group used a prosthesis emulator to evaluate candidate lower-limb prosthetic devices, by measuring user performance metrics and preferences as they 'try on' the different devices [50]. In [50], Caputo et al. mimic only active devices with the exception of an elastic-response passive prosthesis emulated for evaluation as a candidate device.

In Chapter 2, we discussed the need for standardized studies to investigate AFO stiffness effects on the user. Emulators could be a promising solution; providing precise control of key design parameters in one wearable device. While the use of active exoskeletons to emulate passive devices has not been extensively investigated, the prevalence of compliant actuation schemes used in these devices makes them promising for tracking AFO stiffness. Series-elastic actuation is a common form of compliant actuation used for haptic rendering of stiffness [50, 121–124].

Unfortunately, it is not known whether emulated and physical devices have the same influence on human performance. Designers of these emulation systems aim to recreate the torque-angle profiles of active or passive physical devices. The emulators are validated in terms of torque reference tracking errors and bandwidth [25, 124]. However, physical and emulated versions of the same device may have different weight and mass distributions and compliance in other planes of motion not captured in the emulated torque-angle relationship, all of which could influence motion. There is a need to understand how user movement differs when walking in these tethered emulators from walking in the untethered physical devices they are emulating. Moreover, before emulators can be deemed useful for studying the effect of a particular design parameter on the user, we need to understand which performance metrics are affected by emulation and which remain consistent between emulated and physical devices.

Therefore, the objective of this work was to develop a methodology to validate an AFO emulator from a biomechanical sense by comparing kinematic differences between emulated and physical AFOs. We did this by first building an AFO emulator system that used series-elastic actuation of an ankle exoskeleton to track the stiffness of physical AFOs, as measured by methodology developed in Chapter 3. Next, we quantified differences in kinematics while walking with a physical AFO and its emulated representation. The study focused on ankle kinematics since they are the most consistently reported measure to be affected by rotational stiffness in AFO literature (Chapter 2).

5.2 The AFO Emulator System[1]

To test the biomechanical effects of walking with an emulated AFO, we built an AFO emulator system consisting of a hinged ankle exoskeleton, instrumented with a sensing suite, and an off-board motor for applying plantarflexion torques via series-elastic actuation (Figure 5.2).

Exoskeleton Design

The exoskeleton had a single joint at the ankle with one degree of freedom. It was constructed from a surgical shoe with an embedded steel plate for rigidity and to allow it to interface with hinged upright metal struts (Figure 5.1). The metal struts met at the calf,

[1]Supplementary files including code to configure and operate the AFO emulator system can be found at this link: https://drive.google.com/drive/folders/11203bS2ZBxkzoXIUXlWmh7sLdPkfaDYD?usp=sharing

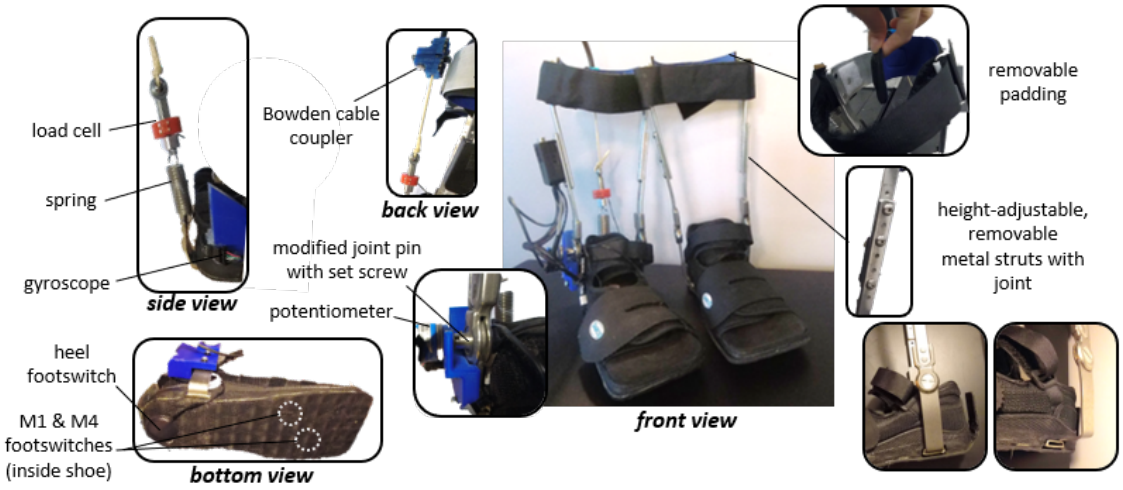

Figure 5.1: The instrumented and uninstrumented exoskeletons of the AFO emulator system worn on the right leg and left leg, respectively.

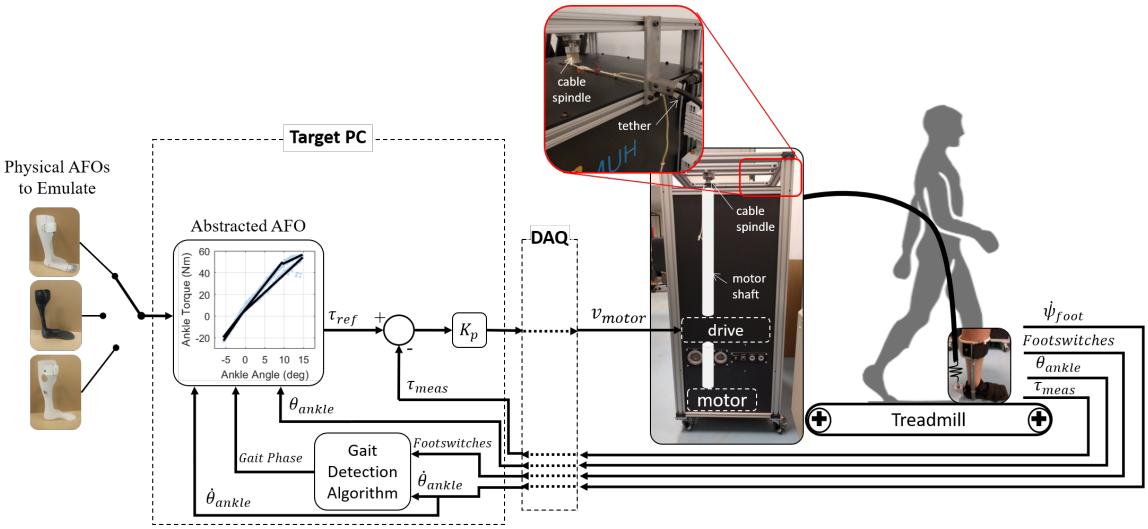

Figure 5.2: The AFO emulator system and its control diagram. A particular AFO is manually selected for emulation, then abstracted to its stiffness representation. Sensors on the exoskeleton measure ankle angle (θ_{ankle}), foot inclination velocity ($\dot{\psi}_{foot}$), torque (T_{meas}), and the state of three footswitches, which are used to calculate an appropriate motor velocity (v_m) command through proportional (P) feedback control.

where they were welded to a cuff outfitted with a hook and loop strap for securing the exoskeleton around the shin. The metal footplate embedded in the shoe also extended past the shoe posterior side, slightly beyond the heel. This extension provided an attachment point for the actuation spring discussed in the following subsection.

The exoskeleton was designed with a certain degree of adjustability in mind to fit a range of users. The metal struts can be adjusted for different calf heights, and can be detached from the surgical shoe to be used with a different shoe size. The metal band around the calf has padding for user comfort; several padding options of different thicknesses are available to accommodate different calf widths or circumferences. The padding pieces are outfitted with hook and loop patches so they can be easily switched out. Finally, the open style of the surgical shoe and its highly adjustable hook and loop straps, make it easy to accommodate a range of foot sizes.

Actuation

Torque was applied about the exoskeleton joint using series-elastic actuation. A Bowden cable was run through a conduit from the motor spindle and attached to a metal plate extending posteriorly from the exoskeleton footplate via an in-line extension spring. As the motor shaft rotates, the cable is wound up around the spindle and extends the spring to apply an upward force on the footplate. The point of force application is located posterior to the hinge joint, which provides the moment arm to convert the force to a plantarflexion moment.

The motor's position and rotation direction dictate the stretch of the spring and, thus, the amount of torque applied to the exoskeleton user's ankle. By commanding motor motion parameters, we can track different torque trajectories to emulate a variety of AFO stiffness patterns. The spring used in the pilot study in this chapter had a stiffness rate of 2.85 N/mm (Extension Spring 37090GS, Gardner Springs). The motor, drive, and Bowden cable assembly was purchased from Humotech (Pittsburgh, PA).

Sensing

The exoskeleton was outfitted with several sensors:

- A load cell (LC201, Omega, Norwalk, CT) was placed in-line between the series-elastic spring and Bowden cable to measure the total force causing a plantarflexion moment about the ankle. Ankle torque was calculated by multiplying the force measurement with the exoskeleton moment arm (0.07 m).

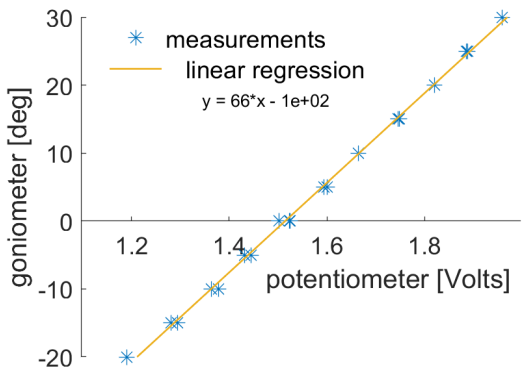

Figure 5.3: The calibration curve of the potentiometer sensor.

- A potentiometer (6637-Precision Potentiometer, Bourns Inc., Riverside, CA) coupled with the exoskeleton hinge joint provided ankle angle measurements.
- Three touch pad switches (7692K3, McMaster-Carr, Elmhurst, IL) were placed in the exoskeleton shoe to serve as footswitches for detecting ground contact at the heel and the first and fourth metatarsals.
- A single-axis gyroscope (ENC-03RC, KNACRO through www.Amazon.com) attached to the exoskeleton shoe measured foot inclination velocity for gait phase detection.

These analog sensor signals were collected by a set of data acquisition modules (DAQ) from Beckholf Automation LLC and transmitted to a target PC through EtherCAT protocol. The DAQ modules consisted of a main EtherCAT coupler (EK1100), a 5-volt power supply terminal (EL9505), a differential analog input module (EL3102) for reading the load cell signal, and an 9-channel single-ended analog input terminal (EL3068) for reading the remaining sensors. The load cell signal was filtered and amplified through a signal conditioner before it was read by the DAQ. The same transmission and receive lines of the EtherCAT protocol handled exoskeleton sensor readings and communication with the motor drive, managed by custom code using Simulink Real-Time software (Mathworks Inc., Natick, MA).

The load cell calibration was tuned before each trial using a shunt calibration resister according to the manufacturer's manual. We also checked the calibration by hanging a weight from the load cell prior to its assembly into the exoskeleton system. The potentiometer sensor was calibrated after it was mounted on the exoskeleton. We used a manual goniometer to position the exoskeleton's ankle joint between -20 and 30° (in increments

of 5°) while the potentiometer voltage was measured, to produce a linear model relating voltage readings to ankle angles (Figure 5.3).

Torque Trajectory Tracking

To emulate a particular physical AFO, we need the abstracted representation of the AFO in the form of its measured stiffness curve (see Chapter 3). From the AFO's torque-angle curve (Figure 5.4b), we get the plantarflexion (PF) neutral angle and the dorsiflexion (DF) loading segment of the curve. These AFO properties are used to determine the desired reference torque the emulator should track during a walking trial based on sensor readings.

A gait detection algorithm, adapted from [125], uses the footswitch and gyroscope sensors to determine the subject's gait cycle phase in real-time. *During stance*, the DF loading portion of the torque-angle curve is used to look up the desired resistance torque for joint angles greater than the emulated AFO's PF neutral angle. The desired torque is divided by the moment arm (0.07 m) to yield a desired force value that is sent to the controller. *During swing* and when the exoskeleton's joint angle is smaller than neutral, the desired force is set to 8 N (ankle torque of 0.56 Nm) to just keep the series elastic actuation cabling taught without transferring significant torque to the user. This passive tension force was found empirically through trial and error.

A proportional feedback control loop compares load cell force readings with the desired force. The force error is multiplied with a proportional gain (k_P = 0.300) and sent as a velocity command to the motor drive, which has its own feedback control inner-loop.

Safety Features

Several features were implemented to maintain the safety of the emulator test bed:

- A hardware stop at the exoskeleton joint limits plantarflexion to a maximum of $42°$. Note that dorsiflexion limits are not needed since the emulator can only apply forces by *pulling* the Bowden cable towards greater plantarflexion, and has no way to apply dorsiflexion moments.
- A manually-activated emergency stop button cuts power to the motor.
- Participants wear a safety harness, tethered to a gantry system, while walking on the treadmill. A magnetic stop switch is also clipped to the participants' clothing, which triggers an emergency stop in the treadmill belt if detached.

(a) AFOQ1

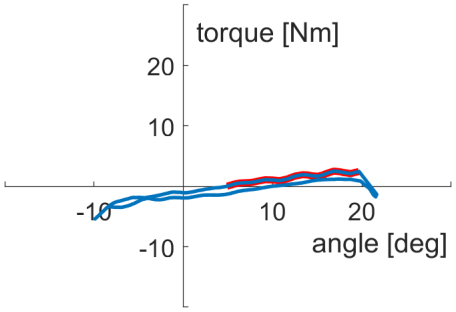

(b) AFO torque

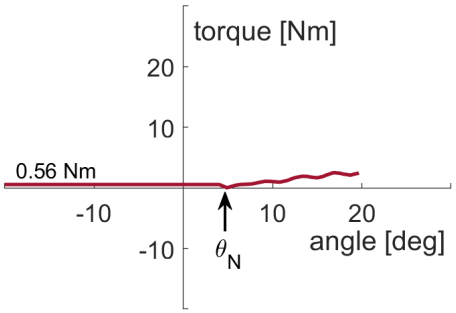

(c) Reference torque

Figure 5.4: This figures shows (a) a photo of the AFO used in the pilot study in this chapter, (b) the AFO's measured torque-angle curve with the dorsiflexion loading segment to be emulated highlighted, and (c) the generated reference torque-angle trajectory for emulating this AFO. The reference torque trajectory follows the AFO's loading torque profile for angles greater than the plantarflexion neutral angle (θ_N), a constant torque (0.56 Nm) at angles smaller than neutral. The emulated AFO (AFOQ1) had a wall thickness of 2.5 mm, foot length of 16.5 cm, and height of 32.5 cm.

- A break-away cable connects the Bowden cable rope to the rope around the emulator's motor spindle, to ensure excessive forces are not transferred to the end-effector exoskeleton.
- A rope is tied in parallel with the series-elastic spring to ensure the Bowden cable, load cell and exoskeleton footplate stay connected in case the physical spring breaks.
- Limits in the control software:
  - Maximum commanded motor velocity saturates at 100 rpm.
  - A safety check triggers a fault to disable motor power if the load cell reads forces exceeding 300 N.

5.3 Pilot Study

One healthy subject (29 yrs, female) with no gait impairments walked on a treadmill (2.2 mph) to a metronome (100 steps/min) for five minutes at each of three test conditions. The conditions tested were: 1) **Physical AFO** - wearing an AFO on the right leg inside the instrumented exoskeleton, disconnected from the motor, 2) **Emulated AFO** - wearing the exoskeleton as it emulates the physical AFO's stiffness, and 3) **No AFO** - wearing the exoskeleton disconnected from the motor. The subject also wore an unactuated exoskeleton on the left leg during all conditions, for symmetry. This study was approved by the University of Michigan's Institutional Review Board.

To accommodate a malfunction of the gyroscope sensor at the start of this collection, two changes were made to the emulator framework. First, the gait detection algorithm was modified to use only the footswitch sensors to detect the current gait phase. Second, during the *emulated AFO* condition, the exoskeleton was set to emulate AFO stiffness for any angle greater than the plantarflexion neutral angle regardless of the current gait phase. This is a change from the emulator's normal operation, where stiffness is emulated past neutral during the stance phase only and not during swing.

The Physical AFO

An off-the-shelf posterior leaf spring, plastic AFO (Figure 5.4) was purchased in a size that would fit the pilot subject. The torque-angle curve, or stiffness curve, of the AFO was measured with a custom stiffness measurement apparatus (SMApp) described in Chapter 3. We determined the ankle angle range and angular speed at which to test the AFO in

the SMApp from ankle trajectories collected from our subject in a prior walk test. The subject walked on a treadmill (2.2 mph, 100 steps/min) while wearing the instrumented exoskeleton for five minutes. The first minute and final minute of data were discarded, leaving three minutes of walking for analysis. Right leg walking strides were isolated from the collected right ankle trajectory and averaged. The maximum dorsiflexion angle ($15°$) and mean absolute angular velocity ($60°/s$) of the averaged stride's stance phase determined the range and speed of AFO testing in the SMApp, respectively.

Data Analysis

Three minutes of data were analyzed after discarding the first and last minutes of each of the five-minute walking trials, to avoid initiation and termination effects. The potentiometer sensor angle data were segmented into individual strides starting at heel-strike and ending at toe-off, as detected by the exoskeleton's footswitch sensors. The stride ankle angle trajectories were then normalized to a percentage of the stance phase of the gait cycle. Finally, we calculated the range of motion, maximum dorsiflexion angle, angle at toe-off, and timing of maximum dorsiflexion. These ankle kinematics features were calculated for each of the three test conditions and any similarities or differences were observed.

5.4 Results

Walking with or without a physical or emulated AFO resulted in similarly shaped ankle trajectories during stance (Figure 5.5). The trials with a physical or emulated AFO had a lower maximum dorsiflexion angle and lower range of motion than the trials without an AFO (Figure 5.6). The timing of the maximum angle occurred at a similar percentage of stance for all three walking conditions. The toe-off angle during the emulated AFO trial was lower than for the physical AFO and no AFO conditions, which had similar toe-off angles. Additionally, the modified gait detection algorithm (excluding gyroscope data) worked well during this pilot study, clearly showing distinct gait phases (Figure 5.7).

5.5 Discussion

An AFO emulator system was successfully constructed and pilot tested with promising results. This study showed that AFO emulation by stiffness trajectory tracking is able to elicit user ankle kinematics similar to those while wearing a physical AFO, for a single-subject pilot. Due to the COVID-19 pandemic, we were unable to conduct a full subject

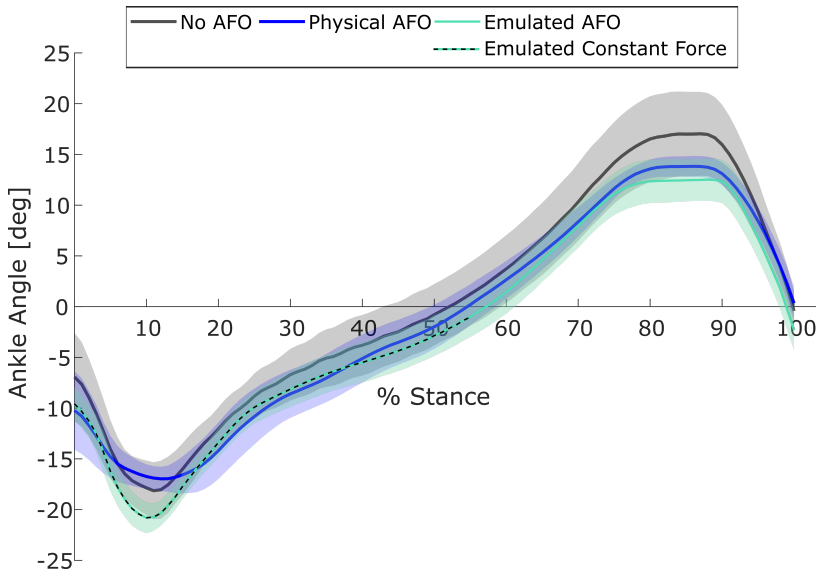

Figure 5.5: Average stride ankle trajectories during stance for the three conditions: without an AFO (No AFO), with a physical AFO, and with the emulator. The emulator condition tracks a constant force for ankle angles below the AFO's neutral angle (Emulated Constant Force) and tracks the AFO torque-angle trajectory when the ankle angle is greater than the neutral (Emulated AFO). Positive angles denote dorsiflexion. The neutral angle for this AFO was $-0.80°$. Time was normalized to a percentage of stance. The shaded regions are $+/-$ one standard deviation of the average.

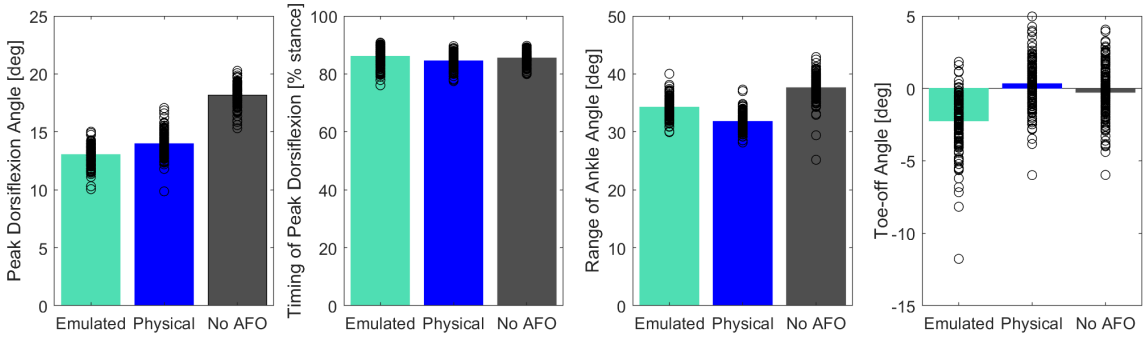

Figure 5.6: Features of ankle kinematics during three walking trials: with an emulated AFO, physical AFO, and without an AFO. The bars show average values and the circles are the values for individual strides.

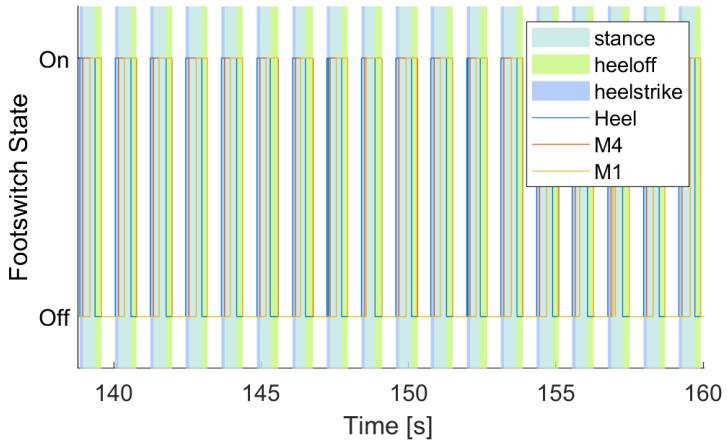

Figure 5.7: An example interval of data from a pilot walking trial showing identified gait phases and the states of the three footswitch signals used to identify them. The footswitches were placed at the heel and first (M1) and fourth (M4) metatarsals. The white (unshaded) regions depict swing phase, which starts at toe-off detected by M1's state change.

trial with a greater number of participants[1]. Nonetheless, these results show promise for emulation as a test bed for studying design parameter effects and encourage further analysis with a full subject trial. The trial should include an evaluation of knee and hip kinematics in addition to ankle kinematics. Future work should also assess emulation effects on other common measures such as heart rate, metabolic cost, and muscle activity.

Future human subject trials should test emulation for a wider range of AFOs of varying stiffnesses. A variety of off-the-shelf physical AFOs of different sizes could be purchased to accommodate different participants. To test the effect of different stiffnesses for a particular AFO design, multiple units of the same AFO could be purchased and modified. We tested this with one plastic AFO and were successfully able to increase the slope of its torque-angle curve (Figure 5.8). The stiffness was increased iteratively by heating and shaping sheets of thermoplastic onto the AFO using a heat gun. We increased the stiffness in three iterations or AFO modifications and measured the torque-angle curve in the SMApp after each modification.

There are a few limitations in the emulator system to consider before conducting a full subject trial. First, the exoskeleton's potentiometer is aligned to it's hinge which may not exactly match the user's ankle location. Adjustability in the hinge joint location would

[1]An experimental protocol for a full subject trial with a larger sample size was designed and approved by the University of Michigan's Institutional Review Board, but could not be completed due to safety restrictions during the COVID-19 pandemic. A copy of the protocol document can be found at this link: https://drive.google.com/drive/folders/11203bS2ZBxkzoXIUXlWmh7sLdPkfaDYD?usp=sharing

be a welcome addition. Second, the emulator can only apply dorsiflexion resistance with plantarflexion torques. A more complex cabling system or the addition of a second actuator could provide the capability for dorsiflexion torque emulation too. Finally, as is the case for series-elastic actuators, the stiffness of the physical series-spring must be greater than the stiffness of the emulated AFO in order to maintain passivity [123]. The spring must also be able to withstand high loads without undergoing plastic deformation.

In conclusion, this AFO emulator system will serve as test bed for understanding the effects of different AFO designs (with corresponding torque-angle trajectories) on AFO users. It will allow the investigation of user performance with, responses to, and perception of changes in torque trajectories. This system not only allows the investigation of passive AFO effects, but also opens the door for investigating the effectiveness of active torque assistance and novel torque trajectories.

The approach presented in this chapter extends beyond ankle-foot orthosis work. This chapter introduces the need to evaluate assistive device emulators of all types in terms of kinematic affects in addition to the current evaluations of tracking error and system bandwidth. The addition of clinically-relevant metrics to the emulator validation process will increase the efficacy of studies conducted with such devices, and enable the translation of design research innovations to measurable improvements in patient outcomes.

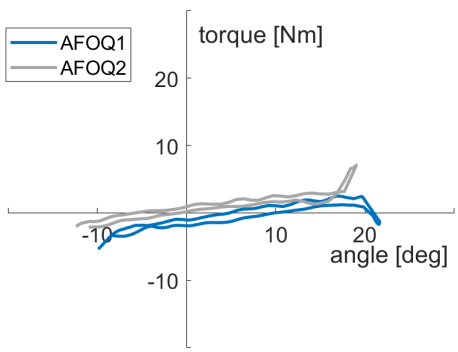

(a)

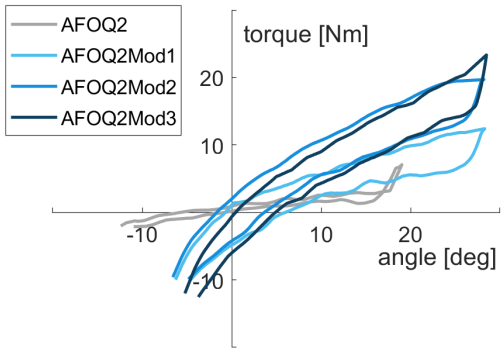

(b)

(c) AFOQ2

(d) AFOQ2Mod3

Figure 5.8: The torque-angle curves of (a) two AFOs and (b) three modifications of one of the AFOs to increase its stiffness. All curves were measured in the SMApp at 800 rpm motor speed. Photos of AFOQ2 and the third modification of the AFO are shown in (c), and (d), respectively. The stiffness was increased by adding layers of thermoplastic, formed with a heat gun, and embedding a steel bar posteriorly along the AFO height.

CHAPTER 6

Conclusions, Broader Impact and Future Work

This work set out to inform AFO design and selection by developing a better understanding of AFO properties and their effects on the user. The findings have improved our understanding of the influence of AFO properties on walking mechanics, through examining the current state of literature evidence, building a device to measure AFO torque-angle dynamics more effectively, finding the small, but significant influence of speed on linear approximations of this torque-angle relationship, and exploring whether AFOs could be effectively emulated for laboratory studies of AFO design changes on user movement.

This dissertation resulted in the development and evaluation of two test beds, one for understanding AFO mechanical properties and another for studying AFO user movement and performance. Accordingly, contributions fell into two areas. Chapters 3 and 4 explored *AFO properties and measurement*, and Chapters 2 and 5 investigated *effects on the AFO user*.

In Chapter 2, I conducted an exhaustive systematic literature review on the effects of AFO stiffness on gait. I found sufficient evidence to indicate that increasing AFO stiffness decreases ankle range of motion and increases stance knee flexion during gait. There was low evidence for the effect of stiffness on other outcome measures including hip mechanics, muscle activity and metabolics. However, differences in measured outcomes, subject populations and stiffness reporting made determining the influence of AFO stiffness on walking performance difficult. Therefore, I called for the establishment of stiffness testing and reporting guidelines and provided recommendations for future research to allow comparison of findings across studies. These recommendations included detailed reporting of trial participant contractures and controlling for footwear and walking speed during data collection.

While reviewing the AFO stiffness literature, it became clear that more effective stiffness measurement techniques were needed to study AFO design before its effects on the user can be investigated. Therefore, I developed an AFO stiffness measurement apparatus

(SMApp) and detail its design in Chapter 3. The SMApp is an automated device that non-destructively flexes an AFO to acquire operator- and trial-independent measurements of its torque-angle dynamics. It was designed to test a variety of AFO types and sizes across a wide range of flexion angles and speeds exceeding current alternatives. The SMApp measurements were shown to be highly repeatable and the stiffness properties were comparable to an alternative manual measurement device.

The SMApp was designed to measure AFO torque-angle dynamics at a controllable fixed speed. These dynamics tend to be non-linear. Common models of AFO torque-angle dynamics in literature have simplified the relationship to a linear fit whose slope represents stiffness. This linear approximation ignores damping parameters. However, as previous studies were unable to precisely control AFO flexion speed, the presence of speed effects has not been adequately investigated. Thus, in Chapter 4, I used the SMApp to explore the effect of rotational speed on AFO properties. I tested a set of AFOs at several speeds typically achieved during walking and evaluated speed effects on AFO loading stiffness, neutral angles, and energy dissipation (i.e. hysteresis area). I found preliminary evidence that both printed and traditional AFOs have viscoelastic properties, suggesting that more complex models that include damping parameters could be more suitable for modeling AFO dynamics.

After establishing a tool for investigating AFO torque-angle dynamics, and determining that flexion speed changes affected these dynamics, I moved on to developing an experimental platform to investigate how these AFO properties affect human movement. In Chapter 5, I explored the potential use of active devices with off-board actuators as AFO emulators. I developed an AFO emulator system and used it to test for the effects of emulation on subject ankle kinematics compared to using a physical AFO. Since the work in Chapter 2 highlighted ankle kinematics as the most consistently reported parameter to be affected by stiffness in literature, I proposed validating the efficacy of AFO emulation by investigating whether ankle movement is affected the same way by emulated AFOs as it is by physical AFOs. This single-subject pilot study showed that AFO emulation by torque-angle trajectory tracking is able to elicit user ankle kinematics similar to those while wearing a physical AFO. These results show promise for the use of emulation as a test bed to study design parameter effects. The results encourage further analysis with a full subject trial.

6.1 Broader Impact

The framework developed in this dissertation, which includes two experimental platforms, provides a unique method for evaluating new AFO designs, materials, and fabrication techniques, in a research-type environment, to better understand the impact of these modifications on AFO properties that affect AFO device efficacy. While these experimental platforms may not be used within a clinical setting, they will directly impact how AFO technology moves forward and provide a quantitative approach to ensuring novel advancements that positively affect AFO user outcomes.

This framework enables researchers to map the effects of different design parameters on AFO properties and then on various user metrics of import, which will inform AFO tuning and selection in the clinic. I published a conceptual example where such information could be used to to select custom-optimal AFO parameters [27] (Appendix D). In [27], a published curve relating exoskeleton ankle stiffness to metabolic cost for healthy individuals was used to inform a multi-objective optimization of AFO design parameters. Emulation test beds make it easier to produce similar curves for specific patient populations, relating any set of design and user metrics that can be measured.

The representations of AFO torque-angle profiles and findings of viscoelastic properties, in Chapters 3 and 4, extend beyond AFO rotational stiffness at the ankle. We should not dismiss the presence of hysteresis or speed-dependence when measuring the footplate torque-angle relationship at the metatarsophalangeal (MTP) joint, evaluating stiffness in motions besides those in the sagittal plane, or studying prosthesis end-effector dynamics, without testing for these effects first. The linear approximations of the torque-angle curve used in literature may not be sufficient models of AFO properties. More complex models that include viscoelasticity and damping parameters could be more appropriate.

The emulator validation approach presented in Chapter 5 also extends beyond ankle-foot orthosis work. The investigation of AFO emulation introduces the need to evaluate assistive device emulators of all types in terms of kinematic affects in addition to the current evaluations of tracking error and system bandwidth. The addition of clinically-relevant metrics to the emulator validation process will increase the efficacy of studies conducted with such devices, and enable the translation of design research innovations to measurable improvements in patient outcomes.

6.2 Recommendations for Future Work

The work accomplished in this dissertation inspires future work in: establishing guidelines and standards for testing AFOs and reporting of future AFO studies, further investigating AFO mechanical properties and modeling, and utilizing emulation to understand user performance, perception, and preferences in relation to torque-angle profile changes. These future directions are enabled by the development of two test beds in this thesis which comprise a framework for investigating AFO properties and user effects.

We propose that the standardization of AFO testing and reporting guidelines for future subject studies will unify the field and facilitate comparisons of findings. We suggest several guidelines for future studies. First, researchers should provide the type, material, pitch, manufacturing method and torque-angle curve for each AFO used. They should also cite the measurement instrument and technique used to obtain those curves. Second, AFO stiffness should be measured in both plantarflexion and dorsiflexion directions and the speed of flexion testing should be reported. Third, participants should be tested at both a prescribed walking speed and preferred speed to facilitate inter-subject comparisons. Fourth, detailed descriptions of subject characteristics should be provided, including noting any contractures. Fifth, each subject's raw data, including preferred walking speed, rather than across-subject averages should be provided to allow deeper analyses for individual stiffness effects. Finally, considering AFO-footwear interaction effects, authors should note the type, make and model of the footwear used with the AFO. When possible, we recommend standardizing footwear across participants. With future studies providing this level of detail we can better understand the effects of a wide range of stiffnesses on specific populations, and thus improve patient outcomes.

The SMApp framework developed in this work should be utilized by future studies to conduct material fatigue testing to ensure longevity of novel and traditional AFO designs; validate finite element models of AFO loading; and investigate how changes in design and manufacturing parameters affect stiffness properties. The preliminary findings of viscoelastic effects in this dissertation should be expanded, by investigating the effects of higher speeds on a variety of AFO materials and designs including different printing techniques and orientations. Additionally, the viscoelastic effects found in more complex models that include viscoelasticity and damping parameters may be able to more fully capture AFO dynamics. It is possible that more complex models could represent AFO behavior regardless of testing speed, flexion direction, or plane of motion. Future studies should also develop models of the AFO's footplate compliance. Such models could also help us understand AFO-shoe interactions to inform user fitting, and facilitate experimental design to avoid

confounding factors during subject trials.

The AFO emulator system should be utilized to investigate changes in user performance, perception, and preferences. Once the COVID-19 pandemic improves and safe trials become possible, a full subject trial will be conducted to verify the preliminary findings of the pilot study in Chapter 5. A full trial with a diverse subject population would reveal the kinematic effects of emulation on individuals with and without gait impairments. Effects on knee and hip kinematics and other physiological measures such as heart rate, metabolic cost, and muscle activity should be investigated as well. Future studies should also assess the effects of small and large variations of AFO stiffness, neutral angle, and energy dissipation to understand whether they have a clinically meaningful impact on user performance. To investigate human stiffness perception, the emulator can be used to quantify the minimum stiffness or torque changes that can be detected by a typical AFO user and the change that has an effect on their movement.

In conclusion, this dissertation has introduced new tools in the form of test beds, AFO property representations, and frameworks to validate these test beds. These tools enable: a) the needed exploration of new models to fully describe AFO dynamics, b) innovations in active and passive AFO design, and c) the investigation of user metrics and how they are affected by design changes. The AFO emulator system can be used to investigate user responses to a variety of torque-angle profiles. Optimal profiles can be translated to designs of passive or active AFOs that can be validated and studied with the SMApp system. This opens doors to a greater understanding of AFO design and how it relates to the user experience, to ultimately revolutionize AFO design and improve clinical outcomes.

APPENDICES

APPENDIX A

Literature Review Search Strategy

Database: Engineering Village (Compendex & Inspec)	
User Query: (Keyword Search)	((ankle-foot orthosis OR AFO OR ankle foot orthosis) AND (stiffness OR resistance OR compliance OR rigidity OR flexibility OR energy storage OR energy return) AND (gait OR patient outcomes OR walking OR outcomes OR patient performance OR subject performance OR performance))
Filters Activated:	none
Autostemming:	ON
Number of Results	177

Database: Web of Science	
User Query: (Keyword Search)	TOPIC: ((ankle-foot orthosis OR AFO OR ankle foot orthosis) AND (stiffness OR resistance OR compliance OR rigidity OR flexibility OR energy storage OR energy return) AND (gait OR patient outcomes OR walking OR outcomes OR patient performance OR subject performance OR performance))
Filters Activated:	none
Number of Results	194

Database: PubMed (includes Medline)		
User Query: (Keyword Search)	((ankle-foot orthosis OR AFO OR ankle foot orthosis) AND (stiffness OR resistance OR compliance OR rigidity OR flexibility OR energy storage OR energy return) AND (gait OR patient outcomes OR walking OR outcomes OR patient performance OR subject performance OR performance))	
Filters Activated:	Humans	
Query Translation:	"joint"[All Fields]) OR "ankle joint"[All Fields]) AND ("foot orthoses"[MeSH Terms] OR ("foot"[All Fields] AND "orthoses"[All Fields]) OR "foot orthoses"[All Fields] OR ("foot"[All Fields] AND "orthosis"[All Fields]) OR "foot orthosis"[All Fields]))) AND (stiffness[All Fields] OR resistance[All Fields] OR ("patient compliance"[MeSH Terms] OR ("patient"[All Fields] AND "compliance"[All Fields]) OR "patient compliance"[All Fields] OR "compliance"[All Fields] OR "compliance"[MeSH Terms]) OR ("muscle rigidity"[MeSH Terms] OR ("muscle"[All Fields] AND "rigidity"[All Fields]) OR "muscle rigidity"[All Fields] OR "rigidity"[All Fields]) OR ("pliability"[MeSH Terms] OR "pliability"[All Fields] OR "flexibility"[All Fields]) OR (("Energy (Oxf)"[Journal] OR "energy"[All Fields]) AND storage[All Fields]) OR (("Energy (Oxf)"[Journal] OR "energy"[All Fields]) AND return[All Fields])) AND (("gait"[MeSH Terms] OR "gait"[All Fields]) OR (("patients"[MeSH Terms] OR "patients"[All Fields] OR "patient"[All Fields]) AND outcomes[All Fields]) OR ("walking"[MeSH Terms] OR "walking"[All Fields]) OR outcomes[All Fields] OR (("patients"[MeSH Terms] OR "patients"[All Fields] OR "patient"[All Fields]) AND performance[All Fields]) OR (subject[All Fields] AND performance[All Fields]) OR performance[All Fields])) AND "humans"[MeSH Terms]	
Translations:	orthosis	"orthotic devices"[MeSH Terms] OR ("orthotic"[All Fields] AND "devices"[All Fields]) OR "orthotic devices"[All Fields] OR "orthosis"[All Fields]
	ankle	"ankle"[MeSH Terms] OR "ankle"[All Fields] OR "ankle joint"[MeSH Terms] OR ("ankle"[All Fields] AND "joint"[All Fields]) OR "ankle joint"[All Fields]
	foot orthosis	"foot orthoses"[MeSH Terms] OR ("foot"[All Fields] AND "orthoses"[All Fields]) OR "foot orthoses"[All Fields] OR ("foot"[All Fields] AND "orthosis"[All Fields]) OR "foot orthosis"[All Fields]
	compliance	"patient compliance"[MeSH Terms] OR ("patient"[All Fields] AND "compliance"[All Fields]) OR "patient compliance"[All Fields] OR "compliance"[All Fields] OR "compliance"[MeSH Terms]
	rigidity	"muscle rigidity"[MeSH Terms] OR ("muscle"[All Fields] AND "rigidity"[All Fields]) OR "muscle rigidity"[All Fields] OR "rigidity"[All Fields]
	flexibility	"pliability"[MeSH Terms] OR "pliability"[All Fields] OR "flexibility"[All Fields]
	energy	"Energy (Oxf)"[Journal] OR "energy"[All Fields]
	gait	"gait"[MeSH Terms] OR "gait"[All Fields]
	patient	"patients"[MeSH Terms] OR "patients"[All Fields] OR "patient"[All Fields]
	walking	"walking"[MeSH Terms] OR "walking"[All Fields]
	Humans[Mesh]	"humans"[MeSH Terms]
Number of Results	110	

APPENDIX B

Literature Quality Assessment Scales

(see tables on the following pages)

Table B.1: The modified PEDro scale used to assess the quality of the reviewed papers. Papers are awarded a point if a criterion is satisfied (Y) and zero points if the criterion is not satisfied (N) for a total score out of 10.

Modified PEDro Criteria	**Satisfied?**
1. Eligibility criteria were specified*	Y/N
2. Subjects were randomly allocated to groups* (in a crossover study, treatment order was randomized)	Y/N
3. Allocation was concealed*	Y/N
4. Groups were similar at baseline in most important indicators*	Y/N
5. Subjects were blinded*	Y/N
6. Data was obtained for more than 85% of the subjects*	Y/N
7. Consideration of available data if subjects did not receive conditions they were allocated to*	Y/N
8. Between-group statistical comparisons were reported*	Y/N
9. Both point measures and variability measures are provided*	Y/N
10. Reliability or accuracy of stiffness measurement devices or analyses was reported†	Y/N

*Criterion adapted from the original PEDro scale [85].

†This additional criterion was adapted from a modified STROBE scale [86].

Table B.2: Quality scores of the reviewed papers.

Criteria	Amerinatanzi, 2016 [87]	Amerinatanzi, 2017 [88]	Arch, 2015 [4]	Arch, 2016 [89]	Bolus, 2017 [90]	Brunner, 1998 [91]	Choi, 2017 [3]	Collins, 2015 [51]	Guillebastre, 2009 [92]	Harper, 2014 [93]	Kerkum, 2015 [94]	Kobayashi, 2011 [95]	Kobayashi, 2013 [2]	Kobayashi, 2015 [33]	Kobayashi, 2016 [34]	Kobayashi, 2017 [73]	Kobayashi, 2017 [96]	Lehmann, 1983 [97]	Ramdharry, 2012 [126]	Russell Esposito, 2014 [98]	Singer, 2014 [5]	Sumiya, 1996 [24]	Telfer, 2012 [99]	Yamamoto, 1993 [36]	Yamamoto, 1997 [45]
1. Eligibility criteria	0	0	0	0	0	0	0	0	0	0	1	0	0	0	0	0	0	0	1	1	0	0	0	0	0
2. Random allocation	0	0	1	1	1	0	1	1	1	1	1	0	1	1	1	0	0	0	1	1	1	0	0	0	0
3. Blind allocation	1	1	1	1	1	1	1	1	1	1	1	1	1	1	1	1	1	1	1	1	1	1	1	0	0
4. Similar at baseline	1	0	1	1	1	0	1	1	1	0	1	0	0	0	0	0	1	0	1	0	0	1	1	0	0
5. Subject blinding	0	0	0	0	0	0	0	0	0	0	0	0	0	0	0	0	0	0	0	1	0	0	0	0	0
6. Outcomes from >85%	1	1	1	1	1	1	1	1	1	1	1	1	1	1	1	1	1	1	1	1	1	1	1	0	0
7. Intention to treat	1	1	1	1	1	1	1	1	1	1	1	1	1	1	1	1	1	1	1	1	1	1	1	0	1
8. Between-group statistics	0	0	0	0	0	1	1	1	1	1	1	1	1	0	0	1	0	1	1	1	0	0	1	1	0
9. Point measures & variability	0	0	1	0	1	1	1	1	1	1	1	1	1	1	1	1	1	1	1	1	1	0	0	0	0
10. Test re-rest reliability	1	1	1	1	1	0	1	0	0	1	1	1	0	1	1	1	0	0	1	0	0	0	0	1	1
Total Score:	5	4	7	6	7	5	8	7	7	7	9	6	6	6	6	6	5	5	9	8	5	4	5	2	2

APPENDIX C

Summary of AFO Stiffness Effects on Gait Outcome Measures in Current Literature

The following tables contain the parameters measured in the studies reviewed in Chapter 2. The trends indicated with the arrows show the changes in that parameter as AFO stiffness was increased (i.e. the AFO was made more stiff). References in this appendix are self-contained, with the bibliography included at the end of the appendix.

Table C.1: Measures of Ankle Joint Kinematics

Ref.	Paper	N	ROM	Peak PF	Peak PF - Early Stance	Peak DF	DF - Initial Contact	DF - Midstance	PF/DF - Late Stance	DF - Foot Clearance
Studies with statistical testing										
[1]	Brunner, 1998	14	↓* [4]			↓*				
[2]	Choi, 2017	8				↓*				
[3]	Harper, 2014	13		- [5]	↓*, - [8]	↓*, - [11]				
[4]	Kerkum, 2015	15	↓*				-	-		
[5]	Kobayashi, 2011	10	↓*	↓*		↓*				
[6]	Kobayashi, 2013	5		↓*						
[7]	Kobayashi, 2017[1]	10					↑*, - [14]			
[8]	Lehmann, 1983	10			↓*, - [9]	↓*, - [12]				
[9]	Ramdharry, 2012	14								-
[10]	Russell Esposito, 2014	13		- [6]		-				-
[11]	Telfer, 2012	1			↓*				- [18]	
Studies without statistical testing										
[12]	Amerinatanzi, 2016	1	↓							
[13]	Amerinatanzi, 2017	2	↓							
[14]	Arch, 2015	2				↓, - [13]				
[15]	Bolus, 2017	1	↓			↓				
[16]	Collins, 2015[2]	9								
[17]	Kobayashi, 2015[1,3]	10			↓*, - [10]		↑*[15]			
[18]	Kobayashi, 2016[3]	6			↓*, - [10]					
[19]	Kobayashi, 2017	1				↓	↑ [16]			
[20]	Singer, 2014	5			↓					
[21]	Sumiya, 1996	1							↓ [19]	
[22]	Yamamoto, 1993	15		↓ [7]			↑ [17]			

Symbol Key

↓ Parameter decreased as stiffness increased
↑ Parameter increased as stiffness increased
- No change observed / change was not significant
* Changes were statistically significant

Abbreviations & Acronyms

N: Number of study participants
DF: Dorsiflexion
PF: Plantarflexion
ROM: Range of Motion

Footnotes

[1] Kobayashi et al. [7] had the same subject population as Kobayashi et al. [17].
[2] Only ankle trajectories are reported and little change can be seen in the curves across stiffnesses.
[3] Did not run between-group statistics for all stiffnesses, only compared to the least stiff (near-zero) baseline condition (S1).
[4] Only resistance to dorsiflexion was varied.
[5] Measured during initial swing.
[6] Measured during late stance.
[7] Curves for only one subject are presented and for a subset of the stiffness conditions, however, the text mentions that more rigid springs resulted in smaller plantarflexion angles.
[8] Significance was only between compliant and nominal stiffnesses, where nominal equaled the prescribed stiffness and compliant and stiff strut conditions were -20% and +20% of the nominal, respectively.
[9] Measured during heelstrike phase (right/affected-side heelstrike to toe-strike). The study tested one trim of two AFOs (Engen and Teufel) and three trims of the Seattle AFO. The trend was significant across all the Seattle AFO trims and between the Teufel and the first two Seattle trims. It was not significant between the Engen and the Seattle trims, between the Engen and the Teufel, or between the Teufel and the most flexible Seattle trim (trim 3).
[10] Only the two stiffest conditions (S3 and S4) were significantly different from the near-zero baseline stiffness (S1).
[11] A significant trend was found only between the nominal and stiff struts, where nominal equaled the prescribed stiffness and compliant and stiff strut conditions were -20% and +20% of the nominal, respectively.
[12] Measured during push off phase (right/affected-side heel-off to toe-off). The study tested one trim of two AFOs (Engen and Teufel) and three trims of the Seattle AFO. The trend was significant across all comparisons except for between the Engen and the first two Seattle trims and between the Teufel and the most flexible Seattle trim (trim 3). Note: This study also found a decrease in peak DF during swing phase (right/affected-side toe-off to heelstrike) without statistical testing.
[13] Trend observed for only one of the two subjects.
[14] Four increasing stiffness levels resisting PF were tested (S1-S4). The trend was significant only between S4 or S3 and S1 or S2 (the two most stiff vs the two least stiff conditions).
[15] All stiffness groups were significantly different from the near-zero baseline condition (S1).
[16] Trend found only when resistance to PF was varied (effects for this parameter were not discussed with DF resistance variation).
[17] The text mentions that PF angle at the time of foot contact decreased for all nine subjects.
[18] PF angle measured at toe-off.
[19] Changes in DF angle in late stance were described only qualitatively for the different stiffness conditions.

Table C.2: Measures of Knee Joint Kinematics

Ref.	Paper	N	ROM	Peak Flexion - Stance	Peak Flexion - Swing	Peak Extension - Stance	Contra. Extension - Stance	Flexion - IC	Angle - Early Stance	Angle - Midstance	Angle - cTO	Angle - Late Swing
Studies with statistical testing												
[1]	Brunner, 1998	14							-			-
[2]	Choi, 2017	8				↓*						
[3]	Harper, 2014	13		↑*, - [5,6]	-							
[4]	Kerkum, 2015	15		- [6]						- [19]	-	
[6]	Kobayashi, 2013	5		↑*, - [7]	-							
[7]	Kobayashi, 2017[1]	10						↑*, - [17]				
[9]	Ramdharry, 2012	14					-					
[10]	Russell Esposito, 2014	13	-	↑*, - [8]								
[11]	Telfer, 2012	1		↑*								
[22]	Yamamoto, 1993[2]	15			*, - [11]	*, - [12]						
Studies without statistical testing												
[16]	Collins, 2015[3]	9										
[17]	Kobayashi, 2015[1,4]	10				↓*, - [13]		↑*, - [18]				
[18]	Kobayashi, 2016[4]	6				↓* [14]						
[19]	Kobayashi, 2017	1		- [9]		↑, - [15, 16]						
[20]	Singer, 2014	5		- [10]								

Symbol Key

↓ Parameter decreased as stiffness increased
↑ Parameter increased as stiffness increased
- No change observed / change was not significant
* Changes were statistically significant

Abbreviations & Acronyms

ROM: Range of Motion
LR: Loading Response
Contra: Contralateral
IC: Initial Contact
cTO: Contralateral Toe-Off

Footnotes

[1] Kobayashi et al. [7] had the same subject population as Kobayashi et al. [17].
[2] Yamamoto et al. [22] performed statistical analyses for each participant individually, they did not run group statistics.
[3] Only knee angle trajectories are reported and little change can be seen in the curves across stiffnesses.
[4] Did not run between-group statistics for all stiffnesses, only compared to the least stiff (near-zero) baseline condition (S1).
[5] Significant differences were seen between the compliant and nominal, and compliant and stiff struts only, where nominal equaled the prescribed stiffness and compliant and stiff strut conditions were -20% and +20% of the nominal, respectively.
[6] Measured during single support phase.
[7] This paper tested four stiffness levels, the increasing trend was significant only when comparing the stiffest condition (level 4) to the lowest two stiffness levels (levels 1 and 2).
[8] Within the parameter, the compliant stiffness was significantly lower than both the nominal and stiff struts, but the nominal and stiff struts were not significantly different.
[9] There was no observable effect for either plantarflexion or dorsiflexion resistance changes.
[10] Increased nominally for two out of five subjects and decreased nominally for three out of five subjects.
[11] Peak knee flexion was measured during stance and during swing, but in the outcomes, it was not specified which was reported. Changes were significant for five out of the nine subjects, but no generalizable trend was indicated.
[12] Change in peak knee extension was significant for seven out of nine subjects, though no generalizable trend was indicated.
[13] Only the two intermediate stiffnesses (S2 and S3) were significantly different from the near-zero baseline stiffness (S1).
[14] All stiffness groups were significantly different from the near-zero baseline condition (S1).
[15] No effect was observed when plantarflexion resistance was increased, only for increasing resistance to dorsiflexion.
[16] Subjects did not go into extension in this study, and the parameter was named “minimum flexion during stance.”
[17] This paper tested four stiffness levels (S1-S4) resisting plantarflexion only. The increasing trend was only significant when comparing the stiffest conditions (S3 & S4) with the least stiff (S1: near-zero stiffness), and the stiffest (S4) with the second least stiff (S2).
[18] Only the two stiffest conditions (S3 and S4) were significantly different from the near-zero baseline stiffness (S1)
[19] Measured during midstance: “the moment that malleolus marker of the contralateral leg passed the malleolus marker of the ipsilateral leg” [23].

Table C.3: Measures of Hip Joint and Pelvis Kinematics

Ref.	Paper	N	ROM - Sagittal	Peak Flex - Stance	Peak Flex - Swing	Peak Ext	Peak Ext - Stance	Angle - Early Stance	Angle - cIC	Peak Abduction - Swing	Min Abduction	Pelvic Elevation - Swing	Max Pelvic Tilt	Min Pelvic Tilt
Studies with statistical testing														
[1]	Brunner, 1998[1]	14			-			-		-	↓*		↓*	↓*
[3]	Harper, 2014	13					- [3]							
[4]	Kerkum, 2015	15							-					
[9]	Ramdharry, 2012	14			-					-		-		
[10]	Russell Esposito, 2014	13	-	-		-								
Studies without statistical testing														
[2]	Choi, 2017	8	-				↑ [4]							
[16]	Collins, 2015[2]	9												

Symbol Key

↓ Parameter decreased as stiffness increased
↑ Parameter increased as stiffness increased
- No change observed / change was not significant
* Changes were statistically significant

Abbreviations & Acronyms

ROM: Range of Motion
Ext: Extension
Flex: Flexion
cIC: Contralateral Initial Contact
Min: Minimum
Max: Maximum

Footnotes

[1] They also measured the minimum, maximum, and difference of pelvic tilt, pelvic obliquity, pelvic rotation, hip flexion, hip abduction, and hip external rotation. The parameters not shown in the table did not have statistically significant stiffness effects.
[2] Only hip angle trajectories are reported and little change can be seen in the curves across stiffnesses.
[3] Measured during second double support phase (from non-AFO Heel-Strike to AFO toe-off).
[4] Only hip angle trajectories for one participant are shown, and the text mentions an increase in late-stance hip extension for this participant.

Table C.4: Measures of Ankle Joint Kinetics

Ref.	Paper	N	Pk PF Mom - Stance	Pk DF Mom - Early Stance	Bio Mom	Mom Trajectory	Mom Zero-cross Point [%GC][14]	Work	Pk Pow Abs - iLoad	Pk Pow Abs - Mid/Late Stance	Pk Pow Gen - Late Stance	Avg Pow Abs/Gen	Avg Net Pow	Timing of Pk Pow Gen - PO
Studies with statistical testing														
[16]	Collins, 2015	9	-		↓* [9]							↓* [19]	- [20]	
[3]	Harper, 2014	13	-	-				-						
[4]	Kerkum, 2015	15	-								↓*, - [16]			-
[9]	Ramdharry, 2012	14		-							↑*, - [17]			
[10]	Russell Esposito, 2014	13	-	-					-	-	-			
[22]	Yamamoto, 1993[1]	15	*, - [5]	↑* [7]		↑ [10]								
Studies without statistical testing														
[12]	Amerinatanzi, 2016[2]	1				↓								
[13]	Amerinatanzi, 2017[2]	2				↓								
[14]	Arch, 2015	2				↓, ↑ [11, 12]								
[24]	Arch, 2016	2				↓								
[17]	Kobayashi, 2015[3, 4]	10		↑*, - [8]			↑* [15]							
[18]	Kobayashi, 2016[4]	6		↑*, - [8]										
[19]	Kobayashi, 2017	1									↓, - [18]			
[7]	Kobayashi, 2017[3]	10				- [13]								
[20]	Singer, 2014	5		↑										
[11]	Telfer, 2012	1	- [6]											

Symbol Key

↓ Parameter decreased as stiffness increased
↑ Parameter increased as stiffness increased
- No change observed / change was not significant
* Changes were statistically significant

Abbreviations & Acronyms

Pk: Peak
PF: Plantarflexion
DF: Dorsiflexion
Mom: Moment
Bio Mom: Biological Moment
Pow: Power
Abs: Absorption
Gen: Generation
PO: Push-off
iLoad: Initial Loading

Footnotes

[1] Yamamoto et al. [22] performed statistical analyses for each participant individually, and only for those that preferred the intermediate stiffness orthotic (nine subjects total). They did not run group statistics.
[2] Only one patient's data was reported, and only trajectories and ranges for the parameters were indicated.
[3] Kobayashi et al. [7] had the same subject population as Kobayashi et al. [17].
[4] Did not run between-group statistics for all stiffnesses, only compared to the least stiff (near-zero) baseline condition (S1).
[5] In this paper, the methods state that peak PF during stance and during swing was measured but the statistical results only state 'plantarflexion moment' and don't specify the gait phase. There was a significant difference in PF moment for three out of the nine participants that preferred the intermediate stiffness, but no general trend was reported.
[6] Statistical significance was only reported for peak plantar flexion moment of AFO conditions compared to the shoes-only condition, no observable difference was inferred between the stiffness conditions.
[7] There was a significant difference for all nine participants that preferred the intermediate stiffness.
[8] Only the most stiff condition (S4) was significantly different from the near-zero baseline stiffness (S1).
[9] This study found a significant decrease in the peak and average biological ankle moment (without the AFO contribution) during a stride and during early to mid-stance.
[10] The ankle moment trajectories of only one subject are presented. The text states that more rigid springs resulted in larger dorsiflexion ankle joint moments for all nine subjects who preferred intermediate stiffness springs.
[11] Only two subjects were tested. One's net moment decreased as stiffness increased, and the other's increased only slightly.
[12] The study stated that the moment reported is the net moment of both the biological ankle and the AFO device.
[13] This paper only provided ankle moment trajectories and no clear trend can be inferred across the stiffness conditions.
[14] Moment Zero-Cross Point is the percentage of the gait cycle at which the ankle moment switches directions, "crosses zero."
[15] All stiffness groups were significantly different from the near-zero baseline condition (S1).
[16] The power generation when wearing the rigid strut was significantly lower than both the stiff and flexible stiffnesses.
[17] Peak power generation decreased significantly when going from the Push Brace (moderate stiffness) to Multifit AFO (high stiffness).
[18] A decrease was found when resistance to dorsiflexion was increased. No change was observed when resistance to plantarflexion was increased.
[19] The magnitude of both the biological and total (combined subject and exoskeleton contribution) average positive (Gen) and negative (Abs) power decreased with greater stiffness.
[20] Average net power calculated as the sum of positive and negative work divided by stride time. Subject biological contribution and exoskeleton contribution reported separately and together.

Table C.5: Measures of Knee Joint Kinetics

Ref.	Paper	N	Peak Extensor Moment - Stance	Peak Flexor Moment - Early Stance	Peak Flexor Moment - Late Stance	Avg. Extensor Moment - Early Stance[7]	Moment - Mst	Avg. Flexor Moment - Late Stance[9]	Avg. Absolute Knee Moment - Whole Stride[10]	Flexor Moment at Timing of Pk Extension - SS	Neg Work - 1st DS	Power Gen - iL	Power Gen - After LR	Power Abs - Early Stance
Studies with statistical testing														
[16]	Collins, 2015[14]	9				↓*		↑*	-					
[3]	Harper, 2014	13	-[2]	-	-						↓*, -[12, 13]			
[4]	Kerkum, 2015	15					-[8]			↑*, -[11]				
[10]	Russell Esposito, 2014	13	↑*, -[3]		-							-	-	-
Studies without statistical testing														
[17]	Kobayashi, 2015[1]	10			↓*, -[5]									
[18]	Kobayashi, 2016[1]	6			↓*, -[5]									
[19]	Kobayashi, 2017	1	↑, ↓[4]		↑, -[6]									
[20]	Singer, 2014	5	↑											
[11]	Telfer, 2012	1	↑											

Symbol Key

↓ Parameter decreased as stiffness increased
↑ Parameter increased as stiffness increased
- No change observed / change was not significant
* Changes were statistically significant

Abbreviations & Acronyms

Mst: Midstance
SS: Single Support
DS: Double Support
iL: Initial Loading
LR: Loading Response
Neg: Negative
Gen: Generation
Abs: Absorption

Footnotes

[1] Did not run between-group statistics for all stiffnesses, only compared to the least stiff (near-zero) baseline condition (S1).
[2] Peak extensor moment was measured during early single leg support phase.
[3] Only the compliant stiffness (20% less stiff than prescribed) was significantly lower than the stiff strut (20% more stiff than prescribed). Comparisons with the nominal condition (prescribed stiffness) were not significant.
[4] Peak extensor moment had a decreasing trend with greater stiffness resisting plantarflexion, and increased only nominally when resistance to dorsiflexion was increased.
[5] Only the two stiffest conditions (S3 and S4) were significantly different from the near-zero baseline stiffness (S1).
[6] Peak flexor moment increased with higher stiffnesses resisting plantarflexion, and remained generally unchanged when resistance to dorsiflexion was increased.
[7] This is the average knee moment during early stance, defined as “the positive impulse within approximately 10–30% stride divided by stride period.”
[8] Moment was measured at midstance (33% of gait cycle), which was close to the timing of peak flexor moment during late stance.
[9] This is the average knee moment during late stance, defined as “the negative impulse within approximately 30–50% stride divided by stride period.” Its magnitude increased as stiffness increased.
[10] Average absolute (rectified) knee moment over the entire stride.
[11] Significant differences were found only between the most and least stiff conditions.
[12] Negative mechanical work was only significantly different between the nominal (prescribed) and stiff (20% greater than prescribed) and between the compliant (20% less stiff than prescribed) and stiff strut conditions.
[13] Changes in positive and negative mechanical work during other regions of the gait cycle were not significant.
[14] This study also measured the knee power trajectory during gait and found no effect.

Table C.6: Measures of Hip Joint Kinetics

Ref. Paper	N	Moment - Contralateral Initial Contact	Peak Moment	Peak Flexor Moment	Peak Extensor Moment - Early Stance	Peak Power Generation - Early Stance	Peak Power Generation - Late Stance	Peak Power Absorption - Late Stance	Work
Studies with statistical testing									
[3] Harper, 2014	13			-	-				-
[4] Kerkum, 2015	15	-							
[9] Ramdharry, 2012	14		-						
[10] Russell Esposito, 2014	13			-	-	-	-	-	
Studies without statistical testing									
[16] Collins, 2015[1]	9								

Symbol Key

- No change observed / change was not significant

Footnotes

[1] Only hip moment and power trajectories are reported and little change can be seen in the curves across stiffnesses.

Table C.7: Ground Reaction Force Measures

Ref.	Paper	N	Vertical - Initial Contact	Peak Vertical - Early SS (First Peak)	Peak Vertical - Late SS (Second Peak)	Peak Vertical - 2nd DS	Minimum Vertical - Stance	Peak A/P - Braking	Peak A/P - Propulsive	Peak M/L
Studies with statistical testing										
[1]	Brunner, 1998[1]	14	-	-	↓*		-	-	-	
[3]	Harper, 2014	13	-[3]	-[4]	-	-		-	-	↑*, -[5]
[10]	Russell Esposito, 2014	13		-	-			-	-	-
Studies without statistical testing										
[13]	Amerinatanzi, 2017[2]	2								

Symbol Key

↓ Parameter decreased as stiffness increased
↑ Parameter increased as stiffness increased
- No change observed / change was not significant
* Changes were statistically significant

Abbreviations & Acronyms

DS: Double Support
SS: Single Support
A/P: Anterior/Posterior
M/L: Medial/Lateral

Footnotes

[1] Brunner et al. [1] also reported the difference between the two vertical peaks, and the load reduction from the first and second peaks to the minimum vertical load. None had significant changes across stiffnesses.
[2] The ground reaction force profile during gait is presented in the paper, but no comparisons or conclusion are made.
[3] Measured the impulse during 1st double support
[4] No effect for both AFO limb and non-AFO (sound) limb.
[5] Significant differences were only seen between the compliant (20% less stiff than prescribed) and stiff (20% stiffer than prescribed) conditions. No change when compared to the prescribed stiffness. These results were the same for both the AFO and non-AFO limbs.

Table C.8: Spatiotemporal Measures

Ref.	Paper	N	SWS	Cadence	Stride Len.	Step Len.	Stride Wid.	Step Wid.	Stride Time	Step Time	tDS	tSS	Stance Time	Swing Phase	Heel Off-On	HC to FC
Studies with statistical testing																
[25]	Brunner, 1998	14	↓*	↓*	↓*	↓*					-	↑*				
[16]	Collins, 2015				-			-								
[26]	Guillebastre, 2009	11	↓*, -[2]			-				-			-[7]		-[8]	
[3]	Harper, 2014	13	-													
[4]	Kerkum, 2015	15	-													
[5]	Kobayashi, 2011	10	-													
[6]	Kobayashi, 2013	5	-													
[10]	Russell Esposito, 2014	13	-		-		-		-							
[22]	Yamamoto, 1993[1]	15							*, -[4]		*, -[5]	*, -[6]		*, -[6]		↑[9]
Studies without statistical testing																
[14]	Arch, 2015	2				-[3]							-[3]			

Symbol Key

↓ Parameter decreased as stiffness increased
↑ Parameter increased as stiffness increased
- No change observed / change was not significant
* Changes were statistically significant

Abbreviations & Acronyms

SWS: Self-selected Walking Speed
Len.: Length
Wid.: Width
tSS: Single Support Time
tDS: Double Support Time
HC: Heel-Contact
FC: Forefoot-Contact

Footnotes

[1] Yamamoto et al. [22] performed statistical analyses for each participant individually, and only for those that preferred the intermediate stiffness spring (nine subjects total). They did not run group statistics.

[2] The study included three stiffness variations of dynamic AFOs (minimal, moderate and stiff) and one rigid AFO. The observed decrease in SWS was significant only when comparing the moderate stiffness to the rigid AFO, but not when comparing minimal and stiff dynamic AFO conditions. Stiffness values were not reported.

[3] The text stated that this parameter remained generally consistent across experimental conditions.

[4] The effect for this parameter was significant for 4/9 subjects that preferred the intermediate stiffness. No general trend was reported, but all nine subject who preferred the intermediate stiffness had a minimum cycle time at that stiffness.

[5] This paper measured first and second DS time separately. Stiffness effects were significant in 5/9 and 4/9 subjects for first and second DS, respectively. No clear trends were reported but first DS time was minimized at the intermediate stiffness for the subjects that chose it as their preferred stiffness.

[6] The effect for this parameter was significant for 3/9 subjects that preferred the intermediate stiffness. No stiffness effect trend was reported.

[7] Guillebastre et al. [26] measured stance time as a percentage of the gait cycle.

[8] Heel off-on was defined as the percentage of time during which the rear third of the foot was on the ground.

[9] The interval from heel-contact to forefoot-contact increased with greater stiffnesses for all nine participants that preferred an intermediate stiffness. Statistical significance was not reported for this parameter.

Table C.9: Muscle Activity Measures

Ref.	Paper	N	Medial Gastrocnemius	Medial + Lateral Gastrocnemius	Soleus	Tibialis Anterior	Gluteus Medius	Biceps Femoris (Long Head)	Rectus Femoris	Vastus Medialis
Studies with statistical testing										
[2]	Choi, 2017	8	- [3]							
[16]	Collins, 2015[1]	9		↑*, - [6]	↓*, - [7]	↑*, - [8]				
[3]	Harper, 2014[2]	13	↓*, - [4]		-	-	-	-	-	-
Studies without statistical testing										
[24]	Arch, 2016	2	- [5]		- [5]					

Symbol Key

↓ Parameter decreased as stiffness increased
↑ Parameter increased as stiffness increased
- No change observed / change was not significant
* Changes were statistically significant

Footnotes

[1] This study calculated average muscle activity as the time integral of the muscle electromyographic signal during the period of interest divided by the stride period. They measured average activity during a whole stride, during early and mid-stance only and during late stance. Activity was normalized to the maximum activity during normal walking.

[2] This study calculated average activity by first time-normalizing the electromyographic signal to 100% of the gait cycle, value-normalizing to the maximum activity during walking, and then integrating the normalized signal across different portions of the gait cycle. Average activity was calculated during six regions of the gait cycle: 1st and 2nd double support, early and late single support, and early and late swing.

[3] Measured peak normalized medial gastrocnemius activity during stance.

[4] Significant differences were only found for integrated activity during late single-leg support and between the nominal (prescribed) and compliant (20% less stiff) struts.

[5] This study reported the electromyography data for only one of the two subjects, no clear trends are observed.

[6] Measured combined average activity of the medial and lateral gastrocnemius. The trend was significant for average activity during the whole stride and during late stance, but not during early and mid-stance.

[7] The decrease was significant only for average activity during the whole stride and during early and mid-stance, but not during late stance.

[8] An increase was found for average activity during a whole stride and during early and mid-stance. The increase was significant only for the whole stride average. No change was found for late stance average activity.

Table C.10: Other Quantitative Measures

Ref.	Paper	N	Lengthwise Plantar CoP	CoP Excursion	Midline Length	COM Power	Peak MTU Length - Stance	Peak MG Length	Peak Achilles Tendon Length	MG Length Change Velocity
Studies with statistical testing										
[2]	Choi, 2017	8				↑*, ↓*, - [4]	↓*	↑*	↑*, ↓* [5]	-
[16]	Collins, 2015[1]	9								
[26]	Guillebastre, 2009	11			- [3]					
[4]	Kerkum, 2015	15		- [2]						
Studies without statistical testing										
[15]	Bolus, 2017	1	↓ [1]							

Symbol Key

↓ Parameter decreased as stiffness increased
↑ Parameter increased as stiffness increased
- No change observed / change was not significant
* Changes were statistically significant

Abbreviations & Acronyms

CoP: Center of Pressure
COM: Center of Mass
MTU: Gastrocnemius Musculotendon Unit
MG: Medial Gastrocnemius Muscle

Footnotes

[1] Measure was defined as the location of the plantar CoP along the lengthwise axis of the subject's right foot over the course of the gait cycle.
[2] Measure was defined as the CoP position with respect to the position of the calcaneus at initial contact.
[3] Midline length was defined as “the length between the pivot points of the two-dimensional sensor structure of heel and toe area.”
[4] This study calculated only the human contribution to power (biological power) by removing the exoskeleton's work contribution. Average rebound power (during mid-stance) increased and average push-off power (during late stance) decreased significantly with greater stiffness. There were no effects for collision or preload power calculated during early and mid-stance, respectively.
[5] Achilles tendon length increased at heel contact and decreased during midstance to terminal stance with increasing AFO stiffness.

Table C.11: Preference and Qualitative Measures

Ref.	Paper	N	Qualitative Measure	Results
[25]	Brunner, 1998	14	Arm swinging motion was assessed qualitatively from video recordings (rated as yes or no improvement)	The stiff AFO slightly improved arm movement compared to no AFO, but arm movements were closest to normal in the spring-type (flexible) AFO. With the flexible AFO, ``the arm on the plegic side was held more extended, less pronated and swing much wider compared with barefoot and the stiff orthosis."
[10]	Russell Esposito, 2014[1]	13	Patient preference	Preferences varied, 3/13 preferred the compliant, 5/13 preferred the nominal, 3/13 preferred the stiff, 1/13 preferred the nominal and stiff AFOs equally, and 1/13 had no preference.
[22]	Yamamoto, 1993	15	Patient preference	No generalizable preference, there were 4 springs to choose from and combine, subjects who didn't use an AFO (2/15) preferred No AFO, 2/15 didn't answer, 2/15 walked with a cane and selected the most rigid, and the remaining 9/15 selected intermediate flexibility spring combinations. (Note: For the 9/15 subjects that preferred intermediate stiffness, the selected stiffness conditions also exhibited the shortest first double support phase and cycle time.)
[27]	Yamamoto, 1997	33	Patient preference	Preferences varied, but only 2/33 hemiplegic patients preferred the stiffest springs, the rest preferred one of the first three stiffness levels, which varied between about 0.5 - 1.5 Nm/deg.

Footnotes

[1] This paper tested three stiffness conditions of the AFO posterior, where nominal equaled the prescribed stiffness and compliant and stiff strut conditions were -20% and +20% of the nominal, respectively.

APPENDIX C REFERENCES

[1] R. Brunner, G. Meier, and T. Ruepp, "Comparison of a stiff and a spring-type ankle-foot orthosis to improve gait in spastic hemiplegic children," *J. Pediatr. Orthop.*, vol. 18, no. 6, pp. 719–726, 1998.

[2] H. Choi, K. M. Peters, M. B. MacConnell, K. K. Ly, E. S. Eckert, and K. M. Steele, "Impact of ankle foot orthosis stiffness on Achilles tendon and gastrocnemius function during unimpaired gait," *J. Biomech.*, 2017.

[3] N. G. Harper, E. R. Esposito, J. M. Wilken, and R. R. Neptune, "The influence of ankle-foot orthosis stiffness on walking performance in individuals with lower-limb impairments," *Clin. Biomech.*, vol. 29, no. 8, pp. 877–884, Sep. 2014.

[4] Y. L. Kerkum, A. I. Buizer, J. C. van den Noort, J. G. Becher, J. Harlaar, and M.-A. Brehm, "The Effects of Varying Ankle Foot Orthosis Stiffness on Gait in Children with Spastic Cerebral Palsy Who Walk with Excessive Knee Flexion," *PLoS One*, vol. 10, no. 11, p. e0142878, Nov. 2015.

[5] T. Kobayashi, A. K. L. Leung, Y. Akazawa, and S. W. Hutchins, "Design of a stiffness-adjustable ankle-foot orthosis and its effect on ankle joint kinematics in patients with stroke," *Gait Posture*, vol. 33, no. 4, pp. 721–723, Apr. 2011.

[6] T. Kobayashi, A. K. L. Leung, Y. Akazawa, and S. W. Hutchins, "The effect of varying the plantarflexion resistance of an ankle-foot orthosis on knee joint kinematics in patients with stroke.," *Gait Posture*, vol. 37, no. 3, pp. 457–459, Mar. 2013.

[7] T. Kobayashi, M. S. Orendurff, M. L. Singer, F. Gao, and K. B. Foreman, "Contribution of ankle-foot orthosis moment in regulating ankle and knee motions during gait in individuals post-stroke," *Clin. Biomech.*, vol. 45, pp. 9–13, 2017.

[8] J. F. Lehmann, P. C. Esselman, M. J. Ko, J. C. Smith, B. J. DeLateur, and A. J. Dralle, "Plastic ankle-foot orthoses: evaluation of function.," *Arch. Phys. Med. Rehabil.*, vol. 64, no. 9, pp. 402–7, Sep. 1983.

[9] G. M. Ramdharry, B. L. Day, M. M. Reilly, and J. F. Marsden, "Foot drop splints improve proximal as well as distal leg control during gait in Charcot-Marie-Tooth disease.," *Muscle Nerve*, vol. 46, no. 4, pp. 512–519, Oct. 2012.

[10] E. Russell Esposito PhD, R. V Blanck CPO, N. G. Harper MS, J. R. Hsu MD, and J. M. Wilken PT, PhD, "How Does Ankle-foot Orthosis Stiffness Affect Gait in Patients With Lower Limb Salvage?," *Clin. Orthop. Relat. Res.*, vol. 472, no. 10, pp. 3026–3035, 2014.

[11] S. Telfer, J. Pallari, J. Munguia, K. Dalgarno, M. McGeough, and J. Woodburn, "Embracing additive manufacture: implications for foot and ankle orthosis design," *BMC Musculoskelet. Disord.*, vol. 13, no. 1, p. 84, Dec. 2012.

[12] A. Amerinatanzi, H. Zamanian, N. Shayesteh Moghaddam, H. Ibrahim, M. S. Hefzy, and M. Elahinia, "On the Advantages of Superelastic NiTi in Ankle Foot Orthoses," in *Volume 2: Modeling, Simulation and Control; Bio-Inspired Smart Materials and Systems; Energy Harvesting*, 2016, vol. 2, p. V002T03A026.

[13] A. Amerinatanzi, H. Zamanian, N. Shayesteh Moghaddam, A. Jahadakbar, and M. Elahinia, "Application of the Superelastic NiTi Spring in Ankle Foot Orthosis (AFO) to Create Normal Ankle Joint Behavior," *Bioengineering*, vol. 4, no. 4, p. 95, Dec. 2017.

[14] E. S. Arch and S. J. Stanhope, "Passive-Dynamic Ankle–Foot Orthoses Substitute for Ankle Strength While Causing Adaptive Gait Strategies: A Feasibility Study," *Ann. Biomed. Eng.*, vol. 43, no. 2, pp. 442–450, Feb. 2015.

[15] N. B. Bolus, C. N. Teague, O. T. Inan, and G. F. Kogler, "Instrumented Ankle-Foot Orthosis: Towards a Clinical Assessment Tool for Patient-Specific Optimization of Orthotic Ankle Stiffness," *IEEE/ASME Trans. Mechatronics*, 2017.

[16] S. H. Collins, M. B. Wiggin, and G. S. Sawicki, "Reducing the energy cost of human walking using an unpowered exoskeleton," *Nature*, vol. 522, no. 7555, pp. 212–215, Apr. 2015.

[17] T. Kobayashi, M. L. Singer, M. S. Orendurff, F. Gao, W. K. Daly, and K. B. Foreman, "The effect of changing plantarflexion resistive moment of an articulated ankle-foot orthosis on ankle and knee

joint angles and moments while walking in patients post stroke," *Clin. Biomech.*, vol. 30, no. 8, pp. 775–780, 2015.

[18] T. Kobayashi, M. S. Orendurff, M. L. Singer, F. Gao, W. K. Daly, and K. B. Foreman, "Reduction of genu recurvatum through adjustment of plantarflexion resistance of an articulated ankle-foot orthosis in individuals post-stroke.," *Clin. Biomech. (Bristol, Avon)*, vol. 35, pp. 81–85, Jun. 2016.

[19] T. Kobayashi *et al.*, "An articulated anklefoot orthosis with adjustable plantarflexion resistance, dorsiflexion resistance and alignment: A pilot study on mechanical properties and effects on stroke hemiparetic gait," *Med. Eng. Phys.*, vol. 44, pp. 94–101, 2017.

[20] M. L. Singer, T. Kobayashi, L. S. Lincoln, M. S. Orendurff, and K. B. Foreman, "The effect of ankle–foot orthosis plantarflexion stiffness on ankle and knee joint kinematics and kinetics during first and second rockers of gait in individuals with stroke," *Clin. Biomech.*, vol. 29, no. 9, pp. 1077–1080, Nov. 2014.

[21] T. Sumiya, Y. Suzuki, and T. Kasahara, "Stiffness control in posterior-type plastic ankle-foot orthoses: effect of ankle trimline. Part 2: Orthosis characteristics and orthosis/patient matching.," *Prosthet. Orthot. Int.*, vol. 20, no. 2, pp. 132–137, Aug. 1996.

[22] S. Yamamoto, S. Miyazaki, and T. Kubota, "Quantification of the effect of the mechanical property of ankle-foot orthoses on hemiplegic gait," *Gait Posture*, vol. 1, no. 1, pp. 27–34, 1993.

[23] Y. L. Kerkum, A. I. Buizer, J. C. van den Noort, J. G. Becher, J. Harlaar, and M.-A. A. Brehm, "The effects of varying ankle foot orthosis stiffness on gait in children with spastic cerebral palsy who walk with excessive knee flexion," *PLoS One*, vol. 10, no. 11, p. e0142878, 2015.

[24] E. S. Arch, S. J. Stanhope, and J. S. Higginson, "Passive-dynamic ankle–foot orthosis replicates soleus but not gastrocnemius muscle function during stance in gait: Insights for orthosis prescription," *Prosthet. Orthot. Int.*, vol. 40, no. 5, pp. 606–616, Oct. 2016.

[25] R. Brunner, G. Meier, and T. Ruepp, "Comparison of a stiff and a spring-type ankle-foot orthosis to improve gait in spastic hemiplegic children," *J. Pediatr. Orthop.*, vol. 18, no. 6, pp. 719–726, 1998.

[26] B. Guillebastre, P. Calmels, and P. Rougier, "Effects of Rigid and Dynamic Ankle-Foot Orthoses on Normal Gait," *Foot Ankle Int.*, vol. 30, no. 1, pp. 51–56, Jan. 2009.

[27] S. Yamamoto, M. Ebina, S. Miyazaki, H. Kawai, and T. Kubota, "Development of a new ankle-foot orthosis with dorsiflexion asist, part 1: desirable charactersitics of ankle-foot orthoses for hemiplegic patients," *J Prosthet Orthot*, vol. 9, no. 4, pp. 174–179, 1997.

APPENDIX D

Manufacturing Choices for Ankle-Foot Orthoses: A Multi-objective Optimization

This appendix was published as [27]: Totah, D., Kovalenko, I., Saez, M., & Barton, K. (2017). Manufacturing Choices for Ankle-Foot Orthoses: A Multi-objective Optimization. In Procedia CIRP (Vol. 65, pp. 145–150).

Summary

Increased interest in additive manufacturing of medical devices leads to a greater number of manufacturing choices, from processes to product designs, with little research comparing these new techniques. This paper proposes a multi-objective optimization approach for choosing the appropriate process, material and thickness that minimizes production cost and time, and maximizes device performance. We tested our framework with a simulated case study to choose between traditional plaster casting and additive manufacturing techniques for an ankle-foot orthosis. This evaluation tool provides early quantitative support for additive manufacturing, and it can be expanded to fit various patient, clinic and insurance provider needs.

D.1 Introduction

An ankle-foot orthosis (AFO) is a custom-made medical device used to correct a patient's walking gait. AFOs are prescribed to individuals with various lower-extremity disabilities, ranging from patients with debilitating disorders like cerebral palsy [13], to multiple sclerosis [9] and stroke recovery patients [10], as well as injuries due to sports and recreation [127].

AFOs come in various shapes and sizes with different stiffness values that correspond to varying levels of movement flexibility to accommodate the diverse populations needing assistance. Some designs involve hinged AFOs that allow/restrict various ranges of ankle motion, others do not include a joint and are referred to as non-articulated AFOs. Both articulated and non-articulated designs may offer energy return either through added elastic components or a leaf spring design [14, 128]. The traditional and most-widely adopted method for AFO manufacturing involves plaster casting [129], which is a highly-customized patient-centered process. Plaster casting is also an imperfect process producing non-repeatable results and is highly dependent on skilled labor.

More recently, additive manufacturing (AM) methods have been proposed as alternatives to the traditional approach. Several published studies [14, 21, 40] outline novel AFO manufacturing methods utilizing foot scanning, computer-aided design (CAD) and additive manufacturing. For example, Faustini et al. [21] outline AFO production through selective laser sintering (SLS), while Jin et al. [14] propose a fused deposition modeling (FDM) AM technique. Both AM approaches require scanning of the foot and utilizing AFO model simulations [14, 40, 41]. AM pioneers claim that these methods will improve production times, lower waste, decrease costs, and improve AFO performance. Additionally, an AM approach has the potential to lead to greater customization, and enhanced repeatability. Despite the multitude of potential benefits, adoption of AM fabrication of AFOs has been very slow. One key reason for this stems from the lack of quantitative and qualitative metrics comparing AM to more standard manufacturing approaches. As AM technologies become more popular, a clinic's ability to identify the optimal manufacturing method for a specific custom device will become increasingly important.

In this paper, we propose a multi-objective optimization approach to compare the different manufacturing methods and associated materials. We present a framework that identifies the optimal combination of process, material and material thickness that balances cost, production time and performance for various AFO sizes. Performance is defined in terms of the user's predicted energy cost while wearing the AFO. The framework is implemented with a simulated clinic case study explained in section D.2. The framework is meant to serve as a guideline and its parameters may be adjusted according to a clinic's available technologies and individual costs as well as to specific patients' performance patterns and anthropometry.

D.2 Current AFO Manufacturing Technique

The most-widely adopted AFO manufacturing method is plaster casting [129]. After a referral from a physician, a patient will come into the clinic where an orthotist takes relevant anthropometric measurements and fits the patient with a cast mold by wrapping the affected leg in a plaster wrap. Plaster is then poured into the resulting negative mold to produce a positive mold of the leg. The orthosis is then made by heating and vacuum-forming sheets of thermoplastic onto the plaster mold, which is left to cool and then cut to the correct orthosis shape. Polypropelyne (PP) and polyehtylene (PE) are commonly used thermoplastics [129]. Alternatively, a carbon fiber (CF) orthosis might be made in a meticulous, manual layering and lamination process. Additional steps might be involved, depending on the patient's needs, where the plaster mold might be modified or additional components added. Accessories and straps are added to finalize the orthosis production and the patient returns for a fitting visit, where further adjustments might be needed. This is a highly customized process and involves one-on-one interaction between the orthotist and the patient, which allows the patient to give verbal feedback regarding the comfort and support of the orthosis. It also allows the orthotist to visually evaluate the AFO's functionality while in use. However, this process lacks quantitative evaluation metrics. Moreover, the process could take from one to several days, sometimes with weeks between patient visits, and might require several return visits depending on the patient's needs. The plaster casting method produces a lot of wasted materials, which can be costly, and it requires skilled labor to complete this highly manual build.

D.3 Simulated Case Study

The framework proposed in this paper solves an optimization problem from a simulated case study of a clinic faced with choosing between traditional plaster casting and additive manufacturing for producing its AFOs. The clinic must decide on the manufacturing method, material and thickness that would minimize production cost and time and maximize performance for an AFO of a specific size. Three sizes are simulated in this implementation (section D.4.1). For simplicity, our implementation considered only a non-articulated AFO with a leaf spring design, however the algorithm is modular and can be expanded to other designs as more data becomes available.

The clinic is assumed to have access to three manufacturing processes: traditional plas-

Table D.1: Manufacturing processes and associated materials and thickness options used in the case study implementation of the optimization framework.

Process	Materials	Thicknesses (inch)
Plaster Casting	Polypropelyne (PP), Polyethelyne (PE)	$\frac{3}{32}, \frac{1}{8}, \frac{3}{16}, \frac{1}{4}$
SLS	Rilsan D80 (RD80), DuraForm PA (DFPA), DuraForm GF (DFGF), PP, PE	0.03 to 1 with resolution 0.01
FDM	Carbon Fiber (CF), PP, PE	0.03 to 1 with resolution 0.01

ter casting, and two additive manufacturing processes, SLS and FDM. Certain materials can be used and certain thicknesses can be produced with each process, as shown in table D.1. For instance, the AM processes can print a range of AFO thicknesses with a minimum resolution of 0.01 inch, while the plaster casting process uses sheets of material with discrete thicknesses. For SLS, process and material information was obtained from [21] and production cost and time from [130]. Information from [15, 129] and [22] informed the plaster casting and FDM process assumptions, as well as word-of-mouth and internal documents at the University of Michigan Orthotics and Prosthetics Center.

D.4 Optimization Framework Setup

The following subsections describe the mathematical setup and implementation of this framework for the simulated case study. Due to the custom nature of these devices and the variability of patient anthropometry, a wide range of AFO sizes may be manufactured. Thus, the model takes the size of the AFO as an input, and in this implementation, three AFO sizes were investigated as explained in section D.4.1. The weights and geometries associated with each size were determined using published weight [6] and anthropometry data [7]. The model uses the AFO size input to determine size-dependent variables, such as stiffness, through regression functions based on finite element analysis (FEA) results (section D.4.2). The design variables used in the mathematical representation of this framework are described in section D.4.3. Finally, section D.4.4 details the optimization constraints in terms of the design variables.

D.4.1 Model Input Variable

The optimization algorithms take the size of the AFO as an input. Our implementation allows the user three sizes to choose from: small, medium and large. Each of the sizes is associated with corresponding patient data: weight, foot length, calf circumference and calf height. The patient measurements for the small, medium and large sizes were respectively chosen as the values of the 10th, 50th, and 90th percentiles of population data published in

[6] and [7]. A CAD model of a non-articulated AFO was produced and adjusted for each of the three sizes. The foot and calf measurements determined the geometry of the CAD model, on which finite element analysis (FEA) was performed (section D.4.2). The patient weight values determined the ankle moment values simulated in the FEA analysis. The FEA results then determined the safety factor constraint (section D.4.4) and performance metric (section D.5.3).

D.4.2 Finite Element Analysis

Part performance is affected by design factors (material, thickness, and dimensions), and external factors (load from the user). In order to analyze the effect of both design and external factors, we performed FEA using Autodesk® Inventor™ software. This tool allowed us to simulate every combination of material, thickness, AFO geometry size and ankle moment, as mentioned in section D.4.1.

The focus of this analysis was: 1) to evaluate yield through the safety factor, and 2) to calculate AFO deflection from the torque applied during ankle plantarflexion. The deflection measurement is used to calculate an effective ankle stiffness of a particular design, which is related to device performance (section D.5.3).

In order to reduce computational time a simplified geometry was created based on the geometry of a scanned 3D model of an AFO. This reduced the number of nodes in the simulation. The mesh in the model was adjusted to increase density in the critical areas. Also, a 10% convergence requirement was specified to ensure correct results. Figure D.1 shows the scanned, simplified and meshed geometry. The load used in the simulation was determined based on ankle torque for patients with disability [17] and converted into $N\,m\,Kg^{-1}$. This value was then multiplied by the appropriate patient weight based on the AFO size (see table D.2), to determine the applied torque value for that size. The anthropometric dimensions of calf circumference, foot length and calf height for the 10,

Table D.2: The anthropometric measurements (calf circumference, calf height, and foot length) and patient weight values used for each AFO size taken from the 10^{th}, 50^{th}, and 90^{th} percentiles of published data from [6] and [7].

		Anthropometry (cm)		
Size	Wt. (Kg)	Calf Circ.	Calf Ht.	Ft. Lgth.
Small	53.5	33.4	320	25.1
Medium	70.3	36.4	354	26.7
Large	101.8	40.1	389	28.4

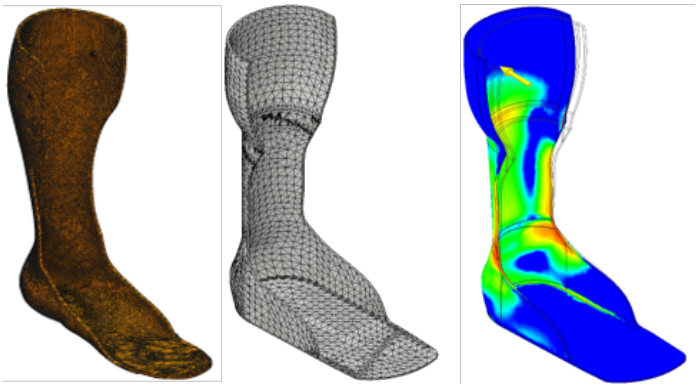

Figure D.1: From left to right, a 3-dimensional scan of a plaster cast AFO, mesh of a modeled AFO, and a contour map showing stresses from an FEA simulation.

50th and 90th percentiles, were similarly used to generate three CAD models of the AFO.

Each of the models was subjected to the appropriate torque loading according to their size. The maximum stress and displacement of the AFO at the calf were extracted from the FEA simulations. The equivalent ankle stiffness was calculated from the resulting displacement. The safety factor was calculated as a ratio of the maximum stress and the material strength.

An FE analysis was run for each of the sizes with each material and each of the four discrete thicknesses of the plaster casting process shown in table D.1. The safety factor and ankle stiffness was determined from the FEA for each size, material and thickness combination. Moreover, a regression model was implemented to correlate safety factor and stiffness to the entire range of thicknesses with an R^2 between 0.8 and 1.0.

D.4.3 Model Design Variables

The mathematical model representing this optimization problem includes several design variables: the type of process, p, the material, m, and the thickness of the material, k, used to create the AFO. There are a processes available with b total possible materials.

One vector, x, was created containing $a + b + 1$ variables:

$$x_i \in \{0, 1\}, \text{ for } i = 1, 2, ..., a + b, \text{ and}$$
$$x_{a+b+1} = k, \text{ where}$$
$$k \in \{y \mid 0.03 < y < 1, y = 0.01n, n \in \mathbb{Z}_+\} \cup \{\tfrac{3}{32}, \tfrac{1}{8}, \tfrac{3}{16}, \tfrac{1}{4}\}$$

$x_1, x_2, ..., x_a$ are binary decision variables indicating the selected process; $x_{a+1}, x_{a+2}, ..., x_{a+b}$ are binary decision variables of the material chosen; and x_{a+b+1} is the variable representing the thickness of that material, which includes all the discrete thicknesses of the additive manufacturing processes (in increments of the minimum resolution) and the four discrete

thicknesses of the plaster casting method. This implementation involved three processes ($a = 3$) and six materials ($b = 6$).

D.4.4 Model Constraints

As mentioned in section D.3, there are certain constraints associated with which materials can be selected given the selection of a process for example. The mathematical model representing the optimization problem included several constraints:

1. Only one process can be selected.

$$(\sum_{j=1}^{a} x_j) - 1 = 0 \tag{D.1}$$

2. Only one material can be selected.

$$(\sum_{a+1}^{a+b} x_j) - 1 = 0 \tag{D.2}$$

3. If casting is selected, then PP or PE must be selected.

$$x_1 + (\sum_{j=6}^{9} x_j) - 1 = 0 \tag{D.3}$$

4. If SLS is selected, then PP, PE, RD80, DFPA, or DFGF must be selected.

$$x_2 + x_4 + x_5 + x_9 - 1 = 0 \tag{D.4}$$

5. If 3D printing is selected, then PP, PE, or CF must be the selected material.

$$x_3 + (\sum_{j=6}^{8} x_j) - 1 = 0 \tag{D.5}$$

6. If casting is selected, then the thickness must be $3/32''$, $1/8''$, $3/16''$, or $1/4''$.

$$x_1 \prod_{i=1}^{4} (x_{10} - k_i) = 0, \text{where } k_i = \frac{3}{32}, \frac{1}{8}, \frac{3}{16}, \frac{1}{4}. \tag{D.6}$$

7. The safety factor must be greater than a specified value, SF_{min}, to prevent product yield and failure. The safety factor is a ratio of material strength to maximum stress, calculated as a function of the material chosen, m, the thickness, k, and the AFO size, z, as depicted in equation D.7. This function was calculated using a combination of FEA and regression analysis (section D.4.2).

$$SF(m, k, z) \geq SF_{min} \tag{D.7}$$

D.5 Multi-Objective Optimization

The AFO fabrication analysis is posed as a multi-objective optimization, where a clinic would aim to minimize production cost and time, while maximizing AFO performance.

$$\begin{aligned} &\underset{x}{\text{minimize}} && f_c(x),\, f_t(x),\, -f_p(x) \\ &\text{subject to} && \text{equations } (D.1) - (D.7) \end{aligned}$$

The mathematical representation of this objective is a function of the cost, $f_c(x)$, and time, $f_t(x)$, to produce a single AFO, and the performance, $f_p(x)$, of the AFO based on the material, size and thickness chosen. The derivation of each of these functions is described below. The cost and time were determined using data from various literature sources and following a cost analysis method termed 'activity-based costing for manufacturing' outlined in [131]. The performance function was more complex to determine; using published data [132], a performance metric based on predicted patient energetic cost was used.

For our implementation, we resolved the multi-objective optimization into minimizing a single weighted-sum (equation D.8). Since production costs are usually carried over to insurance providers, a clinic might value performance and production time more than the cost. The objective weightings chosen followed this logic and were selected empirically after investigating the solution space.

$$F = 0.01 f_c(x) + f_t(x) - 100 f_p(x) \tag{D.8}$$

D.5.1 Cost

Manufacturing cost is calculated as the sum of direct and indirect costs associated with the part [133]. Direct costs include material and labor directly in contact with the part. Indirect

costs include machine cost. Overhead costs such as administrative and production overhead are not evaluated at this stage, working under the assumption that all the manufacturing processes are available in the same shop and processes share administrative expenses. The cost model, f_c, with material, labor and equipment cost terms, is shown in equation D.9.

For the casting process, the material is available in specific sheet dimensions and the price is a function of the material and thickness chosen. Because of the discrete set of sizes available, excess material might be wasted and is included in the cost. For the laser sintering process, a powder block of material of a fixed volume must be used for each production cycle. Only a portion of this material can be recycled and this is reflected in the cost. Finally, for the 3D printing process, the excess material is in the form of support material needed to support the shape of the AFO while printing. This is a fixed volume of material, $9\,inch^3$ in our case study, with a cost dependent on the material chosen.

$$f_c = C_M + C_L + C_{EQ} \tag{D.9}$$

$$\begin{aligned} C_M = &\sum_{i=a}^{a+b} c_{m_{i-a}}[(kx_i + 123.34/c_{m_{i-a}})x_1 \\ &+ \rho_{i-a}(V_{build}(1-\alpha) + V_{bed}\alpha)x_i x_2 + (V_{part} + V_{sup})x_i x_3] \end{aligned}$$

$$C_L = \sum_{i=1}^{3}\sum_{h=1}^{2} c_{l_{i,h}} t_{l_{i,h}} x_i \qquad C_{EQ} = \sum_{i=1}^{3}\sum_{e=1}^{n} c_{eq_{i,e}} t_{eq_{i,e}} x_i$$

ρ : material density

α : material waste rate

V_{part} : volume of part

V_{bed} : volume of machine bed

V_{sup} : volume of support material

e : machine $\in \{1, 2, 3, ..., n\}$

h : operator class $\in \{1, 2 \mid 1$: orthotist, 2: technician$\}$

c_m : cost of material

c_l : cost of labor

c_{eq} : cost of equipment

t_l : labor time

t_{eq} : machine runtime

Table D.3: An example of a breakdown for calculating time taken for each process for a medium-sized AFO.

Plaster Casting					
Total Time: 29 hours 11 minutes					
	(1) Impression	(2) Plaster Mold	(3) Adjustment	(4) Shaping	(5) Finishing
Value added time (hr):	1	0.5	1	0.58	0.5
Non-value added time (hr):	0.1	1	0	24.5	0
Number of operators:	1 (Orthotist)	1 (Technician)	1 (Orthotist)	1 (Technician)	1 (Orthotist)
Equipment:	N/A	Miscellaneous	Miscellaneous	Kiln + Vacuum	Miscellaneous
Laser Sintering					
Total Time: 32 hours 57 minutes					
	(1) Surface Model	(2) Build CAD	(3) Fabrication	(4) Cleaning	
Value added time (hr):	0.2	0.45	26	0.3	
Non-value added time (hr):	0	0	6	0	
Number of operators:	1 (Orthotist)	1 (Technician)	1 (Technician)	1 (Technician)	
Equipment:	Laser Scanner	PC + Software	SLS Machine	Miscellaneous	
FDM					
Total Time: 26 hours 9 minutes					
	(1) Surface Model	(2) Build CAD	(3) Fabrication	(4) Finishing	
Value added time (hr):	0.45	0.45	0.1	1.5	
Non-value added time (hr):	0	0	24	0	
Number of operators:	1 (Orthotist)	1 (Technician)	1 (Technician)	1 (Technician)	
Equipment:	Laser Scanner	PC + Software	3-D Printer	Miscellaneous	

D.5.2 Time

Each manufacturing processes has a specific flow and steps involved in making the part. Time taken by each step as considered in our implementation depends on part size. A value stream mapping was developed for every process to identify time and equipment involved. A simplified version of the map for the medium size case is shown in table D.3.

The effect of size on the production time was assumed to be negligible for our purposes. The justification of this choice being that the change in size is small compared to the overall product volume and would not greatly affect the additive manufacturing time. As for the plaster casting process, the orthotist and technician would need to spend the same amount of time on a device regardless of its size.

D.5.3 Performance

Metabolic rate is a widely used metric for evaluating the performance of wearable medical devices. For this particular device, the patient metabolic rate is most directly affected by the bending stiffness of the AFO [132, 134]. A study varying the bending stiffness of an exoskeleton device, emulating an AFO, worn by healthy subjects while they walked on a

treadmill showed a relationship to metabolic rate [132]. Leveraging their research, averaged metabolic rate data they obtained from nine subjects were fit to a quadratic function, resulting in equation D.10, where k is the stiffness at the ankle measured in $N\,m\,rad^{-1}$ and r is the predicted metabolic rate at that stiffness with units of $W\,Kg^{-1}$. Since reduced metabolic rate indicates better performance, we aimed to maximize performance, which we defined as the reciprocal of metabolic rate.

$$r = 5e^{-6}k^2 - 0.0019k + 2.9 \tag{D.10}$$

As explained in section D.4.2, FEA was used to create functions which took material, thickness and AFO size as an input and returned the stiffness of the device. This stiffness was then inputted into equation D.10 to calculate metabolic rate and thus performance. This allowed us to relate material choice, thickness and AFO size to a performance metric for our objective function. FEA was performed for each of the four discrete thicknesses used by traditional plaster casting manufacturing technique (see table D.1). A linear regression model, fit to the FEA results, for each size category was used to calculate bending stiffness for the entire range of thickness values.

D.5.4 Optimization Algorithms

An exhaustive search of the variable space, implemented using Matlab® software (Mathworks Inc., Natick, MA), was possible in our implementation because of the limited number of materials and possible thicknesses associated with the three manufacturing processes. Nonetheless, the optimization problem was also solved using a heuristic search method, Simulated Annealing (SA), and results were compared with the exhaustive search optima. The heuristic, also implemented in Matlab®, was tested for practicality, since it might have to be used if the number of points in our feasible set increases. The increase could be due to the addition of process, materials, and ranges of possible thickness. Eventually, an exhaustive search might not be able to solve the optimization problem in a reasonable time. Because of the large number of local minima, a heuristic will have to be implemented in order to relatively quickly solve our optimization problem.

D.6 Results and Discussion

Using an exhaustive search, all of the design variable combinations were created and evaluated. The result was a total of 1818 points in the design space. After the model constraints were applied, 744, 726, and 669 points remained as part of the feasible set for

Table D.4: The global optimal selections and corresponding optimization function values for each AFO size considered.

	Process	Material	Thickness (in.)	Cost ($)	Time (hr.)	Performance ($Kg\,W^{-1}$)	Obj. Func. Value
Small	FDM	PE	0.17	425.91	26.5	0.35	-3.79
Medium	FDM	PP	0.11	425.90	26.5	0.36	-5.13
Large	FDM	PP	0.19	425.95	26.5	0.23	8.10

small, medium, and large sizes respectively. The optimal process, material, and thickness, resulting in a minimum weighted objective function, were found for each size category and are summarized in table D.4.

In this case study, 3-D printing was the optimal process. It is the fastest process, incurring only a small increase in cost from the plaster casting method, while maintaining comparable performance. It is worth mentioning that machine cycle time is low in SLS, however, SLS-manufactured parts require a long cool down time before extraction. In addition, the SLS machine has to warm up before initiation. Casting is a less expensive process, but it also requires a long cooling time after the plastic has been heat-molded to the plaster. It is worth noting that SLS and 3D printing both allow batch production. These technologies can leverage economies of scale to produce multiple parts simultaneously, thus shortening setup and production time as well as cost per part. This analysis did not take into account economies of scale as it only considered the production of one AFO per batch.

PE and PP were the chosen optimal materials. Upon further investigation, the performance of the PE material was found to be only slightly better (by $0.005\,Kg\,W^{-1}$) than the PP material. It was also observed that a larger thickness was chosen for the small AFO compared to the medium one. This result could be due to the different materials chosen and the change in AFO geometry due to size-specific anthropometric measurements and ankle moment. It seems that the relationship between AFO size and optimal thickness is not a linear one. Further experimental data is required to form a proper stiffness-performance model.

The simulated annealing method was able to found the global optimal solution. However, due to the small number of variables in this problem, simulated annealing proved to be more computationally intensive than the exhaustive search method as shown in table D.5. Heuristic methods like simulated annealing are expected to have better performance as the number of variables and options increases. A future implementation that includes a larger thickness range, and more materials and process choices could benefit from such a heuristic method. The model could be further expanded to include other sizes, dimensions and AFO designs. The model could be adapted to take patient anthropometric measurements

Table D.5: Comparison of the heuristic simulated annealing (SA) optimization method with an exhaustive search (ES) for the three sizes: small (S), medium (M), and large (L). The success rate was evaluated by running 10 trials of the optimization. The runtime is an average of the runtimes of the 10 trials.

	ES			SA		
Size	S	M	L	S	M	L
Optimal Found?	yes	yes	yes	yes	yes	yes
Success Rate (%)	100	100	100	90	100	100
Runtime (sec.)	2.88	2.84	2.78	4.36	4.99	4.12

as an input instead of a set size and build a geometry that fits the patient then automatically adjust FEA results accordingly. Such a model would add even more customizability, with potential for creating non-traditional AFO designs. Machine tool paths and AFO geometries could be optimized simultaneously and scalability could be incorporated to reduce cost and time. The limitation lies in the availability of experimental data to validate FEA results and any resulting models.

This framework provides a quantitative tool for evaluating the optimal choices for these custom devices. For example, it relies on a quantitative model of metabolic rate and stiffness to predict performance. Quantitative models are necessary for insurance reimbursement justification. However, qualitative orthotist input is also necessary. The integration of qualitative feedback can complement the quantitative choices and provide a better full picture. The weights of the multi-objective function could be altered according to the various interests of patient, clinic and insurance provider. With the weights selected in this paper, our quantitative model provides early support for the development of additive manufacturing techniques for AFO manufacturing. However, the material properties of the printed materials still need experimental verification.

D.7 Conclusion

An optimization framework was developed for evaluating and comparing manufacturing choices for AFO devices. The framework was successfully tested with a case study of three example AFO devices in a range of sizes, where a manufacturing method, material and material thickness were chosen to optimize cost, time and patient performance. The case study implemented in this paper is merely an example to show the feasibility of an optimization approach to choosing optimal manufacturing techniques and materials to meet several objectives. As additive manufacturing techniques make their way further into

custom-manufactured devices, and as more and more choices become available to patients and clinics, an optimization framework could automate part of the decision process and find a quantitatively optimal solution. This framework provides a guideline for a clinic to evaluate and optimize its choices. This versatile framework can be altered to include different objective functions, weighted according to the interested party's preferences. Clinics may use their own parameter values and cost data as well. However, the framework is limited to available experimental data. A greater understanding of patient performance as various AFO design variables are altered is necessary. With the advancement of sensing techniques, the proposed optimization framework could be coupled with real-time sensing methods to more accurately determine an AFO's *performance* metric. Moreover, more complex FEA studies coupled with experimental validation and a better understanding of the properties of additively-manufactured materials is needed.

BIBLIOGRAPHY

[1] David Moher, Alessandro Liberati, Jennifer Tetzlaff, Douglas G. Altman, Doug Altman, Gerd Antes, David Atkins, Virginia Barbour, Nick Barrowman, Jesse A. Berlin, Jocalyn Clark, Mike Clarke, Deborah Cook, Roberto D'Amico, Jonathan J. Deeks, P. J. Devereaux, Kay Dickersin, Matthias Egger, Edzard Ernst, Peter C. Gøtzsche, Jeremy Grimshaw, Gordon Guyatt, Julian Higgins, John P.A. Ioannidis, Jos Kleijnen, Tom Lang, Nicola Magrini, David McNamee, Lorenzo Moja, Cynthia Mulrow, Maryann Napoli, Andy Oxman, Bá Pham, Drummond Rennie, Margaret Sampson, Kenneth F. Schulz, Paul G. Shekelle, David Tovey, and Peter Tugwell. Preferred reporting items for systematic reviews and meta-analyses: The PRISMA statement. PLoS Medicine, 6(7), jul 2009. ISSN 15491277. doi: 10.1371/journal.pmed.1000097. ix, 14, 15

[2] Toshiki Kobayashi, Aaron K L Leung, Yasushi Akazawa, and Stephen W Hutchins. The effect of varying the plantarflexion resistance of an ankle-foot orthosis on knee joint kinematics in patients with stroke. Gait & posture, 37(3):457–459, mar 2013. ISSN 1879-2219 (Electronic). doi: 10.1016/j.gaitpost.2012.07.028. ix, 17, 19, 20, 21, 23, 24, 25, 28, 31, 90

[3] Hwan Choi, Keshia M Peters, Michael B MacConnell, Katie K Ly, Eric S Eckert, and Katherine M Steele. Impact of ankle foot orthosis stiffness on Achilles tendon and gastrocnemius function during unimpaired gait. Journal of Biomechanics, 2017. ISSN 00219290. ix, 4, 17, 19, 20, 21, 22, 24, 25, 29, 31, 33, 90

[4] Elisa S Arch and Steven J Stanhope. Passive-Dynamic Ankle–Foot Orthoses Substitute for Ankle Strength While Causing Adaptive Gait Strategies: A Feasibility Study. Annals of Biomedical Engineering, 43(2):442–450, feb 2015. ISSN 0090-6964. doi: 10.1007/s10439-014-1067-8. ix, 17, 19, 20, 21, 24, 25, 28, 29, 90

[5] Madeline L. Singer, Toshiki Kobayashi, Lucas S. Lincoln, Michael S. Orendurff, and K. Bo Foreman. The effect of ankle–foot orthosis plantarflexion stiffness on ankle and knee joint kinematics and kinetics during first and second rockers of gait in individuals with stroke. Clinical Biomechanics, 29(9):1077–1080, nov 2014. ISSN 02680033. doi: 10.1016/j.clinbiomech.2014.09.001. ix, 18, 19, 20, 21, 22, 24, 25, 26, 27, 90

[6] Margaret A McDowell, Cheryl D. Fryar, Cynthia L. Ogden, and Katherine M. Flegal.

Anthropometric reference data for children and adults United States, 2003-2006. Technical report, National Center for Health Statistics (U.S.), 2008. xiii, 113, 114

[7] Robert M. White. Comparative Anthropometry of the Foot. Technical report, Army Natick Research and Development Labs (Individual Protection Lab), MA, USA, dec 1982. xiii, 113, 114

[8] Lynne R. Sheffler, Maureen T. Hennessey, Jayme S. Knutson, Gregory G. Naples, and John Chae. Functional Effect of an Ankle Foot Orthosis on Gait in Multiple Sclerosis. American Journal of Physical Medicine & Rehabilitation, 87(1):26–32, January 2008. ISSN 0894-9115. doi: 10.1097/PHM.0b013e31815b5325. 1

[9] Emma Davidson and Roy Bowers. A systematic literature review comparing ankle-foot orthoses and functional electrical stimulation in the treatment of patients with multiple sclerosis, feb 2013. 1, 14, 110

[10] Kyle A. Sherk, Vanessa D. Sherk, Mark A. Anderson, Debra A. Bemben, and Michael G. Bemben. Lower Limb Neuromuscular Function and Blood Flow Characteristics in AFO-Using Survivors of Stroke. Journal of Geriatric Physical Therapy, 38(2):56–61, 2015. ISSN 1539-8412. doi: 10.1519/JPT.0000000000000017. 1, 110

[11] Jonathan Bean, Andrea Walsh, and Walter Frontera. Brace Modification Improves Aerobic Performance in Charcot-Marie-Tooth Disease. American Journal of Physical Medicine & Rehabilitation, 80(8):578–582, 2001. ISSN 0894-9115. doi: 10.1097/00002060-200108000-00006. 1

[12] Hank White, Jennifer Jenkins, William P Neace, Chester Tylkowski, and Janet Walker. Clinically prescribed orthoses demonstrate an increase in velocity of gait in children with cerebral palsy: a retrospective study. Developmental medicine and child neurology, 44(4):227–232, May 2002. ISSN 0012-1622. doi: 10.1017.S0012162201001992. 1

[13] D. Maltais, ODED Bar-Or, VICTORIA Galea, and MICHAEL Pierrynowski. Use of orthoses lowers the O2 cost of walking in children with spastic cerebral palsy. Medicine and Science in Sports and Exercise, 33(2):320–325, feb 2001. ISSN 0195-9131. doi: 10.1097/00005768-200102000-00023. 1, 13, 110

[14] Constantinos Mavroidis, Richard G Ranky, Mark L Sivak, Benjamin L Patritti, Joseph DiPisa, Alyssa Caddle, Kara Gilhooly, Lauren Govoni, Seth Sivak, Michael Lancia, Robert Drillio, and Paolo Bonato. Patient specific ankle-foot orthoses using rapid prototyping. Journal of neuroengineering and rehabilitation, 8(1):1, January 2011. ISSN 1743-0003. doi: 10.1186/1743-0003-8-1. 1, 4, 60, 111

[15] Roland K. Chen, Yu-an Jin, Jeffrey Wensman, and Albert Shih. Additive manufacturing of custom orthoses and prostheses – A review. Additive Manufacturing, 12: 77–89, October 2016. ISSN 22148604. doi: 10.1016/j.addma.2016.04.002. 2, 60, 113

[16] International Committee of the Red Cross's Physicial Rehabilitation Programme. Manufacturing Guidelines: Ankle Foot Orthosis. Technical report, The Red Cross, 2010. 2, 3, 13

[17] Barry Meadows. Tuning of rigid ankle-foot orthoses is essential. Prosthetics and Orthotics International, 38(1):83, January 2014. ISSN 0309-3646. doi: 10.1177/0309364613498333. 2

[18] Nicola Eddison, Nachiappan Chockalingam, and Stephen Osborne. Ankle foot orthosis–footwear combination tuning: An investigation into common clinical practice in the United Kingdom. Prosthetics and Orthotics International, 39(2):126–133, February 2014. ISSN 0309-3646. doi: 10.1177/0309364613516486.

[19] E Owen, R Bowers, and CB Meadows. Tuning of afo-footwear combinations for neurological disorders. In Proceedings of the 11th World Congress of the International Society for Prosthetics and Orthotics, pages 1–6, 2004.

[20] Roy Bowers and Karyn Ross. A review of the effectiveness of lower limb orthoses used in cerebral palsy. In Recent Developments in Healthcare for Cerebral Palsy: Implications and Opportunities for Orthotics, pages 235–297. International Society for Prosthetics and Orthotics, 2009. 2

[21] Mario C. Faustini, Richard R. Neptune, Richard H. Crawford, and Steven J. Stanhope. Manufacture of Passive Dynamic Ankle–Foot Orthoses Using Selective Laser Sintering. IEEE Transactions on Biomedical Engineering, 55(2):784–790, February 2008. ISSN 0018-9294. doi: 10.1109/TBME.2007.912638. 2, 3, 39, 111, 113

[22] Yuan Jin, Yong He, and Albert Shih. Process Planning for the Fuse Deposition Modeling of Ankle-Foot-Othoses. Procedia CIRP, 42:760–765, 2016. ISSN 22128271. doi: 10.1016/j.procir.2016.02.315. 2, 3, 113

[23] R E Major, P J Hewart, and A M MacDonald. A new structural concept in moulded fixed ankle foot orthoses and comparison of the bending stiffness of four constructions. Prosthetics and orthotics international, 28(1):44–48, apr 2004. ISSN 0309-3646. doi: 10.3109/03093640409167924. 2, 13, 39, 40

[24] Tsuyoshi Sumiya, Y. Suzuki, and T. Kasahara. Stiffness control in posterior-type plastic ankle-foot orthoses: effect of ankle trimline. Part 2: Orthosis characteristics and orthosis/patient matching. Prosthetics and Orthotics International, 20(2):132–137, August 1996. ISSN 0309-3646. doi: 10.3109/03093649609164431. 2, 4, 13, 18, 19, 20, 21, 24, 90

[25] Juanjuan Zhang, Pieter Fiers, Kirby A Witte, Rachel W Jackson, Katherine L Poggensee, Christopher G Atkeson, and Steven H Collins. Human-in-the-loop optimization of exoskeleton assistance during walking. Science, 356(6344):1280 LP – 1284, June 2017. 2, 67, 68

[26] Jeffrey R Koller, Deanna H Gates, Daniel P Ferris, and C David Remy. "Body-in-the-Loop" Optimization of Assistive Robotic Devices: A Validation Study. Robotics: Science and Systems, page Submitted, 2016. 2, 6

[27] Deema Totah, Ilya Kovalenko, Miguel Saez, and Kira Barton. Manufacturing Choices for Ankle-Foot Orthoses: A Multi-objective Optimization. In Procedia CIRP, volume 65, pages 145–150, 2017. ISBN 22128271 (ISSN). doi: 10.1016/j.procir.2017.04.014. 3, 4, 82, 110

[28] Amanda E. Chisholm and Stephen D. Perry. Ankle-foot orthotic management in neuromuscular disorders: recommendations for future research. Disability and Rehabilitation: Assistive Technology, 7(6):437–449, November 2012. ISSN 1748-3107. doi: 10.3109/17483107.2012.680940. 3, 4, 13, 14, 33

[29] E Condie, J Campbell, and J Martina. Report of a consensus conference on the orthotic management of stroke patients. copenhagen: International society for prosthetics and orthotics; 2004, 2008.

[30] DJ Hoy and M Reinthal. Articulated ankle foot orthosis designs. In Report of a consensus conference on the orthotic management of stroke patients. Copenhagen: ISPO, pages 95–111, 2004. 3

[31] Toshiki Kobayashi, Aaron K. L. Leung, and Stephen W. Hutchins. Techniques to measure rigidity of ankle-foot orthosis: A review. The Journal of Rehabilitation Research and Development, 48(5):565, 2011. ISSN 0748-7711. doi: 10.1682/JRRD.2010.10.0193. 4, 19, 32, 39, 60

[32] Bryan S. Malas. What Variables Influence the Ability of an AFO to Improve Function and When Are They Indicated? Clinical Orthopaedics and Related Research®, 469(5):1308–1314, May 2011. ISSN 0009-921X. doi: 10.1007/s11999-010-1684-y. 4, 32

[33] Toshiki Kobayashi, Madeline L. Singer, Michael S. Orendurff, Fan Gao, Wayne K. Daly, and K. Bo Foreman. The effect of changing plantarflexion resistive moment of an articulated ankle-foot orthosis on ankle and knee joint angles and moments while walking in patients post stroke. Clinical Biomechanics, 30(8):775–780, 2015. ISSN 18791271. doi: 10.1016/j.clinbiomech.2015.06.014. 4, 7, 18, 19, 20, 21, 22, 24, 26, 27, 90

[34] Toshiki Kobayashi, Michael S. Orendurff, Madeline L. Singer, Fan Gao, Wayne K. Daly, and K. Bo Foreman. Reduction of genu recurvatum through adjustment of plantarflexion resistance of an articulated ankle-foot orthosis in individuals post-stroke. Clinical Biomechanics, 35:81–85, June 2016. ISSN 02680033. doi: 10.1016/j.clinbiomech.2016.04.011. 18, 19, 20, 21, 22, 24, 26, 27, 90

[35] Toshiki Kobayashi, Michael S Orendurff, Grace Hunt, Lucas S Lincoln, Fan Gao, Nicholas LeCursi, and K Bo Foreman. An articulated anklefoot orthosis with adjustable plantarflexion resistance, dorsiflexion resistance and alignment: A pilot

study on mechanical properties and effects on stroke hemiparetic gait. Medical Engineering and Physics, 44:94–101, 2017. ISSN 13504533.

[36] Sumiko Yamamoto, Shinji Miyazaki, and Toshio Kubota. Quantification of the effect of the mechanical property of AFOs on hemiplegic gait. Gait & Posture, 1(1):27–34, 1993. ISSN 09666362. doi: 10.1016/0966-6362(93)90040-8. 4, 18, 19, 20, 21, 22, 24, 26, 28, 29, 30, 31, 90

[37] Nicole G. Harper, Elizabeth Russell Esposito, Jason M. Wilken, and Richard R. Neptune. The influence of ankle-foot orthosis stiffness on walking performance in individuals with lower-limb impairments. Clinical biomechanics (Bristol, Avon), 29(8):877–884, September 2014. ISSN 1879-1271 (Electronic). doi: 10.1016/j.clinbiomech.2014.07.005. 4

[38] Elizabeth Russell Esposito PhD, Ryan V Blanck CPO, Nicole G Harper MS, Joseph R Hsu MD, and Jason M Wilken PT, PhD. How Does Ankle-foot Orthosis Stiffness Affect Gait in Patients With Lower Limb Salvage? Clinical Orthopaedics and Related Research, 472(10):3026–3035, 2014. ISSN 0009-921X. doi: 10.1007/s11999-014-3661-3. 4

[39] Elizabeth Russell Esposito, Harmony S Choi, Johnny G Owens, Ryan V Blanck, and Jason M Wilken. Biomechanical response to ankle-foot orthosis stiffness during running. Clinical biomechanics (Bristol, Avon), 30(10):1125–1132, December 2015. ISSN 1879-1271 (Electronic). doi: 10.1016/j.clinbiomech.2015.08.014. 4

[40] Samuel J. Lochner, Jan P. Huissoon, and Sanjeev S. Bedi. Simulation Methods in the Foot Orthosis Development Process. Computer-Aided Design and Applications, 11(6):608–616, June 2014. ISSN 1686-4360. doi: 10.1080/16864360.2014.914375. 4, 111

[41] J Munguia and Kw. Dalgarno. Ankle foot orthotics optimization by means of composite reinforcement of free-form structures. In 24th Annual International Solid Freeform Fabrication Symposium: An Additive Manufactuing Conference, pages 766–776, Austin, Texas, USA, 2013. 4, 111

[42] Amy K. Hegarty, Anthony J. Petrella, Max J. Kurz, and Anne K. Silverman. Evaluating the Effects of Ankle-Foot Orthosis Mechanical Property Assumptions on Gait Simulation Muscle Force Results. Journal of Biomechanical Engineering, 139(3): 031009, 2017. ISSN 0148-0731. doi: 10.1115/1.4035472. 4

[43] Paolo Cappa, Fabrizio Patane, and Giuseppe Di Rosa. A continuous loading apparatus for measuring three-dimensional stiffness of ankle-foot orthoses. Journal of biomechanical engineering, 127(6):1025–1029, November 2005. ISSN 0148-0731 (Print). 5, 39, 40, 41, 57

[44] B Klasson, P Convery, and S Raschke. Test apparatus for the measurement of the flexibility of ankle-foot orthoses in planes other than the loaded plane. Prosthetics

and Orthotics International, 22(1):45–53, April 1998. ISSN 0309-3646. doi: 10.3109/03093649809164456. 5, 39, 40, 57

[45] S Yamamoto, M Ebina, S Miyazaki, H Kawai, and T Kubota. Development of a new ankle-foot orthosis with dorsiflexion asist, part 1: desirable charactersitics of ankle-foot orthoses for hemiplegic patients. J Prosthet Orthot, 9(4):174–179, 1997. 5, 18, 19, 20, 21, 30, 90

[46] D. J J Bregman, A. Rozumalski, D. Koops, V. de Groot, M. Schwartz, and J. Harlaar. A new method for evaluating ankle foot orthosis characteristics: BRUCE. Gait and Posture, 30(2):144–149, August 2009. ISSN 09666362. doi: 10.1016/j.gaitpost.2009.05.012. 5, 21, 36, 37, 39, 40, 41, 54, 56, 57

[47] Sumiko Yamamoto, Masahiko Ebina, Mitsuo Iwasaki, Shigeru Kubo, Hideo Kawai, and Takeo Hayashi. Comparative Study of Mechanical Characteristics of Plastic AFOs. JPO: Journal of Prosthetics and Orthotics, 5(2), 1993. ISSN 1040-8800. 5, 32, 60

[48] S Yamamoto, a Hagiwara, T Mizobe, O Yokoyama, and T Yasui. Development of an ankle – foot orthosis with an oil damper. Prosthet Orthot Int, 29(3):209–219, 2005. ISSN 0309-3646. doi: 10.1080/03093640500199455. 5, 60

[49] Tom F. Novacheck, Cammie Beattie, Adam Rozumalski, George Gent, and Gary Kroll. Quantifying the spring-like properties of ankle-foot orthoses (AFOs). Journal of Prosthetics and Orthotics, 19(4):98–103, 2007. ISSN 10408800. doi: 10.1097/JPO.0b013e31812e555e. 5, 32, 36, 39, 41, 56, 60, 64

[50] Joshua M Caputo, Peter G Adamczyk, and Steven H Collins. Informing Ankle-Foot Prosthesis Prescription through Haptic Emulation of Candidate Devices. 2015 Ieee International Conference on Robotics and Automation (Icra), pages 6445–6450, 2015. ISSN 1050-4729. 6, 8, 67

[51] Steven H. Collins, M. Bruce Wiggin, and Gregory S. Sawicki. Reducing the energy cost of human walking using an unpowered exoskeleton. Nature, 522(7555):212–215, apr 2015. ISSN 0028-0836. doi: 10.1038/nature14288. 6, 17, 19, 20, 21, 22, 26, 27, 28, 29, 30, 90

[52] Jeffrey R Koller, Deanna H Gates, Daniel P Ferris, and C David Remy. Confidence in the curve: Establishing instantaneous cost mapping techniques using bilateral ankle exoskeletons. Journal of Applied Physiology, 122(2):242–252, November 2016. ISSN 8750-7587. doi: 10.1152/japplphysiol.00710.2016. 7, 67

[53] Philippe Malcolm, Wim Derave, Samuel Galle, and Dirk De Clercq. A Simple Exoskeleton That Assists Plantarflexion Can Reduce the Metabolic Cost of Human Walking. PLoS ONE, 8(2):e56137, February 2013. ISSN 19326203. doi: 10.1371/journal.pone.0056137. 6

[54] Koji Ohata, Tadashi Yasui, Tadao Tsuboyama, and Noriaki Ichihashi. Effects of an ankle-foot orthosis with oil damper on muscle activity in adults after stroke. Gait & posture, 33(1):102–107, January 2011. ISSN 1879-2219 (Electronic). doi: 10.1016/j.gaitpost.2010.10.083. 6

[55] John H. Hollman, Eric M. McDade, and Ronald C. Petersen. Normative spatiotemporal gait parameters in older adults. Gait and Posture, 34(1):111–118, 2011. ISSN 09666362. doi: 10.1016/j.gaitpost.2011.03.024. 6

[56] S. Fritz and M. Lusardi. Walking speed: the sixth vital sign. Journal of Geriatric Physical Therapy, 32(2):1–5, 2009. ISSN 1539-8412. doi: 10.1519/00139143-200932020-00002. 6

[57] Larry W Forrester, Anindo Roy, Hermano Igo Krebs, and Richard F Macko. Ankle training with a robotic device improves hemiparetic gait after a stroke. Neurorehabilitation and neural repair, 25(4):369–77, 2011. ISSN 1552-6844. doi: 10.1177/1545968310388291. 6, 7

[58] Stefan Hesse, Cordula Werner, Konrad Matthias, Kirker Stephen, and Michael Berteanu. Non–Velocity-Related Effects of a Rigid Double-Stopped Ankle-Foot Orthosis on Gait and Lower Limb Muscle Activity of Hemiparetic Subjects With an Equinovarus Deformity. Stroke, 30(9):1855 LP – 1861, September 1999. 6

[59] Sarah Prenton, Laurence Pj Kenney, Glen Cooper, and Matthew J Major. A sock for foot-drop: a preliminary study on two chronic stroke patients. Prosthetics and orthotics international, 38(5):425–430, October 2014. ISSN 1746-1553 (Electronic). doi: 10.1177/0309364613505107. 6

[60] Karen J. McCain, Patricia S. Smith, and Ross Querry. Ankle-Foot Orthosis Selection to Facilitate Gait Recovery in Adults After Stroke. JPO Journal of Prosthetics and Orthotics, 24(3):111–121, July 2012. ISSN 1040-8800. doi: 10.1097/JPO.0b013e31825f860d. 6

[61] L M Schutte, U Narayanan, J L Stout, P Selber, J R Gage, and M H Schwartz. An index for quantifying deviations from normal gait. Gait & Posture, 11(1):25–31, 2000. ISSN 0966-6362. doi: 10.1016/S0966-6362(99)00047-8. 6

[62] M Romei, M Galli, F Motta, M Schwartz, and M Crivellini. Use of the normalcy index for the evaluation of gait pathology. Gait & Posture, 19(1):85–90, 2004. ISSN 0966-6362. doi: 10.1016/S0966-6362(03)00017-1. 6

[63] Michael H Schwartz and Adam Rozumalski. The gait deviation index: A new comprehensive index of gait pathology. Gait & Posture, 28(3):351, 2008. ISSN 0966-6362. 6

[64] Richard Baker, Jennifer L McGinley, Michael H Schwartz, Sarah Beynon, Adam Rozumalski, H Kerr Graham, and Oren Tirosh. The Gait Profile Score and Movement Analysis Profile. Gait & Posture, 30(3):265–269, 2009. ISSN 0966-6362. doi: 10.1016/j.gaitpost.2009.05.020. 6

[65] Gabor J Barton, Malcolm B Hawken, Mark A Scott, and Michael H Schwartz. Movement Deviation Profile: A measure of distance from normality using a self-organizing neural network. Human Movement Science, 31(2):284–294, 2012. ISSN 0167-9457. doi: 10.1016/j.humov.2010.06.003. 6

[66] Jessica L. Burpee and Michael D. Lewek. Biomechanical gait characteristics of naturally occurring unsuccessful foot clearance during swing in individuals with chronic stroke. Clinical Biomechanics, 30(10):1102–1107, 2015. ISSN 18791271. doi: 10.1016/j.clinbiomech.2015.08.018. 7

[67] Kavi C. Jagadamma, Elaine Owen, Fiona J. Coutts, Janet Herman, Jacqueline Yirrell, Thomas H. Mercer, and Mariëtta L. Van Der Linden. The effects of tuning an Ankle-Foot Orthosis Footwear Combination on kinematics and kinetics of the knee joint of an adult with hemiplegia. Prosthetics and Orthotics International, 34(3): 270–276, 2010. ISSN 0309-3646. doi: 10.3109/03093646.2010.503225. 7

[68] Megan E. Reissman and Yasin Y. Dhaher. A functional tracking task to assess frontal plane motor control in post stroke gait. Journal of Biomechanics, 48(10):1782–1788, 2015. ISSN 18732380. doi: 10.1016/j.jbiomech.2015.05.008. 7

[69] Jeffrey R. Koller, Daniel A. Jacobs, Daniel P. Ferris, and C. David Remy. Learning to walk with an adaptive gain proportional myoelectric controller for a robotic ankle exoskeleton. Journal of NeuroEngineering and Rehabilitation, 12(1):97, 2015. ISSN 1743-0003. doi: 10.1186/s12984-015-0086-5. 7, 67

[70] Deema Totah, Meghna Menon, Carlie Jones-hershinow, Kira Barton, and Deanna H. Gates. The Impact of Ankle-Foot Orthosis Stiffness on Gait: A Systematic Literature Review. Gait and Posture, 69(January):101–111, 2019. ISSN 09666362. doi: S0966636218303084. 12, 36, 60

[71] Bartonek Åsa, Eriksson Marie, and Gutierrez-Farewik Elena M. Effects of carbon fibre spring orthoses on gait in ambulatory children with motor disorders and plantarflexor weakness. Developmental Medicine & Child Neurology, 49(8):615–620, jul 2007. ISSN 0012-1622. doi: 10.1111/j.1469-8749.2007.00615.x. 13, 14

[72] Gita M. Ramdharry, Brian L. Day, Mary M. Reilly, and Jonathan F. Marsden. Foot drop splints improve proximal as well as distal leg control during gait in Charcot-Marie-Tooth Disease. Muscle and Nerve, 46(4):512–519, 2012. ISSN 0148639X. doi: 10.1002/mus.23348. 13, 14, 18, 19, 20, 21, 22, 24, 26, 28, 32

[73] Toshiki Kobayashi, Michael S Orendurff, Madeline L Singer, Fan Gao, and K Bo Foreman. Contribution of ankle-foot orthosis moment in regulating ankle and knee motions during gait in individuals post-stroke. Clinical Biomechanics, 45:9–13, 2017. ISSN 02680033. 13, 18, 19, 20, 21, 22, 24, 90

[74] Cathleen E Buckon, Susan Sienko Thomas, Sabrina Jakobson-Huston, Michael Moor, Michael Sussman, and Michael Aiona. Comparison of three ankle–foot orthosis configurations for children with spastic hemiplegia. Developmental Medicine

& Child Neurology, 43(6):371–378, 2001. ISSN 0012-1622. doi: DOI:10.1017/S0012162201000706. 13

[75] E. Cakar, O. Durmus, L. Tekin, U. Dincer, and M. Z. Kiralp. The ankle-foot orthosis improves balance and reduces fall risk of chronic spastic hemiparetic patients. European Journal of Physical and Rehabilitation Medicine, 46(3):363–368, 2010. ISSN 19739087. doi: R39102251[pii]. 13

[76] Michael W. Whittle and Jim Richards. Whittle's Gait Analysis. Churchill Livingstone, fifth edition, 2012. 13

[77] Report of a consensus conference on the orthotic management of stroke patients. In E Condie, J Campbell, and J Martina, editors, Report of a consensus conference on the orthotic management of stroke patients., Coopenhagen, Denmark, 2004. International Society for Prosthetics and Orthotics. doi: ISBN87-89809-14-9. 13

[78] Hiroaki Abe, Akira Michimata, Kazuyoshi Sugawara, Naoki Sugaya, and Shin-Ichi Izumi. Improving Gait Stability in Stroke Hemiplegic Patients with a Plastic Ankle-Foot Orthosis. The Tohoku Journal of Experimental Medicine, 218(3):193–199, 2009. doi: 10.1620/tjem.218.193. 13

[79] J F Lehmann, S M Condon, R Price, and B J DeLateur. Gait abnormalities in hemiplegia: their correction by ankle-foot orthoses. Archives of physical medicine and rehabilitation, 68(11):763–771, nov 1987. ISSN 0003-9993 (Print). 13, 19

[80] Mael Lintanf, Jean-Sébastien Bourseul, Laetitia Houx, Mathieu Lempereur, Sylvain Brochard, and Christelle Pons. Effect of ankle-foot orthoses on gait, balance and gross motor function in children with cerebral palsy: a systematic review and meta-analysis. Clinical Rehabilitation, 32(9):1175–1188, 2018. doi: 10.1177/0269215518771824. 14

[81] M Arazpour, M Samadian, K Ebrahimzadeh, M Ahmadi Bani, and S W Hutchins. The influence of orthosis options on walking parameters in spinal cord-injured patients: a literature review. Spinal Cord, 54(6):412–422, 2016. ISSN 1362-4393. doi: 10.1038/sc.2015.238. 14

[82] S. F. Tyson, E. Sadeghi-Demneh, and C. J. Nester. A systematic review and meta-analysis of the effect of an ankle-foot orthosis on gait biomechanics after stroke. Clinical Rehabilitation, 27(10):879–891, 2013. ISSN 02692155. doi: 10.1177/0269215513486497. 14, 16

[83] N Eddison, M Mulholland, and N Chockalingam. Do research papers provide enough information on design and material used in ankle foot orthoses for children with cerebral palsy? A systematic review. Journal of Children's Orthopaedics, 11 (4):263–271, aug 2017. ISSN 1863-2521. doi: 10.1302/1863-2548.11.160256. 14

[84] M Jason Highsmith, Leif M Nelson, Neil T Carbone, Tyler D Klenow, Jason T Kahle, Owen T Hill, Jason T Maikos, Mike S Kartel, and Billie J Randolph. Outcomes Associated With the Intrepid Dynamic Exoskeletal Orthosis (IDEO): A Systematic Review of the Literature. Military Medicine, 181(S4):69–76, nov 2016. ISSN 0026-4075. doi: 10.7205/MILMED-D-16-00280. 14, 19, 31

[85] PEDro. PEDro Physiotherapy Evidence Database, 2016. 16, 89

[86] Kaitlyn Weiss and Chris Whatman. Biomechanics Associated with Patellofemoral Pain and ACL Injuries in Sports. Sports Medicine, 45(9):1325–1337, 2015. ISSN 11792035. doi: 10.1007/s40279-015-0353-4. 16, 89

[87] Amirhesam Amerinatanzi, Hashem Zamanian, Narges Shayesteh Moghaddam, Hamdy Ibrahim, Mohamed Samir Hefzy, and Mohammad Elahinia. On the Advantages of Superelastic NiTi in Ankle Foot Orthoses. In Volume 2: Modeling, Simulation and Control; Bio-Inspired Smart Materials and Systems; Energy Harvesting, volume 2 of ASME 2016 Conference on Smart Materials, Adaptive Structures and Intelligent Systems, SMASIS 2016, page V002T03A026, Stowe, VT, United states, sep 2016. ASME. ISBN 978-0-7918-5049-7. doi: 10.1115/SMASIS2016-9267. 17, 19, 20, 21, 22, 90

[88] Amirhesam Amerinatanzi, Hashem Zamanian, Narges Shayesteh Moghaddam, Ahmadreza Jahadakbar, and Mohammad Elahinia. Application of the Superelastic NiTi Spring in Ankle Foot Orthosis (AFO) to Create Normal Ankle Joint Behavior. Bioengineering, 4(4):95, dec 2017. ISSN 2306-5354. doi: 10.3390/bioengineering4040095. 17, 19, 20, 21, 22, 28, 30, 90

[89] Elisa S Arch, Steven J Stanhope, and Jill S Higginson. Passive-dynamic ankle–foot orthosis replicates soleus but not gastrocnemius muscle function during stance in gait: Insights for orthosis prescription. Prosthetics and Orthotics International, 40 (5):606–616, oct 2016. ISSN 0309-3646. doi: 10.1177/0309364615592693. 17, 19, 20, 21, 22, 29, 90

[90] Nicholas B Bolus, Caitlin N Teague, Omer T Inan, and Geza F Kogler. Instrumented Ankle-Foot Orthosis: Towards a Clinical Assessment Tool for Patient-Specific Optimization of Orthotic Ankle Stiffness. IEEE/ASME Transactions on Mechatronics, 2017. ISSN 10834435. 17, 19, 20, 21, 22, 24, 28, 90

[91] R. Brunner, G. Meier, and T. Ruepp. Comparison of a stiff and a spring-type ankle-foot orthosis to improve gait in spastic hemiplegic children. Journal of Pediatric Orthopaedics, 18(6):719–726, 1998. ISSN 02716798. doi: 10.1097/00004694-199811000-00005. 17, 19, 20, 21, 22, 24, 26, 28, 29, 30, 31, 33, 90

[92] Bastien Guillebastre, Paul Calmels, and Patrice Rougier. Effects of Rigid and Dynamic Ankle-Foot Orthoses on Normal Gait. Foot & Ankle International, 30(1): 51–56, jan 2009. ISSN 1071-1007. doi: 10.3113/FAI.2009.0051. 17, 19, 20, 21, 28, 29, 30, 31, 32, 33, 90

[93] Nicole G. Harper, Elizabeth Russell Esposito, Jason M. Wilken, and Richard R. Neptune. The influence of ankle-foot orthosis stiffness on walking performance in individuals with lower-limb impairments. Clinical Biomechanics, 29(8):877–884, sep 2014. ISSN 02680033. doi: 10.1016/j.clinbiomech.2014.07.005. 17, 19, 20, 21, 22, 24, 26, 27, 28, 29, 31, 32, 90

[94] Yvette L. Kerkum, Annemieke I. Buizer, Josien C. van den Noort, Jules G. Becher, Jaap Harlaar, and Merel-Anne Brehm. The Effects of Varying Ankle Foot Orthosis Stiffness on Gait in Children with Spastic Cerebral Palsy Who Walk with Excessive Knee Flexion. PLOS ONE, 10(11):e0142878, nov 2015. ISSN 1932-6203. doi: 10.1371/journal.pone.0142878. 17, 19, 20, 21, 22, 24, 26, 27, 28, 30, 31, 90

[95] Toshiki Kobayashi, Aaron K.L. Leung, Yasushi Akazawa, and Stephen W Hutchins. Design of a stiffness-adjustable ankle-foot orthosis and its effect on ankle joint kinematics in patients with stroke. Gait & Posture, 33(4):721–723, apr 2011. ISSN 09666362. doi: 10.1016/j.gaitpost.2011.02.005. 17, 19, 20, 21, 22, 24, 28, 31, 39, 90

[96] Toshiki Kobayashi, Michael S Orendurff, Grace Hunt, Lucas S Lincoln, Fan Gao, Nicholas LeCursi, and K Bo Foreman. An articulated anklefoot orthosis with adjustable plantarflexion resistance, dorsiflexion resistance and alignment: A pilot study on mechanical properties and effects on stroke hemiparetic gait. Medical Engineering and Physics, 44:94–101, 2017. ISSN 13504533. 18, 19, 20, 21, 22, 24, 26, 27, 90

[97] J F Lehmann, P C Esselman, M J Ko, J C Smith, B J DeLateur, and A J Dralle. Plastic ankle-foot orthoses: evaluation of function. Archives of physical medicine and rehabilitation, 64(9):402–7, sep 1983. ISSN 0003-9993. 18, 19, 20, 21, 22, 32, 90

[98] Elizabeth Russell Esposito PhD, Ryan V Blanck CPO, Nicole G Harper MS, Joseph R Hsu MD, and Jason M Wilken PT, PhD. How Does Ankle-foot Orthosis Stiffness Affect Gait in Patients With Lower Limb Salvage? Clinical Orthopaedics and Related Research, 472(10):3026–3035, 2014. ISSN 0009-921X. doi: http://dx.doi.org/10.1007/s11999-014-3661-3. 18, 19, 20, 21, 22, 24, 26, 27, 28, 30, 31, 32, 90

[99] Scott Telfer, Jari Pallari, Javier Munguia, Kenny Dalgarno, Martin McGeough, and Jim Woodburn. Embracing additive manufacture: implications for foot and ankle orthosis design. BMC Musculoskeletal Disorders, 13(1):84, dec 2012. ISSN 1471-2474. doi: 10.1186/1471-2474-13-84. 18, 19, 20, 21, 22, 24, 26, 27, 31, 32, 90

[100] Elizabeth Russell Esposito, Harmony S Choi, Johnny G Owens, Ryan V Blanck, and Jason M Wilken. Biomechanical response to ankle-foot orthosis stiffness during running. Clinical biomechanics (Bristol, Avon), 30(10):1125–1132, December 2015. ISSN 1879-1271 (Electronic). doi: 10.1016/j.clinbiomech.2015.08.014. 27, 33

[101] Derek J Haight, Elizabeth Russell Esposito, and Jason M Wilken. Biomechanics of uphill walking using custom ankle-foot orthoses of three different stiffnesses. Gait & Posture, 41(3):750–756, mar 2015. ISSN 09666362. doi: 10.1016/j.gaitpost.2015.01.001. 33

[102] Gary G Bedard, Jennifer Motylinski, Benjamin Call, Fan Gao, and Leslie Gray. Bench Test Validation of a Dynamic Posterior Leaf Spring Ankle-Foot Orthosis. Journal of Prosthetics & Orthotics (JPO), 28(1):30–37, 2016. ISSN 10408800. doi: 10.1097/JPO.0000000000000081. 36, 39, 40

[103] William W. DeToro. Plantarflexion Resistance of Selected Ankle-Foot Orthoses: A Pilot Study of Commonly Prescribed Prefabricated and Custom-Molded Alternatives. Biomechanical Analyses, pages 39–44, 2001. 36, 39, 40

[104] T Kasahara. Stiffness control in posterior-type plastic ankle-foot orthoses: effect. Prosthetics and Orthotics International, pages 132–137, 1996. 36, 39, 40, 41

[105] Shinji Miyazaki. A System for the Continuous Measurement of Ankle Joint Moment in Hemiplegic Patients Wearing Ankle-Foot Orthoses. Frontiers of medical and biological engineering, 5(3):215–232, 1993. ISSN 0921-3775. 39

[106] Wesley Golay, Thomas Lunsford, Brenda Rae Lunsford, and Jack Greenfield. The effect of malleolar prominence on polypropylene AFO rigidity and buckling, 1989. ISSN 10408800. 39, 40

[107] Thomas R. Lunsford, Thomas Ramm, and Joseph A. Miller. Viscoelastic Properties of Plastic Pediatric AFOs. JPO Journal of Prosthetics and Orthotics, 6(1):3–9, 1994. 39, 40

[108] Masahiro Nagaya. Shoehorn-type ankle-foot orthoses: Prediction of flexibility. Archives of Physical Medicine and Rehabilitation, 78(1):82–84, 1997. ISSN 00039993. doi: 10.1016/S0003-9993(97)90015-0.

[109] Adrian a. Polliack, Christopher Swanson, Samuel E. Landsberger, and Donald R. McNeal. Development of a Testing Apparatus for Structural Stiffness Evaluation of Ankle-Foot Orthoses. JPO Journal of Prosthetics and Orthotics, 13(3):74–82, 2001. ISSN 1040-8800. doi: 10.1097/00008526-200109000-00012. 39, 57

[110] Young-shin Lee, Kyung-joo Choi, Kang Hee Cho, Young-jin Choi, Hyun Kyun Lim, and Bong-ok Kim. Plastic Ankle Foot Orthosis for Hemiplegics and Structural Analysis. Key Engineering Materials, 328:855–858, 2006. ISSN 1662-9795. doi: 10.4028/www.scientific.net/KEM.326-328.855. 40

[111] M. Walbran, K. Turner, and A.J. McDaid. Customized 3D printed ankle-foot orthosis with adaptable carbon fibre composite spring joint. Cogent Engineering, 3(1):1–11, 2016. ISSN 2331-1916. doi: 10.1080/23311916.2016.1227022. 39

[112] Kota Z Takahashi and Steven J Stanhope. Estimates of Stiffness for Ankle Foot Orthoses Are Sensitive to Loading Conditions. Journal of Prosthetics & Orthotics (JPO), 22(4):211, 2010. 39

[113] Robert Singerman, David J. Hoy, and Joseph M. Mansour. Design Changes in Ankle-Foot Orthosis Intended to Alter Stiffness Also Alter Orthosis Kinematics. JPO Journal of Prosthetics and Orthotics, 11(3):48–53, 1999. ISSN 1040-8800. doi: 10.1097/00008526-199907000-00003. 39, 40

[114] Toshiki Kobayashi, Aaron K L Leung, Yasushi Akazawa, Hisashi Naito, Masao Tanaka, and Stephen W. Hutchins. Design of an Automated Device to Measure Sagittal Plane Stiffness of an Articulated Ankle-Foot Orthosis. Prosthetics and Orthotics International, 34(4):439–448, dec 2010. ISSN 0309-3646. doi: 10.3109/03093646.2010.495370. 39

[115] A. Ielapi, E. Vasiliauskaite, M. Hendrickx, M. Forward, N. Lammens, W. Van Paepegem, J. P. Deckers, M. Vermandel, and M. De Beule. A novel experimental setup for evaluating the stiffness of ankle foot orthoses. BMC Research Notes, 11(1):1–7, 2018. ISSN 17560500. doi: 10.1186/s13104-018-3752-4. 39, 40, 41, 56, 64

[116] Joseph P. Weir. Quantifying Test-Retest Reliability Using the Intraclass Correlation Coefficient and the SEM. The Journal of Strength and Conditioning Research, 19 (1):231, 2005. ISSN 1064-8011. doi: 10.1519/15184.1. 52, 53

[117] L Portney and M Watkins. Foundations of clinical research: applications to practice. Pearson Prentice Hall, New Jersey, 3rd edition, 2009. 52

[118] Deema Totah, Ilya Kovalenko, Miguel Saez, and Kira Barton. Manufacturing Choices for Ankle-Foot Orthoses: A Multi-objective Optimization. In Procedia CIRP, volume 65, pages 145–150, 2017. ISBN 22128271 (ISSN). doi: 10.1016/j.procir.2017.04.014. 60

[119] Deema Totah, Meghna Menon, Deanna H. Gates, and Kira Barton. Design and Evaluation of the SMApp: a Stiffness Measurement Apparatus for Ankle-Foot Orthoses. Mechatronics, 2020 (submitted). 61, 62, 64

[120] Daan J J Bregman, Vincent De Groot, Peter Van Diggele, Hubert Meulman, Han Houdijk, and Jaap Harlaar. Polypropylene ankle foot orthoses to overcome drop-foot gait in central neurological patients: A mechanical and functional evaluation. Prosthetics and Orthotics International, 34(3):293, 2010. ISSN 0309-3646. 63

[121] Heike Vallery, Jan Veneman, Edwin van Asseldonk, Ralf Ekkelenkamp, Martin Buss, and Herman van Der Kooij. Compliant actuation of rehabilitation robots. IEEE Robotics and Automation Magazine, 15(3):60–69, 2008. ISSN 10709932. doi: 10.1109/MRA.2008.927689. 67

[122] Emma Treadway, Yi Yang, and R. Brent Gillespie. Decomposing the performance of admittance and series elastic haptic rendering architectures. 2017 IEEE World Haptics Conference, WHC 2017, (June):346–351, 2017. doi: 10.1109/WHC.2017.7989926.

[123] Fabrizio Sergi and Marcia K. O'Malley. On the stability and accuracy of high stiffness rendering in non-backdrivable actuators through series elasticity. Mechatronics, 26:64–75, 2015. ISSN 09574158. doi: 10.1016/j.mechatronics.2015.01.007. 78

[124] Rachel W Jackson and Steven H Collins. An experimental comparison of the relative benefits of work and torque assistance in ankle exoskeletons. Journal of applied physiology (Bethesda, Md. : 1985), 119(5):jap.01133.2014, July 2015. ISSN 1522-1601. doi: 10.1152/japplphysiol.01133.2014. 67, 68

[125] Ion P I Pappas, Thierry Keller, Sabine Mangold, Milos R Popovic, Volker Dietz, and Manfred Morari. A Reliable Gyroscope-Based Gait-Phase Detection Sensor Embedded in a Shoe Insole. IEEE Sensors Journal, 4(2):268–274, 2004. ISSN 1530437X. doi: 10.1109/JSEN.2004.823671. 72

[126] Gita M Ramdharry, Brian L Day, Mary M Reilly, and Jonathan F Marsden. Foot drop splints improve proximal as well as distal leg control during gait in Charcot-Marie-Tooth disease. Muscle & nerve, 46(4):512–519, oct 2012. ISSN 1097-4598 (Electronic). doi: 10.1002/mus.23348. 90

[127] Thomas L. Pommering, Lisa Kluchurosky, and Scott L. Hall. Ankle and Foot Injuries in Pediatric and Adult Athletes. Primary Care: Clinics in Office Practice, 32 (1):133–161, mar 2005. ISSN 00954543. doi: 10.1016/j.pop.2004.11.003. 110

[128] S Ounpuu, K J Bell, R B Davis, and P a DeLuca. An evaluation of the posterior leaf spring orthosis using joint kinematics and kinetics. Journal of pediatric orthopedics, 16(3):378–84, 1996. ISSN 0271-6798. doi: 10.1097/01241398-199605000-00017. 111

[129] International Committee of the Red Cross's Physicial Rehabilitation Programme. Manufacturing Guidelines: Ankle Foot Orthosis, 2010. 111, 112, 113

[130] M Ruffo, C Tuck, and R Hague. Cost estimation for rapid manufacturing - laser sintering production for low to medium volumes. Proceedings of the Institution of Mechanical Engineers, Part B: Journal of Engineering Manufacture, 220(9):1417–1427, jan 2006. ISSN 0954-4054. doi: 10.1243/09544054JEM517. 113

[131] Charles Horngren, Gary Sundem, William Stratton, and Howard Teall. Management Accounting. Pearson Canada, 4th editio edition, 2001. 117

[132] Steven H. Collins, M. Bruce Wiggin, and Gregory S. Sawicki. Reducing the energy cost of human walking using an unpowered exoskeleton. Nature, 522(7555):212–215, apr 2015. ISSN 0028-0836. doi: 10.1038/nature14288. 117, 119, 120

[133] George Ellwood Dieter and Linda C Schmidt. Engineering design, volume 3. McGraw-Hill New York, 2013. 117

[134] Y. Kerkum, J. Harlaar, J. van den Noort, J. Becher, A. Buizer, and M.-A. Brehm. The effects of different degrees of ankle foot orthosis stiffness on gait biomechanics and walking energy cost. Gait & Posture, 42:S89–S90, sep 2015. ISSN 09666362. doi: 10.1016/j.gaitpost.2015.06.163. 119